uOttawa

L'Université canadienne
Canada's university

FACULTÉ DES ÉTUDES SUPÉRIEURES ET POSTOCTORALES

uOttawa

L'Université canadienne
Canada's university

FACULTY OF GRADUATE AND POSDOCTORAL STUDIES

Yishan Li

AUTEUR DE LA THÈSE / AUTHOR OF THESIS

M.Sc. (Microbiology and Immunology)

GRADE / DEGREE

Department of Biochemistry, Microbiology and Immunology

FACULTÉ, ÉCOLE, DÉPARTEMENT / FACULTY, SCHOOL, DEPARTMENT

Mapping IFN Resistance in the NS1 Gene of Influenza A Virus

TITRE DE LA THÈSE / TITLE OF THESIS

Dr. Earl Brown

DIRECTEUR (DIRECTRICE) DE LA THÈSE / THESIS SUPERVISOR

CO-DIRECTEUR (CO-DIRECTRICE) DE LA THÈSE / THESIS CO-SUPERVISOR

EXAMINATEURS (EXAMINATRICES) DE LA THÈSE / THESIS EXAMINERS

Dr. John Bell

Dr. Yu-Wen Hu

Gary W. Slater

Le Doyen de la Faculté des études supérieures et postdoctorales / Dean of the Faculty of Graduate and Postdoctoral Studies

Mapping IFN Resistance In The NS1 Gene Of Influenza A Virus

By

Yishan Li

Thesis Submitted to the
Faculty of Graduate and Postdoctoral Studies
In Partial Fulfillment of the Requirements
for the Master of Science Degree in Microbiology and Immunology

Department of Biochemistry, Microbiology and Immunology
Faculty of Medicine
University of Ottawa

Your file Votre référence
ISBN: 978-0-494-18439-4
Our file Notre référence
ISBN: 978-0-494-18439-4

ABSTRACT

Inhibition of the interferon-mediated antiviral response is a major determinant of virulence in influenza A virus. The NS1 protein of influenza A virus has been identified as the IFN antagonist. However, the specific mechanisms for IFN antagonism are not known. NS1 binds both the PKR as well as single and double stranded RNA to inhibit activation of PKR. Adaptation of human influenza virus to the mouse lung may likewise involve mutations that affect IFN antagonism. The prototype human influenza A virus A/HK/1/68 (H3N2 subtype) was utilized for this project. Six mouse-adapted variants possessing four different point mutations on NS gene were obtained from independently derived mouse-adapted variants. The mutations were located in the RNA binding domain and several sites in an 8 amino acid region from aa 98 to 106. Mutant HKMA20c was of interest because it possessed a mutation in common with highly pathogenic avian influenza virus H5N1 (Leucine on AA 103 on NS1 protein). Base on these phenomena, a hypothesis was brought out that this region may encode a site of interaction with a host or viral factor and that mutation(s) on it may enhance the ability of NS1 protein to function as an IFN antagonist. The approach was to first characterize the IFN resistance and IFN induction properties of HK mouse-adapted mutants as well as pathology in mice lung, followed by the generation of defined recombinant viruses possessing desired mutation(s), then analysis of these recombinant viruses for IFN induction and IFN resistance. Rescuing of the HK wild type NS gene and those of HK mouse-adapted NS mutant genes into the backbone of parental HK genome discovered that NS20, NS20c and NS411 produced attenuating phenotypes on their own. Finally, all these mutant NS genes were inserted into backbone of WSN (lab adapted strain,

A/WSN/33, H1N1) genome to construct recombinant viruses. Using recombinant viruses that differ due to individual NS1 gene showed that all of the NS1 mutations increased resistance to IFN in mouse cells. The extent of IFN resistance due to individual mutation was influenced by cell types: epithelium versus fibroblast, as well as host type: mouse versus human. Interestingly most of the NS1 mutations attenuated growth of virus which suggests that resistance to IFN involves changes in host interaction that are not optimal for growth in the absence of IFN. Infection assay showed mouse-adapted mutant NS genes conferred resistance to mouse IFN and vulnerability to human IFN. And mutant NS1 protein NSMA20c had the most potent ability to resist human and mouse IFN. IFN assay showed that mutant NS1 protein NSMA20c had the highest ability to induce mouse IFN. Furthermore, all synthetic recombinant viruses induced low amounts of IFN in human cells. Immunopathology of infected lungs showed that mouse adapted progeny virus HKMA20C had acquired a crucial ability to spread to and infected alveoli which may be influenced by IFN resistance. Mouse-adapted variants possess mutations that increase IFN resistance that in some instances leads to higher IFN induction. One of the key discussions was that most of these mutations cluster in a small region that has been previously mapped to involve a region of host protein (eIF4GI) interaction.

ACKNOWLEDGEMENTS

I am very pleased to have this chance to give special thanks to Dr. Earl G. Brown for providing me with the opportunity to work in his laboratory and gave me this wonderful project! His guidance, inspiration and patience are greatly appreciated.

Also, I would like to thank the members of my thesis advisory committee, Dr. Ken Dimock and Drs. Kathryn E. Wright for their precious advices.

Thanks also go to my labmates and coworkers: Liya Keleta, Irene Chau, Qingwen Zheng, Jennifer Haley, Jasminka Bozic, Neil McKenna, Reza Nokhbeh and Louise Pelletier for their technical and friendly help during the project.

Special thanks to Drs. Kathryn Wright and Dr. Yu-wen Hu, for their helpful feedback on this thesis writing, also to Liya and Jennifer, for their nicely proof-readings.

Finally, I am grateful to my parents and my husband, for their encouragement and support throughout my education.

I would like to dedicate this work to my dearest daughter, LeAnn.
She is the source of my strength and happiness.

TABLE OF CONTENTS

LIST OF FIGURES

LIST OF TABLES

LIST OF APPENDICES

LIST OF ABBREVIATIONS

5'-UTR	5' end untranslated reagion
CDNA	complementary DNA
CPE	cytopathic effect
CPSF	cleavage and polyadenylation specificity factor
DEPC	diethyl pyrocarbonate
DNA	deoxyribonucleic acid
dNTP	deoxyribonucleotide
DMSO	dimethyl sulfoxide
DTT	dithiothreitol
eIF4GI	eukaryotic translation initiation factor 4GI
ELISA	enzyme linked immunosorbant assay
HA	hemagglutinin protein
HPAI	highly pathological avian influenza A virus
HK	influenza virus A/Hong Kong/1/68
HK-MA	influenza virus A/Hong Kong/1/68 mouse adapted progenies
hStaufen	human homologue of Drosophila Melanogaster protein Staufen
IFN	interferon
IFNAR	IFN-α/β receptor
IRF	IFN regulatory factor
ISRE	IFN stimulated response element
JAK	Janus family of tyrosine kinase
M1	matrix protein

M2	ion channel protein
MA	mouse-Adapted
MDCK	Madin-Darby canine kidney cells
MEF	mouse embryo fibroblast
MEM	minimal essential medium
mLD_{50}	median lethal dose for mice
MMuLV RT	Moloney's murine leukemia virus reverse transcriptase
MOI	multiplicity of infection
mRNA	messenger RNA
NA	neuraminidase protein
NAI	neuraminidase inhibitor
NEP (NS2)	nuclear export protein
NF-κB	nuclear factor- κB
NP	nucleocapsid protein
NS1	nonstructural protein
NS1-BP	NS1-binding protein
NS1-I	NS1-interactor
OAS	2',5'-oligoadenylate synthetase
ORF	open reading frame
PA, PB1, PB2	polymerase complex protein
PABII	poly(A)-binding protein II
PABPI	poly(A)-binding protein I
PBS	phosphate buffered saline
PCR	polymerase chain reaction

PEG	polyethylene glycol
pfu	plaque forming unit
PKR	RNA dependent protein kinase PKR
RBC	red blood cells
RNA	ribonucleic acid
RNP	ribonucleoprotein
rpm	revolutions per minute
STAT	signal transducer and activator of transcription
STE	sodium, Tris and EDTA containing buffer
TBE	Tris, borate, EDTA containing buffer
TE	Tris and EDTA containing buffer
TLR	Toll-like receptor
U	Units
VRNSD	vanadyl ribonucleoside complex
VSV	Vesicular Stomatitis Virus

INTRODUCTION

While influenza epidemics occur yearly, the emergence of pandemic strains of influenza virus is a constant threat, thus influenza continues to be a significant health concern. Influenza infection causes more hospitalization and fatal pneumonia than all other respiratory viruses combined. Each year in the United States, approximately 36,000 people die from influenza-related illness with the most mortality occurring among seniors and young children (Harper et al, CDC recommendations of ACIP, 2005). Global influenza pandemics have appeared at irregular and unpredictable intervals throughout history. During the 1918 pandemic, an H1N1 influenza A virus killed 40 million people worldwide, with an unusual mortality pattern as most deaths were in young adults (Taubenberger et al., 2005(a)). More recently, an unprecedented epizootic of avian influenza A (H5N1) virus that is highly pathogenic for poultry and wild birds has occasionally crossed the species barrier to infect human in Southeast Asia and thus represents an increasing pandemic threat (Chen, 2002; Chotpitayasunondh et al, 2005; Ellis et al, 2004; Horimoto and Kawaoka, 2001; Liem and Lim, 2005). There is a need to understand and interpret influenza genomic features so that virus behavior can be determined for novel influenza viruses. Moreover, there is also a need to more fully understand the virulence determinants of the influenza A virus and to predict the possibility of pandemics. This thesis is concerned with the role of the non-structural protein NS1 in influenza virus adaptation to increased virulence in mice. Recent studies of the z strain of H5N1 showed that it was resisted to IFN due to properties of its NS1 protein (Seo et al, 2002 & 2004).

1.1 Virion Structure, Genome Organization and Encoded Proteins

Influenza A virus belongs to Orthomyxoviridae family which includes the genera of influenza virus A, B, C, and thogotovirus (the 11th meeting of the International Committee on Taxonomy of Viruses). Based on the antigenic character of its envelope proteins, hemagglutinin (HA) and neuraminidase (NA), influenza A virus can be classified into subtypes. Currently there are 16 HA and 9 NA subtypes that have been detected in wild birds and poultry throughout the world (Fouchier et al, 2005; Hinshaw et al, 1982; Kawaoka et al, 1990; Rohm et al, 1996; Webster et al, 1987). Occasionally, avian influenza strains have become adapted to humans and animals to give rise to animal and human strains of influenza. (Please refer to Figure 1 for an explanation of influenza virus nomenclature)

Influenza A virus is an enveloped virus containing a segmented genome consisting of eight pieces of negative sense single stranded RNA. The lipid bilayer envelope of influenza A virus is derived from the plasma membrane of the host cell when the virus buds out. There are three envelope proteins: hemagglutinin, neuraminidase and the M2 protein. Hemagglutinin and neuraminidase form spikes that radiate outward from the envelope; M2 protein forms a channel through the lipid bilayer. The inner surface of the envelope is covered with a matrix protein that also interacts with the nucleocapsid. The eight ribonucleoproteins (RNPs) reside within the virion surrounded by matrix protein. Each RNP structure contains one segment of genomic single-stranded RNA coated by nucleocapsid (NP) protein, associated with the RNA-dependent RNA polymerase complex consisting of three polymerase proteins: PB2, PB1, and PA (Brown, 2000; Lamb and Krug, 2001). (See Figure 2)

Figure 1: Nomenclature for influenza A virus

Note that host of origin is indicated only if strain is isolated from non-humans.

Influenza A Virus Nomenclature

Of human origin:

A/HK/1/68 (H3N2)

Genus/Location/Isolation #/Year (Hemagglutinin & Neuraminidase subtypes)

Host of origin is non-human:

A/Chicken/HK/786/97 (H5N1)

Figure 2: Schematic Diagram of Influenza A Virion Structure

(Taken from Lamb and Krug, 2001)

PB2, PB1, PA: polymerase complex proteins

HA: hemagglutinin protein

NP: nucleoprotein

NA: neuraminidase protein

M1: matrix protein

M2: ion channel protein

NS1: non structural protein

NEP (NS2): nuclear export protein

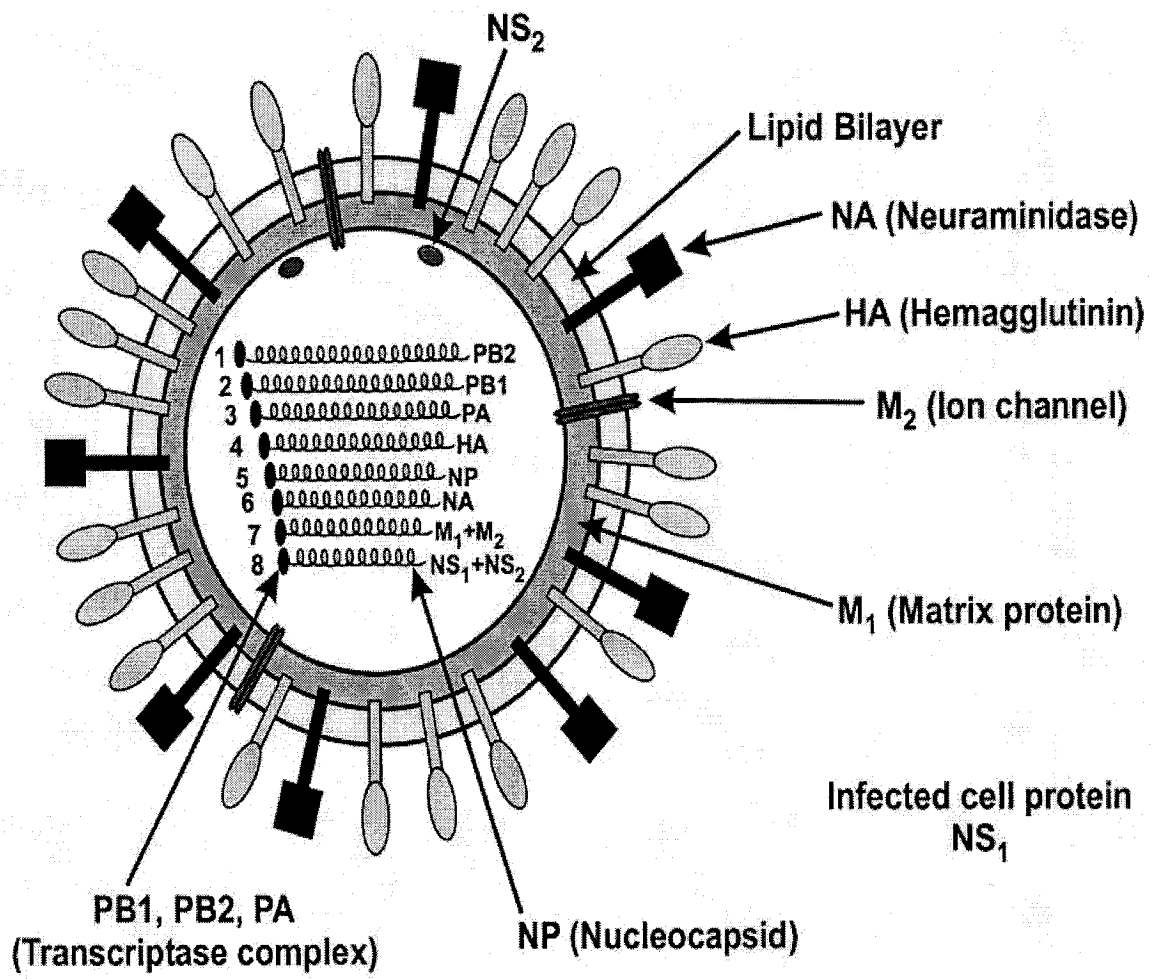
NS2
Lipid Bilayer
NA (Neuraminidase)
HA (Hemagglutinin)
M2 (Ion channel)
M1 (Matrix protein)
Infected cell protein
NS1
1 PB2
2 PB1
3 PA
4 HA
5 NP
6 NA
7 M1+M2
8 NS1+NS2
PB1, PB2, PA
(Transcriptase complex)
NP (Nucleocapsid)

The coding assignment of each of the eight genome segments is showed in Table 1.

TABLE 1: Gene Assignment for Influenza A Virus

Segment	gene	length* (nucleotides)	Encoded protein	function
1	PB2	2313	PB2	Pol. complex subunit
2	PB1	2341	PB1	Pol. complex subunit
			PB1-F2	Apoptosis
3	PA	2209	PA	Pol. complex subunit
4	HA	1736	HA	Hemagglutinin
5	NP	1520	NP	Nucleocapsid
6	NA	1467	NA	Neuraminidase
7	M	1002	M1	Matrix
			M2	Ion channel
8	NS	890	NS1	IFN antagonism
			NEP(NS2)	Nuclear export

- For A/Hong Kong/1/68 strain. (Brown, 2001)

The first three segments encode the polymerase complex: PB2 protein, the cap-recognizing molecule (Fechter et al, 2003; Shi et al, 1995); PB1 protein, the ribonucleotide polymerizing and endonuclease molecule (Lee et al, 2003; Perez and Donis, 2001); and the PA protein that is involved in genome replication (Area et al, 2004; Deng et al, 2005; Fodor et al, 2002 and 2004; Murti et al, 1988). The PB1 gene also encodes another protein from an alternative reading frame, named PB1-F2. This protein was reported to function in apoptosis induction (Chanturiya et al, 2004; Henklein et al, 2005). The fourth segment encodes the Hemagglutinin (HA)

protein which is the dominant envelope protein. The HA protein binds the sialic acid-containing receptors on the cell surface mediating the attachment and fusion of the virus to the cell and subsequently leading to the uncoating of the virus. (Hernandez et al, 1996; Jardetzky and Lamb, 2004) The HA protein exists as a trimer and must undergo a conformational change when fusion occurs (Skehel and Wiley, 2000; Wiley and Skehel, 1987). Furthermore, this protein is the major antigen for influenza A virus to which neutralizing antibodies are made (Abe et al, 2004; Li et al, 2005; Wagner et al, 2005). The fifth segment encodes the nucleocapsid (NP) protein that encapsidates the genomic RNA (Compans et al, 1972; Heggeness et al, 1982; Martin-Benito et al, 2001). The sixth segment encodes the second envelope protein, neuraminidase (NA), which cleaves terminal sialic acid residues from glycoprotein on the surfaces of host cells, as well as the sialic acid present on the carbohydrate chains of HA, the influenza virus envelope protein, facilitating the release and spread of the progeny virus from the host cell (Gottschalk, 1957; Schulman and Palese, 1977; Suzuki et al, 2005). The seventh segment encodes the M1 and M2 proteins through alternative reading frames. The open reading frames (ORF) of these two proteins are in different frames but are overlapping for M1 and a spliced transcript that encodes M2 (Allen et al, 1980; Lamb and Lai, 1981). The M1 matrix protein is the most abundant protein in the virion. M1 associates with RNP, HA, NA and M2 proteins (Bui et al, 1996; Ruigrok et al, 1989; Schulze, 1972). M2 is an ion channel inserted in the envelope membrane (the third envelop protein) (Mould et al, 2000; Pinto et al, 1992). The eighth segment encodes non-structure protein (NS1) and nuclear export protein (NEP) (also named NS2) through alternative reading frames. The ORFs of these two proteins are in different but overlapping reading

frames. The NS1 protein is the focus of this project and it will be described below. The NEP protein, which is encoded by a spliced transcript, binds to the M1 protein in infected cells to direct the nucleo-cytoplasmic export of RNP (Akarsu et al, 2003; Huang et al, 2001; Neumann et al, 2000).

1.2 Expression and Properties of the NS1 Protein

The eighth genome segment is approximately 890 nucleotides in length. Two mRNA transcripts derived from this segment have been identified: the full-length mRNA encoding the NS1 protein, and a spliced mRNA encoding the NEP (Lamb et al, 1980). Depending on the virus strain, NS1 proteins are between 202 to 237 amino acid residues in length (Lamb and Krug, 2001). The NS1 protein is not a component for the virion, however, it is the most abundantly expressed protein in influenza virus-infected cells. The NS1 protein exists as a dimer, and occasionally as higher order multimers (Nemeroff et al, 1995; Wang et al, 1999). As the NS1 protein functions in both nucleus and cytoplasm, there are two nuclear localization signals (NLS) (Greenspan et al, 1988) and one nuclear export signal (NES) (Li et al, 1998) that have been mapped on the NS1 protein. The amino-terminal region of 73 amino acids represents the RNA-binding domain (Hatada and Futada, 1992; Qian et al, 1995). The remaining portion of NS1 protein interacts with several proteins and is called the effector domain (Qian et al, 1994; Wang and Krug, 1996) (See Figure 3). Several molecules have been shown to bind the NS1 protein: dsRNA, poly(A), viral mRNA 5'UTR, U6 snRNA, U6atac snRNA, RNA dependent protein kinase (PKR), eukaryotic translation initiation factor 4GI (eIF4GI), poly(A)-binding protein 1 (PABPI), cleavage and polyadenylation specificity factor (CPSF), poly(A)-binding protein II (PABII), NS1-binding protein (NS1-BP), NS1 interactor (NS1-I), and

Figure 3: Functional Genetic Map of Influenza A Virus NS1 Protein.

(Taken from Krug et al., 2003)

The location of RNA binding, CPSF and PABII are shown.

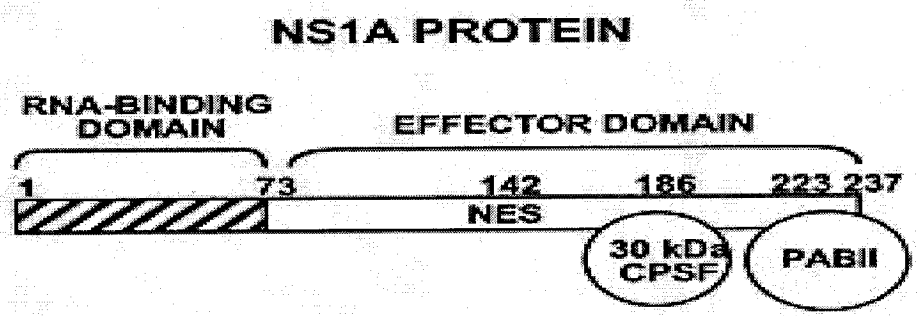
NS1A PROTEIN
RNA-BINDING DOMAIN
EFFECTOR DOMAIN
1
73
142
186
223
237
NES
30 kDa CPSF
PABII

hStaufen (Garfinkel MS and Katze MG, 1993; Qiu and Krug, 1994; Qiu et al, 1995; Wang and Krug, 1998). The binding locations for several of these factors have been determined. The first 73 amino acid residues are associated with dsRNA binding (Hatada and Futada, 1992; Qian et al, 1995). The N-terminal 98 residues that includes the RNA binding sites has been mapped to be the PKR binding region (Tan and Katze, 1998). Sequences between residues 81 and 113 are sufficient to recognized eIF4GI (Aragon et al, 2000). Interaction with PABPI was mapped between residues 1 and 81(Burgui et al, 2003). It was shown that amino acid 186 was in the center of a site required to bind CPSF and amino acid 223-237 for PABII (Chen et al, 1999; Krug et al, 2003; Nemeroff et al, 1998). The N-terminal region was shown to be insufficient for hStaufen binding (Falcon et al, 1999). The regions on NS1 protein involved in binding the rest of the molecules mentioned above have not yet been determined.

1.3 Viral Replication

The first event of replication is viral attachment and entry to the host cell. The HA protein binds to the sialic acid receptors on the cellular surface and the virus is internalized through endocytosis. HAs from different influenza A viruses of different animal sources have different binding preferences for sialic acids with either a α2,3 or a α2,6 linkage to galactose, and this is determined by specific residues in the HA receptor-binding pocket (Weis et al, 1988). This limitation of specific binding preference is believed to constitute a host restriction factor for cross species infection because sialic acid with α2,3 linkage is dominant in avian tissues while sialic acid with α2,6 linkage is dominant in humans'. After endocytosis, the virus goes from early to late endosome and the viral envelope fuses with the membrane

of the late endosome, fusion is mediated by the HA protein. The key to this event is a conformational change of the HA protein that is triggered by low-pH (around pH 5.3) resulting the exposure of the fusion peptide (Eckert and Kim, 2001; Lamb and Choppin, 1983; Ramalho-Santos and de Lima, 1998; Skehel and Wiley, 2000). Another important factor for viral uncoating is the dissociation of M1 from RNP (Martin and Helenius, 1991). This is achieved by the acidification of the inside of the virion as a result of protons being pumped into the virion through the M2 channel (Bui M et al, 1996; Sugrue and Hay 1991). Due to the fusion event, the RNPs are released into the cytoplasm and subsequently migrate into the nucleus (Bui et al, 2000; Helenius, 1992; O'neill et al, 1995; Whittaker et al, 1996).

During replication, there are three types of RNAs synthesized: mRNA (positive sense), template RNA (positive sense), and progeny viral RNA (minus sense). The viral RNA has 12 conserved nucleotides at the 3' end and 13 conserved nucleotides at the 5' end. Depending on the RNA segment, there is a U/A or C/G at position 4 (Lamb and Krug, 2001). The cellular mRNA cap structure, m^7GpppX^m, is required to prime the synthesis of viral mRNA. At the beginning, RNA polymerase complex binds the 5' and 3' end of viral RNA, at the same time PB2 recognizes and binds the capped cellular mRNA, then the cap structure is cleaved by PB1 (Plotch et al, 1981; Rao et al, 2003). Consequently, PB1 catalyzes nucleotide addition using the cap structure as a primer and the viral RNA as template. Polyadenylation occurs at the 3' end of the viral mRNA at a site 15 to 22 nucleotides before the 5' end of the viral RNA segment. The PB1 protein physically blocks the nascent mRNA going through before it can finish copying the full-length of the mRNA thus resulting in the reiterative copying of the U residues (de la Luna et al, 1993; Huang et al, 1990;

Kimura et al, 1992; Mena et al, 1994). The template RNA is positive sense and is a complete copy of the viral RNA segment. The switch from synthesis of mRNA to template RNA requires a change from capped RNA-primed initiation to unprimed initiation that involves encapsidation of the RNA with NP protein, and this is required for both the template and viral RNA synthesis (Honda et al, 1988; Lee et al, 2002; Mena et al, 1999). During the early phase of gene expression, NS1 and NP proteins are the most abundantly expressed protein due to selective transcription of their mRNAs. At the late phase, NS1 and NP mRNAs production declines and the synthesis of structural proteins such as M1 and HA proteins increases (Krug et al, 1989; Shapiro et al, 1987).

The encapsidated viral RNAs are transported from the nucleus to the cytoplasm by interacting with M1 and NEP proteins (Akarsu et al, 2003; Bui et al, 1996; Huang et al, 2001; Martin and Helenius, 1991; Neumann et al, 2000; Patterson et al, 1988). The envelope proteins are translocated onto the plasma membrane, where they appear to aggregate in patches in lipid rafts. These patched areas are the sites for viral budding and where the eight RNPs are packaged into the progeny virus (Leser and Lamb, 2005; Nayak et al, 2004; Schmitt and Lamb, 2005). (See Figure 4)

1.3.1 Roles of NS1 Protein Contributed to Viral Replication

NS1 protein plays a key role for redirecting the host cell translation to viral translation. The NS1 protein binds and recruits eukaryotic initiation factor 4GI (eIF4GI), the cellular translation machinery to the 5' untranslated region (5'UTR) of viral mRNA; it also interacts poly(A)-binding protein 1 (PABPI), a cellular protein involved in translation, hence promoting viral protein translation (Aragon et al, 2000; Burgui et al, 2003). Also, it was proposed that NS1 protein interfered with cellular

Figure 4: Schematic diagram of the life cycle of influenza A virus.

(Taken from Lamb and Krug, 2001)

Influenza A virus attaches host cell by HA protein, followed by endocytosis, and fusion. After the transportation of viral nucleocapsid to the nucleus, viral primary transcription starts. Viral mRNA translocates to cytoplasm, and the protein synthesis begins. Newly synthesized polymerases, NP, NS1 and NEP are transported into the nucleus. Complementary RNA (cRNA) and vRNA are synthesized, followed by secondary transcription. Structural proteins are synthesized and aggregate to specific patch on the cell membrane, together with viral nucleocapsids. Progeny viruses bud out of the infected cell.

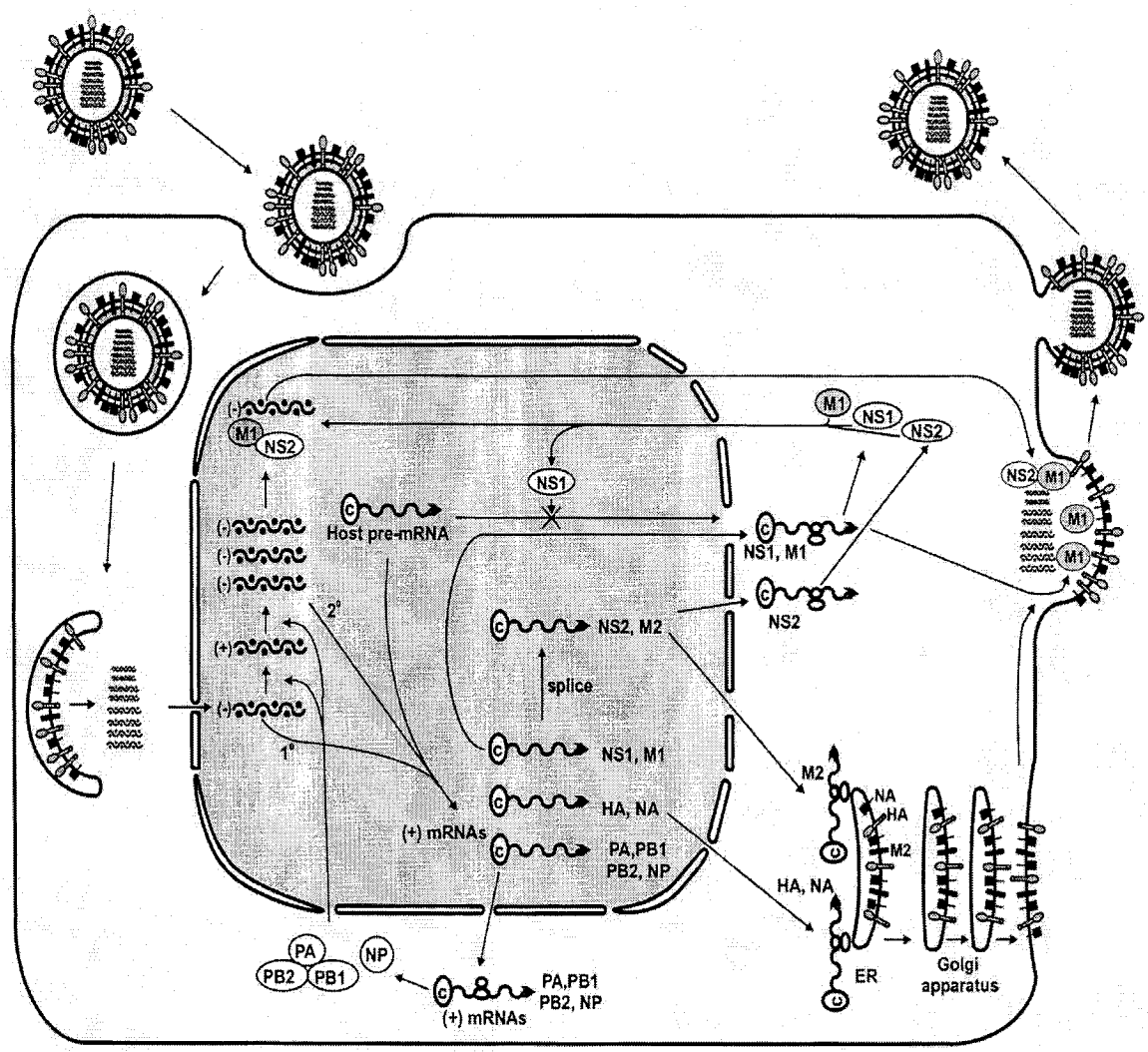
(-)
M1
NS2
NS1
Host pre-mRNA
NS1, M1
NS2
NS2, M2
splice
NS1, M1
HA, NA
PA,PB1
PB2, NP
(+) mRNAs
2°
1°
M1
NS1
NS2
NS2
M1
M1
M1
M2
NA
HA
M2
HA, NA
ER
Golgi
apparatus
PA
PB2
PB1
NP
PA,PB1
PB2, NP
(+) mRNAs

protein synthesis by interacting with a human homologue of Staufen, a protein that is associated with polysomes and localized to the rough endoplasmic reticulum and is also speculated to enhance efficient host translation (Falcon et al, 1999; Marion et al, 1999). Hence the cellular translational machinery and material are redirected to the viral translation, viral protein synthesis is enhanced whereas cellular translation is gradually shutting down. NS1 protein also inhibits the maturation of cellular pre-mRNAs by binding and inhibiting the function of two cellular proteins that are required for mRNA 3'-end polyadenylation: the 30-kDa subunit of the cleavage and polyadenylation specificity factor (CPSF) and poly(A)-binding protein II (PABII) (Chen and Krug, 2000; Chen et al, 1999; Li et al, 2001; Nemeroff et al, 1998; Noah et al, 2003). It has been demonstrated that the NS1 protein binds two molecules involved in mRNA splicing: the key spliceosomal RNA, U6 snRNA, on the specific stem-bulge structure; and the NS1-binding protein (NS1-BP), which is localized to nuclear regions enriched with the spliceosome assembly factor SC35. The ability of NS1 protein to bind splicing components has been implicated in one of NS1's functions of inhibition of cellular pre-mRNA splicing (Agris et al, 1989; Lu et al, 1994; Nemeroff et al, 1992; Qiu et al, 1995; Wang and Krug, 1998; Wolff et al, 1998). It has also been reported that the NS1 protein binds the poly(A) structure of mRNA and causes the nuclear retention of poly(A) containing mRNA (Qiu and Krug, 1994). These activities which block the cellular pre-mRNA maturation and the nucleocytoplasmic export of cellular poly (A) containing mRNA (Alonso-Caplen et al, 1992; Fortes et al, 1994; Li et al, 1998; Qian et al, 1994; Qiu and Krug, 1994), in turn suppress host protein synthesis and provide more materials for viral replication. Finally, the NS1 protein was also found to be associated with NS1 interactor (NS1-

I), a human homologue of the porcine 17β-estradiol dehydrogenase precursor protein, which may play a role in steroid hormones synthesis related to the immune system modulation (Wolff et al, 1996). Mutations in several viral proteins including NS1 protein have been implicated in host range and may involve interaction with host proteins.

1.4 Influenza Virus Genetics and Epidemiology

There are two major processes in influenza A virus genetics: RNA mutation, and genome segment reassortment. RNA viruses have a high mutation rate since their RNA polymerase lacks a proofreading activity. It has been estimated that the mutation rate of influenza A virus is around 1.5×10^{-5} mutations per nucleotide per infection cycle (Parvin et al, 1986). The time required for a complete replication cycle of influenza A virus is about 4-6 hours (Mohler et al, 2005). Mutations result in the accumulation of amino acid changes. There are three different patterns of changes: deletion, insertion, and mismatch. If these changes occur on envelope proteins HA or NA, the main antigen, it is termed antigenic drift. The reassortment of genome segments occurs when two parent viruses coinfect one host cell resulting in the formation of virions containing mixtures of genes derived from the parental strains (Burnet and Lind, 1949). When this event occurs and results change of different subtypes of HA or NA, it is termed antigenic shift. Both antigenic drift and antigenic shift contribute to viral escape from the attack of the host immune response. Antigenic drift gives minor alteration, while on the other hand antigenic shift causes major alteration that can sometimes trigger an epidemic.

1.4.1 Host-Range of Influenza Viruses

Most influenza A viruses are able to efficiently replicate in only one host. Natural hosts for influenza A virus include birds, swine, horses, seals, whales, minks and humans. Influenza A virus can also infect mice and ferrets experimentally (Easterday, 1975). When virulent forms of gene(s) combine with novel genes from virus strains of different hosts, a new virus can arise with high virulence to a new host. For instance, both human and waterfowl influenza A viruses are able to infect swine. Swine can serve as the intermediate host and has been termed the mixing vessel where the human-avian influenza A viruses are thought to be produced.

The influenza pandemic of 1918 to 1919 which called "Spanish flu" killed between 20 and 40 million people worldwide (Taubenberger et al, 2005 and 2005(a)). A novel avian H1N1 virus was responsible for this and it is postulated that the subtypes that circulated before were H3N2 and H2N2. The next pandemic resulted from another antigenic shift that occurred in 1957, when the H2N2 (Asian influenza) appeared. The next pandemic occurred in 1968, due to the H3N2 (Hong Kong) strain that was a human H2N2/avian H3 reassortant. In 1977, a Russian H1N1 virus showed up which was suspected to be the result of an escaped virus from a lab culture. Currently, the H3N2 and H1N1 are co-circulating in the human population (Wright and Webster, 2001). Every pandemic was caused by introduction of new gene segments into human viruses, especially when it involved the introduction of novel HA and NA genes. Waterfowl is the natural host for influenza A virus and acts as a gene library of influenza A subtypes. Currently all the 16 HAs and 9 NAs have been isolated from waterfowl. Most influenza A viruses cause asymptomatic infection in waterfowl. The common subtypes that infect human are H1, H2, H3, and N1, N2 (Webster et al, 1992; Wright and Webster, 2001). There is always a risk that

an influenza A virus gene from the waterfowl reservoir could be introduced into the human population to produce a novel virus to human but with susceptibility. However, in 1997, there was direct transmission of avian H5N1 influenza A virus to humans causing six deaths out of the eighteen cases of infection without any reassortment process, yet, this virus was not able to spread among humans efficiently. Since then, human infection of highly pathogenic H5N1 has reoccurred in subsequent years in Southeast Asia (Chen, 2002; Chotpitayasunondh et al, 2005; Ellis et al, 2004; Horimoto and Kawaoka, 2001; Liem and Lim, 2005).

1.5 Pathogenesis and Clinical Features in Human

Influenza A is highly contagious, causing seasonal epidemics. Infection of the respiratory epithelium induces pathologic changes throughout the respiratory tract, usually involving the lower respiratory tract. Typical influenza A infection causes tracheobronchitis. Symptoms include headache, chills, dry cough, fever, myalgia, malaise and anorexia. Interstitial pneumonitis or secondary bacterial pneumonia is the most severe complication and may result in respiratory failure and fatality. Patients with cardiovascular diseases, chronic bronchitis, obstructive pulmonary disease, diabetes or asthma have a higher chance to develop secondary bacterial pneumonia and are associated with high mortality rates. Children are more likely to develop complications such as otitis media, conjunctivitis, and sputum production. Myositis, gastrointestinal complications, and viremia occur with low incidence. Rarely, Reye's syndrome and other neurological complications have been reported after influenza A infection especially in association with aspirin therapy in children (Cox and Subbarao, 1999; Douglas, 1990; Julkunen et al, 2001(a); Ray, 1990).

Pathologically, the larynx and trachea display diffuse inflammation, and the bronchi show mucosal inflammation and edema. There are patchy areas of necrosis on the surface epithelium while leaving large areas of ciliated epithelium intact. In a more severe primary viral pneumonia, interstitial pneumonitis occurs with the alveoli structure destroyed and the infiltration of immune cells (Wright and Webster, 2001). Viral antigen presents predominantly in epithelial cells. The virus replicates to reach peak titres approximately two days after inoculation, and viral shedding disappears around day 6 to 8 (Wright and Webster, 2001).

1.6 Human Immune Response to Influenza A Infection

Upon infection, the innate immune response is stimulated in the local respiratory tract. Virus infects and is released from the apical surface of epithelial cells in the respiratory tract, does not lead to systemic spread. Potent cytokines are induced and display their antiviral response, notably IFN-α. Other protective cytokines that stimulate the immune response include interleukin-6 (IL-6), IL-8, and IL-2, etc (Blau and Compans, 1996; Hayden et al, 1998). The adaptive immune response is important for the eventual clearance of influenza viruses. Both local mucosal and systemic humoral antibodies are induced. In human nasal secretion, HA-specific immunoglobulins (Ig) Ig-A are detected. Ig-A has neutralizing ability and can inhibit viral replication (Mazanec et al, 1992; Mazanec and Huang, 1996). In experimental mouse infection, these antibodies are also detected in bronchial secretions (Renegar and Small, 1991). Serum antibodies are detected in approximately 80% of human infections (Wright and Webster, 2001). The presence of Ig-G, Ig-A, and Ig-M antibodies specific to HA, NA, NP and M proteins following infection has been documented (Potter and Oxford, 1979). However, mainly those

against HA and NA are protective antibodies (Clements et al, 1986; Epstein et al, 1993). In cellular immunity, both the cytotoxic lymphocytes (CTL) restricted by class I histocompatibility antigens with CD8+ phenotype and the T cells restricted by class II histocompatibility antigens with CD4+ phenotype (helper T cell) are involved during infection (Ennis et al, 1981; Kaplan et al, 1984; Lamb et al, 1982 & 1987; Sterkers et al, 1985). Class I-restricted CTLs recognize HA, M, NP, or PB2 proteins. They target cells infected by homologous subtype virus, as well as different subtypes, depending on the specific subpopulation of the CTLs (Fleischer et al, 1985; Yewdell and Hackett, 1989). CD8+ T cells are sufficient to clear influenza A virus in CD4+ deficient animals, however, whether this clearance is carried out by cytolysis or antiviral cytokine secretion mechanism is unknown (Eichelberger et al, 1991). Class II-restricted T cells contribute to immunity by assisting B cells and class I-restricted CTLs (Lamb et al, 1982 & 1987). They also can have a similar cytolytic activity to the class I-restricted CTLs (Yewdell and Hackett, 1989). In CD8+ deficient animals, influenza A virus can be cleared in a CD4+ dependent manner by promoting B cells to make antiviral antibodies (Bender et al, 1992; Caton and Gerhard, 1992; Scherle et al, 1992).

1.6.1 Type I Interferons (IFN)

In 1956, interferons were first identified by their ability to interfere with virus replication (Isaacs and Lindenmann, 1957; Lindenmann, 1982). IFNs are generally grouped into two types: type I IFNs (including IFN-α, IFN-β, and IFN-ω), and type II IFN (IFN-γ) (Biron and Sen, 2001). IFN-α/β are the best characterized members in the family. There are 13 IFN-α genes and one IFN-β gene. The majority of the IFN gene products are simple unmodified polypeptides, however, some are

posttranslationally modified by N- and O-glycosylation (Biron and Sen, 2001). IFN-α/β is around 18 kd in size (Abbas et al, 1997). IFN-α functions as a monomer whereas IFN-β exists as a homodimer (Samuel, 2001). Type I IFNs can be produced by most cell types after being challenged by infectious agents, particularly by viruses, however, IFN-α and IFN-β are produced predominantly by leukocytes and fibroblasts, respectively. The immune response cascade can be divided into three stages based on response kinetics and antigen specific protection: initial, innate, and adaptive response (Biron and Sen, 2001). Type I IFNs are classified as initial/innate cytokines.

1.6.1.1 Anti-Viral Functions of Type I Interferons (IFN)

The signal transduction pathway of IFN-stimulated genes includes several component families: IFN-α/β receptors (IFNAR), the Janus family of tyrosine kinase (JAK), the signal transducer and activator of transcription (STAT) family, and the IFN regulatory factor (IRF) family. IFNAR is expressed on the surface of all nucleated cells, forming a heterodimer containing two subunits, IFNAR1 and IFNAR2. Tyk2 and JAK1 that belong to the JAK family (Levy and Adolfo, 2001; Samuel, 2001) are involved in this pathway. STAT family proteins latently exist in the cytoplasm and require activation through phosphorylation. The IRF family is an important regulatory factor in the IFN induction and the IFN response system. The N-terminal DNA-binding domains of IRF family members are homologous. They associate with the IFN-α/β gene promoter, as well as the IFN stimulated response element (ISRE) of IFN responsive promoters (Nguyen et al, 1997).

On binding IFN-α/β, the intracellular domain of IFNAR1 associates with Tyk2 and that of IFNAR2 associates with JAK1. The JAKs are activated to tyrosine

phosphorylate STAT1 and STAT2. The majority of activated STAT1 and STAT2 heterodimerize, although some of the STAT1 homodimerize. IRF9 (also known as p48 or ISGF-3γ) contains a nuclear localization signal, and is recruited by the STAT1-STAT2 complex to form the multimeric transcription factor ISGF. ISGF rapidly translocates to the nucleus, binds to ISREs on the promoters of IFN-α/β inducible genes and activates their expression (Biron and Sen, 2001; Samuel, 2001).

More than 300 genes are transcriptionally regulated by Type I IFNs. IFN-α/β-inducible proteins include dsRNA-activated protein kinase PKR, 2',5'-oligoadenylate synthetases (OAS) and Rnase L, Mx protein GTPases, RNA-specific adenosine deaminase (ADAR), ISG56 family, and a form of nitric oxide synthase (iNOS2) along with others. Furthermore, IFN-α/β regulates aspects of the immune response, such as major histocompatibility complex expression, and hence modulates antigen presentation; IFN-α/β also guides the maturation of dendritic cells and differentiation of T helper cells (Biron and Sen, 2001; Muller et al, 1994; Samuel, 2001; Sen and Ransohoff, 1993). In this section, only those genes related to influenza A virus infection will be discussed. Although IFN-α/β induces PKR expression, dsRNA is required to activate PKR, causing its autophosphorylation at serine-threonine residues and dimerization. Activated PKR phosphorylates eukaryotic translation initiation factor eIF-2α, resulting in its inactivation, leading to inhibition of the protein synthesis. Thus, the infected cells, as well as the replicating resident viruses, are inhibited or removed (Biron and Sen, 2001; Samuel, 2001). The OAS is also activated by dsRNA to catalyze the synthesis of 2',5'-oligoadenylates, which in turn bind to inactivated monomeric Rnase L, inducing its dimerization and activation.

Activated Rnase L acts as an endoribonuclease to cleave both mRNA and rRNA, also leading to an inhibition of protein synthesis (Biron and Sen, 2001; Samuel, 2001). The Mx protein GTPases that are induced by IFN have been characterized in human as MxA (cytoplasmic) and murine as Mx1 (nuclear). These GTPases are normally involved in endocytosis and vesicle transportation, but they also act to interfere with virus replication through nucleocapsid transport (MxA) or transcriptional activity (Mx1) (Arnheiter et al, 1996; Haller et al, 1998; Staeheli et al, 1993; Weber et al, 2000). (See Figure 5)

1.6.1.2 Type I Interferon Induction

Double stranded RNA (dsRNA), an intermediate product of viral replication, is a potent inducer of IFN-α/β. Other inducers include viral proteins, the whole viral particle, etc. Both nuclear factor-κB (NF-κB) and IRF3, IRF7 are involved in IFN induction. Toll-like receptor 3 (TLR3) recognizes dsRNA that is released from infected cells. Binding of dsRNA to TLR3 initiates a signal transduction pathway that leads to the liberation of NF-κB and activation of IRF3 (Alexopoulou et al, 2001; Marie et al, 1998; Sen and Sarkar, 2005; Weaver et al, 1998). Both the activated NF-κB and IRF3 translocate from cytoplasm to nucleus. In the nucleus they associate with each other and interact with co-activators p300 and the creb-binding protein (CBP), to form a complex that binds to the IFN promoter region to induce IFN-β and early IFN-α subtype (IFN-α4) synthesis (Alexopoulou et al, 2001). These nascent IFNs then act through the IFNAR-JAK-STAT pathway and induce IRF7 expression. IRF7 in turn activates the synthesis of other members of IFN-α. Consequently, a positive feedback induction loop is established for further IFN

Figure 5: IFN-inducible and Influenza related proteins.

Selected IFN-inducible pathways related to influenza A virus infection response. Among the many proteins induced by IFNs are PKR, 2-5(A), and Mx protein. Activated PKR inhibits translation initiation through phosphorylation of protein synthesis initiation factor eIF-2α; it can also cause cellular apoptosis and participate in specific transcriptional signaling pathways. The 2-5(A) synthetase family and RNase L nuclease mediate RNA degradation. The family of Mx protein GTPases target viral nucleocapsids and inhibit RNA synthesis. PKR and 2-5(A) can be activated by either IFN or directly by dsRNA.

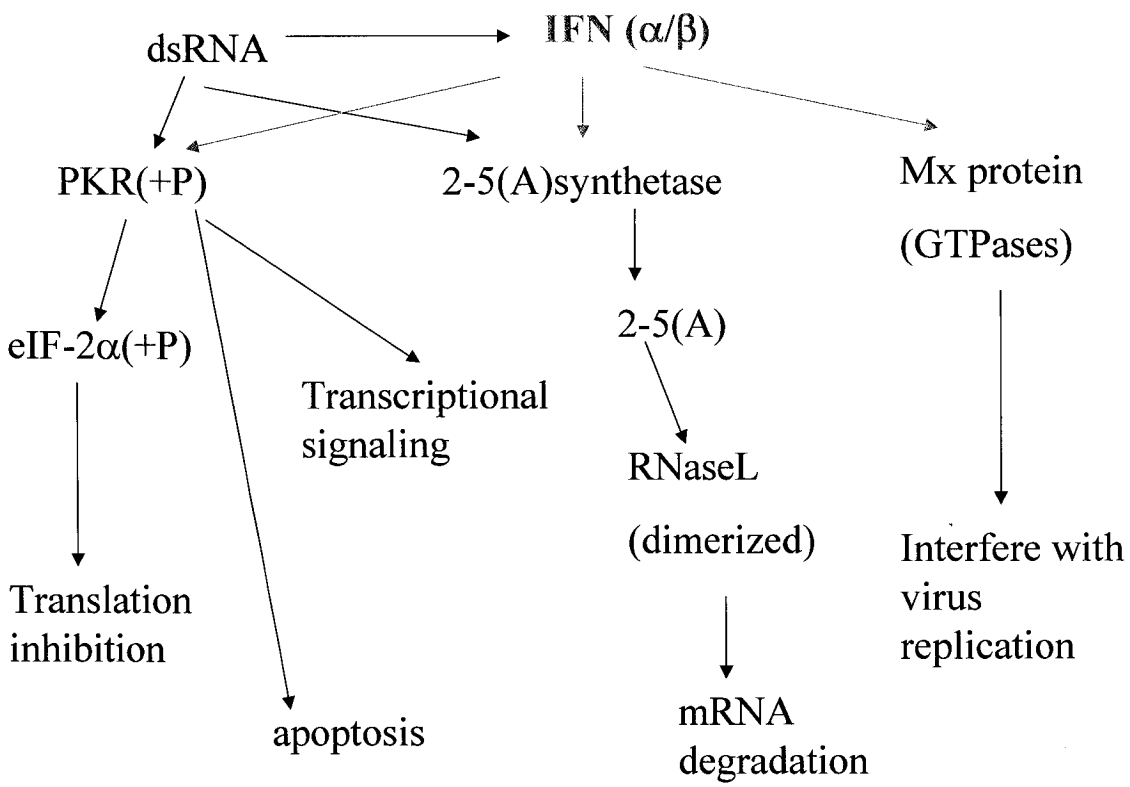
dsRNA
IFN (α/β)
PKR(+P)
2-5(A)synthetase
Mx protein
(GTPases)
eIF-2α(+P)
Transcriptional
signaling
2-5(A)
RNaseL
(dimerized)
Translation
inhibition
apoptosis
mRNA
degradation
Interfere with
virus
replication

induction (Biron and Sen, 2001; Takeda and Akira, 2004 & (b); Marie I., 1998; Smith P.L., 2005). (See Figure 6)

1.7 Prevention and Control

The most effective measure for preventing influenza is vaccination. Inactivated (killed) influenza A vaccines are licensed for parenteral administration in humans (Harper et al, CDC, 2004). Normally the influenza vaccine contains three virus strains (usually two type A strains: H3N2 and H1N1, and one type B strain), representing the influenza viruses that are predicted to circulate in the upcoming influenza season. Chicken embryos are utilized for viral propagation before inactivation of infectivity. Currently, whole-virus (WV), subvirion (SV), and purified-surface-antigen preparations are available (Johansson and Kilbourne, 1998; Lakey et al, 1996; Ogra et al, 1977). The recommended time to be vaccinated is before the peak of the flu season, which typically occurs between December and March. People who are recommended to be vaccinated are seniors, infants, healthcare workers, and patients with chronic diseases (Harper et al, CDC, 2004). When the vaccines are antigenically similar to the circulating viruses, it is effective in preventing illness in approximately 70%-90% of healthy adults (Harper et al, CDC, 2004). Currently, a live vaccine, FluMist, is under investigation in Canada and has been licensed in the USA. It is believed that the attenuated vaccine will provide stronger protection and have the ability to induce local immunity in the respiratory tract (Boyce et al, 2000; Nichol et al, 1999). This vaccine contains virulent wild type HA and NA genes from the current virus strain(s) infecting human, as well as attenuated internal genes donated by a cold-adapted virus (Edwards et al, 1994; Murphy, 1993).

Figure 6: The cascade operating in IFN induction.

(Taken from Smith P.L., 2005)

The two phases of type I IFN induction. IFN-β is induced by IRF3 and NF-κB through TLR3 pathway. IFN-β acts in autocrine manner to induce expression of IFN-α and other ISGs through IFNαR and STAT pathway.

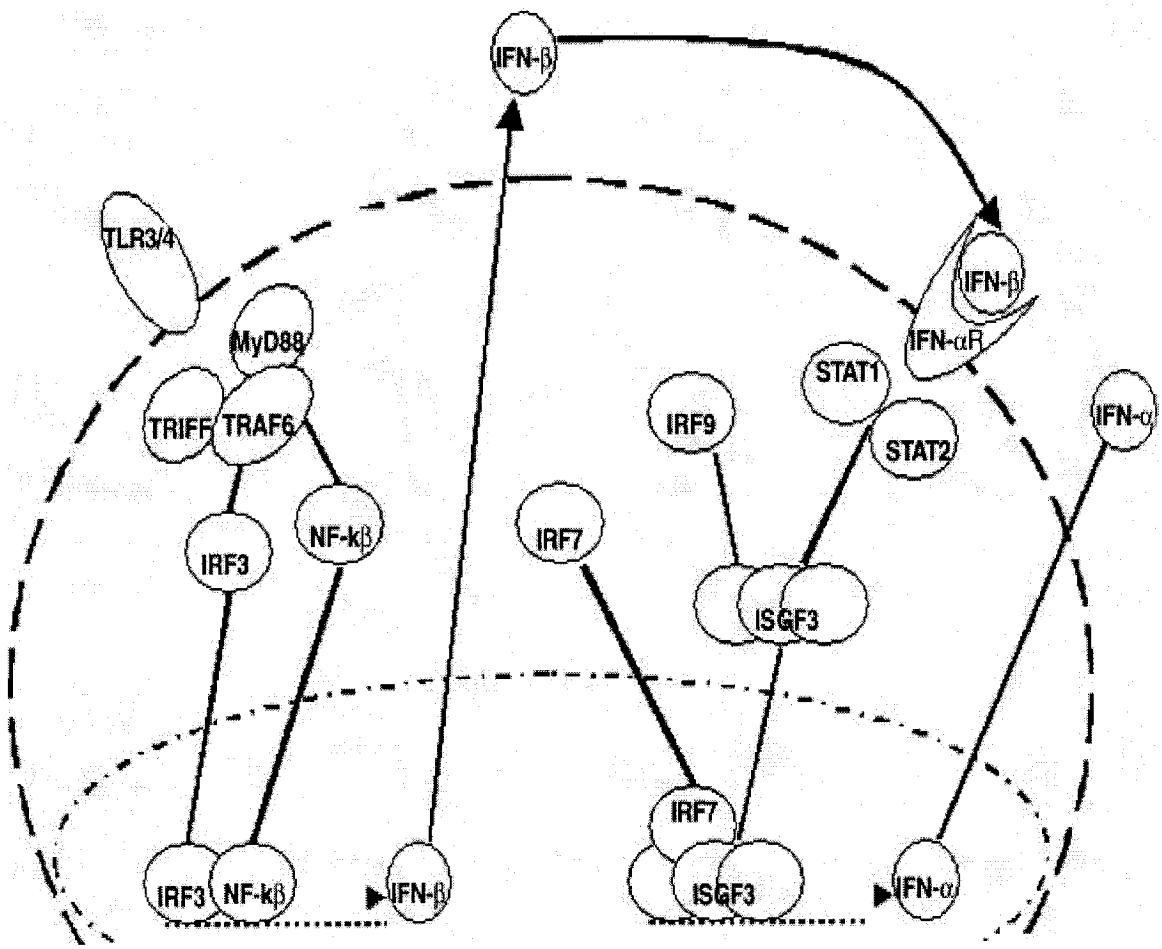
IFN-β
TLR3/4
MyD88
TRIFF
TRAF6
IRF3
NF-kβ
IRF3
NF-kβ
IFN-β
IFN-β
IFN-αR
STAT1
STAT2
IFN-α
IRF9
IRF7
ISGF3
IRF7
ISGF3
IFN-α

Antiviral drugs are important supplements to vaccination. In the United States, four antiviral agents are licensed for preventing or treating influenza: amantadine, rimantadine, zanamivir, and oseltamivir. One class of drugs represented by amantadine and its analogue, rimantadine, possess a tricyclic structure with an amine side group. These drugs block the proton ion flow through the M2 channel after viruses are internalized in the endosome, preventing the acidification of the viral internal, hence the uncoating process is inhibited (Hay, 1992). Amantadine treatment of A/chicken/Germany/34 (H7N1) infected cells resulted in the trapping of the nascent HA protein inside the trans-Golgi network (TGN) leading to their fusion to each other in a low pH environment, implying that the M2 ion channel is also important for maintaining HA function for some variant viruses (Hay, 1992; Lamb et al, 1994; Sakaguchi et al, 1996; Sugrue et al, 1990; Takeuchi and Lamb, 1994). Zanamivir and oseltamivir are neuraminidase inhibitors (NAI). They are analogues of sialic acid and bind tightly to block the active site of neuraminidase. The uncleaved sialic acid molecules that result from NAI treatment bind the HA protein, leading to the aggregation of the progeny viruses on the host cell surface (Palese and Compans, 1976; von Itzstein et al, 1996; Wang et al, 2002), thus preventing viral release and spread.

1.8 Convergent Evolution in RNA Viruses

Evolution operates through the process of adaptation where genome modifications of biological descendents are selected under novel environmental conditions. The mechanisms of RNA virus genetic diversity include mutation, recombination, and genome segment reassortment. RNA viruses have extremely high rates of spontaneous mutation, in the range of 10^{-3} to 10^{-5} misincorporation per

nucleotide (nt) and per round of copying, this results in approximately one mutation per genome (Drake and Holland, 1999; Malet et al, 2003). The high mutation rate results from the lack of proofreading-repair activities associated with RNA replicases and transcriptases (Domingo and Holland, 1997). Recombination is a process of exchange of genetic material usually through breakage and reunion, producing a descendent nucleic acid containing a combination of genetic information from two parental genomes. Influenza virus can recombine genome segments but this occurs at a very low frequency and is not observed to occur often in nature. Reassortment, the exchange of complete genome segments, occurs in segmented RNA viruses. As a consequence of having a segmented genome, influenza A virus can exchange genome segments with high frequency through reassortment. Progeny virus obtained from co-infected cells can possess different combinations of genome segments from both parent viruses. Since influenza A virus has eight genome segments, mathematically, two co-infecting influenza A viruses may give rise to 2^8 potential progeny genotypes (Cann, 2001).

Convergent evolution is defined as repeated and independent occurrence of common mutations in adapted variants. It includes two instances: parallel evolution, on the occurrence of identical mutations; and directional evolution, where mutations are selected at the same sites but with different amino acid. Convergent evolution is a strong evidence of adaptive mutations that are controlling biological processes. Exposure to new selection pressures drives the process of adaptation, leading the selection of viruses with increased replicative fitness for improved survival. Theoretically, under the same selection pressure, parallel adaptive evolution experiments will result in convergent phenotypes and genotypes which bear the

mutant forms of beneficial genes. The individuals suited most will have the best replication rate in the host, which normally is associated with increased virulence; but attenuation could not be ruled out.

1.9 Virulence Factors of Influenza A Virus

Virulent influenza A viruses cause severe disease or even fatality in human and other hosts. With the exception of the extreme virulent virus 1918 H1N1 strain, human influenza appears to have a constant level of virulence for humans. It is therefore not possible to obtain virulent forms of human influenza for analysis. Highly virulent forms of avian influenza are often associated with poultry farming and are the result of continuous high dosages transmission of influenza into susceptible birds. Experimental adaptation of influenza A virus has been done for many animals with most of the published genetic analysis being done on mice. Serial high dose intranasal transmission of human influenza A virus in mice results in selection of virulent variants that possess mutations that increase replication in mouse lung and result in increased virulence. The experimental basis for virulence has been assessed by reassortment analysis of both highly virulent mouse-adapted variants as well as natural isolates of pathogenic avian influenza virus. Groups of genes have been reported to control the property of virulence. Mouse-adapted variants of A/FM/1/47 possessed single amino acid changes in each of the five proteins: PB2, PB1, HA, NA, and M2, that each increased growth and virulence for the mouse lung. The accumulated evidence demonstrates that all the eight genome segments promote virulence among mouse-adapted influenza A virus variants (Brown and Bailly, 1999). As influenza viruses are host restricted, genetic analysis of virulence will demonstrate genetic features of host specificity as well as virulence.

It is expected that for mouse-adapted strains of human influenza, specific functional regions will be identified and the derived amino acid substitutions may confer a mouse specific function, but substitutions providing human specificity could not be ruled out. In studies of influenza virulence, it is important to know the genetic roles that are controlled by each viral gene in pathogenesis. The polymerase complex proteins of the 1918 influenza virus has minor differences from the avian influenza A virus strain consensus sequence and this was believed to contribute to the high virulence of this virus (Taubenberger et al, 2005). PB2 was believed to be one of the important determinants for an avian influenza virus to cross the host species barrier and infect mice (Li et al, 2005). It has been reported that a mutation of E627K on PB2 converted a nonlethal H5N1 influenza virus to a lethal virus in mice (Shinya et al, 2004). Mutations in HA change host range, cleavability and receptor specificity (Couciero et al, 1993; Horimoto and Kawaoka, 1997; Ito and Kawaoka, 2000), and has been associated with replication (Asaoka et al, 2005) and virulence in hosts (Ward and Koning-Ward, 1995(a)). NP is possibly involved in attenuation of the cold adapted virus (Herlocher et al, 1993). Neuraminidase is involved in neurovirulence (Li et al, 1993) and replication in mice (Goto et al, 2001; Ward, 1995 & 1996). The M1 protein is associated with increased replication in mouse lung and cultured cells (Smeenk et al, 1996). M1 protein was also found important in naturally occurring temperature-sensitive (ts) strain of influenza A viruses (Chu et al, 1982). NS1 protein's IFN antagonism function and its contribution to virulence are going to be discussed in the text below. It is also reported that the NS gene was a secondary determinant of neurovirulence (Ward, 1995). In summary, previous documentations demonstrated that virulence determinants of influenza A virus were multigenically

determined. Exceptional virulence has been exemplified by the 1918 pandemic influenza virus and the H5N1 avian influenza virus. This investigation mainly focuses on the role of NS1 protein in virulence.

1.9.1 Roles of NS1 Protein Contributing to Virulence and its IFN Antagonism

The non-structural protein, NS1, is synthesized in large amounts throughout infection and has several functions including counteracting the effects of interferon. Type I IFNs are an essential component of the innate immune response to virus infection (See "Anti-viral Functions of Type I IFN"). Mice defective in STAT1, a component of IFN-dependent signaling pathway, have increased susceptibility to viral infection (Durbin et al, 1996). Influenza virus normally replicates restrictedly in murine lungs, but develops a fulminant systemic infection in STAT1-/- mice (Garcia-Sastre et al, 1998(a)). Thus IFN antagonism is beneficial for viral survival and replication. Influenza A virus NS1 protein has been identified as an IFN antagonist (Garcia-Sastre, 2001). Synthetic influenza A virus lacking the NS1 gene is only able to replicate in Vero cells (no IFN expression) and STAT-1(-/-) mice (lack of IFN signaling) (Garcia-Sastre et al, 1998). Strong IFN antagonism has also been reported to be associated with the virulent H5N1 z genotype strain, which is a loosely defined category based on the constellation of the eight influenza genes including genotypes A, B, C, D, E, V, W, X, Y, Z and Z+ (Guan et al, 2002; Kou et al, 2005; Li et al, 2004). There is a point mutation of D92E on NS1 protein of the highly pathogenic avian influenza (HPAI) virus H5N1 as well as human isolates, A/HK/156/97 strain. This mutant NS1 protein confers increased resistance to interferon inhibition in vitro and prolonged viral replication in swine (Seo et al, 2002 & 2004).

Although the specific mechanism for IFN antagonism by NS1 protein remains uncertain, there are several functions of NS1 protein that could account on contribution to this property. First, the NS1 protein inhibits maturation of cellular mRNA and its nuclear-cytoplasmic transport, utilizes cellular translation machinery for viral protein expression (De La Luna et al, 1995; Fortes et al, 1994; Lu et al, 1994; Lu et al, 1995). Hence it shuts off the host protein synthesis, including the IFN synthesis and its stimulated antiviral gene expression. Second, the NS1 protein has two methods of inhibiting the double-stranded RNA-activated protein kinase (PKR). Binding to dsRNA prevents activation of PKR, and direct binding to PKR may also inhibit PKR activation (Bergmann et al, 2000; Hatada et al, 1999; Lu et al, 1995; Tan and Katze, 1998). PKR is a key effector of the IFN-antiviral response and therefore inhibition of PKR is inhibition of an important part of IFN antiviral response. Third, NS1 protein inhibits the activation of nuclear factor-kappaB (NF-κB) (Wang et al, 2000), interferon regulatory factor 3 (IRF3) (Talon et al, 2000), and IRF7 (Smith et al, 2001), hence suppressing IFN production. And lastly, NS1 protein has been found to be a suppressor of RNA silencing which may be important in blocking an antiviral response (Bucher et al, 2004; Delgadillo et al, 2004; Li et al, 2004(a)). Although IFN antagonism functions include inhibition of IFN induction and resistance to the IFN-mediated antiviral response, and reduced IFN during infection is generally associated with increased virulence, the HPAI H5N1 viruses induces very high levels of IFN. (See "role of NS1 protein contributed to viral replication")

1.10 Background for this project

Infection of mice with human influenza A viruses results in viral replication in murine lungs without disease. Variants that have been selected through serial lung

passages acquire the ability to produce interstitial pneumonia and cause fatality in mice (Raut et al, 1975; Wyde and Cate, 1978). The mouse model of influenza is a practical tool for the study of influenza virus pathogenesis (Kilbourne, 1997; Ward, 1997) since pneumonia in the mouse and pneumonia in the human are pathologically similar (Sweet and Smith, 1980). On adaptation of human virus strains to the mouse lung under conditions of high viral dosage, competition exists among all possible single amino acid mutations, and results in the selection of the most optimal genotypes. Convergent evolution appears to be a common feature of viral evolution, where the same functions are repeatedly selected. Virulence or pathogenicity is the ability of a microorganism to cause damage and disease in the host (Mims, 1987). Viral replication can be a virulence factor if increased replication results in increased pathology and higher morbidity and mortality. Analysis of a virulent mouse-adapted variant FM-MA derived from the avirulent FM strain had previously demonstrated that adaptation to increased virulence is multigenically determined (Bailly and Brown, 1998; Brown, 1990 & 1999; Smeenk and Brown, 1993; Smeenk et al, 1996; Zoueva et al, 2002).

In the present study, virulent mouse-adapted variants were generated from the prototype H3N2 isolate A/HK/1/68, which does not have a history of mouse passage. Again, analysis of the virulent strains demonstrated that virulence is a multifactorial process and a combination of factors is required in order to explain the elevated virulence where eight to eleven mutations were selected in mouse adapted variants after 20 mouse-lung passages (Brown et al, 2001). The key to understanding influenza virus pathogenesis is to clarify the role(s) played by each viral gene in each stage of pathogenesis. Furthermore, assessment of the

contribution to virulence from each gene's specific mutations needs to be performed in isogenic backgrounds. This project is focused on the role of NS1 gene variation in increased virulence during adaptation. Recombinant influenza A viruses were generated as that their genome consist mouse-adapted NS genes (with mutation(s) only on NS1 protein coding region but not in NS2 protein coding region) with seven other genes as wild type HK strain, in order to perform a genetic analysis to measure and characterize properties of the specific NS1 mutation(s) in virulence.

Mouse adaptation experiments were done prior the start of this project. There were two independent mouse adaptation experiments of prototype H3N2 isolate, A/HK/1/68 which is totally avirulent for mice (median mouse lethal dose (mLD_{50}) >> $10^{7.7}$). In the first experiment, A/HK/1/68 was passaged 20 times in mouse lung. Six clonal isolates were obtained from the passage 20th population by two cycles of plaque purification. The plaque-purified clones were designated as HK-MA20(clone#). All progeny clones had decreased mLD_{50}. One clone, HK-MA20c decreased more than $10^{5.1}$ fold in mLD_{50}. Genomic sequence analysis of HK-MA20c discovered eleven amino acid substitutions involving eight of the ten viral proteins. Mutant hemagglutinin protein has already been shown to change in biology and contribution to the increased virulence (Brown et al, 2001; and unpublished data). A separate mouse adaptation experiment was also conducted to assess convergent evolution. In this second experiment, ten sister clones were plaque purified from A/HK/1/68, the same stock utilized in the first experiment. Then the isolates were passaged 21 times in mouse lung. Three clones were plaque purified from each of the ten independent mouse-adapted passage 21st populations. The plaque-purified clones were designated as HK(sister clone #)-MA(mouse passage #)(clone#).

Sequence analysis of the NS1 gene of the HK-MA20 series and some clones HK-MA21 series discovered five mutations at four sites (See Table 2). However, MA variants 21 series had not been tested for their LD_{50} in mice.

Mutations were repeatedly and independently selected in specific regions: aa23, aa98, aa103, and aa106. This phenomenon strongly suggested that mutations on these areas in NS1 protein might be involved in enhanced viral replication and virulence (since HKMA20 series had higher mLD_{50} than their parent virus HK). Convergent mutations occur at position 106 and the cluster of mutations from 98 to 106 identifies a convergently affected region. The goal of this project is to map and characterize the molecular basis of NS1 protein contributing to increased virulence with respect to IFN antagonism.

1.11 Hypothesis

Identification of mutations acquired during adaptation to a new host may give clue to the molecular basis for the IFN antagonist function of NS1 protein.

1.12 Objectives

(A) Characterization the anti-IFN responses of mouse adaptive variants.

First of all, a study of pathology and tissue tropism of HK parent virus and HKMA20c progeny was carried out. HKMA20c was chosen to be investigated for its high pathology developed in mouse lung because it is the most virulent strain among the MA variants 20 series that had been tested for their LD_{50} in mice. Groups of mice were infected by either of these two viruses. Lung sections were Hematoxylin-Eosin stained or labeled with fluorescent antibodies (anti-HK). Inflammatory response as well as the extent and location of viral infection were assessed.

Table 2: Location of mutations in the NS1 protein of independent series of mouse-adapted variants of A/HK/1/68. A map is supplemented for showing.

-, indicates wild type sequence. The locations of mutations are indicated on the map.

Viruse	Amino Acid Position			
	23	98	103	106
HK	V	L	F	M
HKMA20	A	-	-	-
HKMA20a	A	-	-	-
HKMA20b	-	-	L	-
HKMA20c	-	-	L	-
HKMA20d	-	-	L	-
HKMA20e	-	-	-	-
HK4MA21-1	-	-	-	V
HK5MA21-1	-	-	-	I
HK5MA21-2	-	S	-	I
HK5MA21-3	-	S	-	I
HK6MA21-1	-	-	-	-
HK6MA21-3	-	-	-	-
HK8MA21-1	-	-	-	-
HK9MA21-3	-	-	-	-
HK10MA21-1	-	-	-	-
HK10MA21-3	-	-	-	-
HK12MA21-1	-	-	-	-

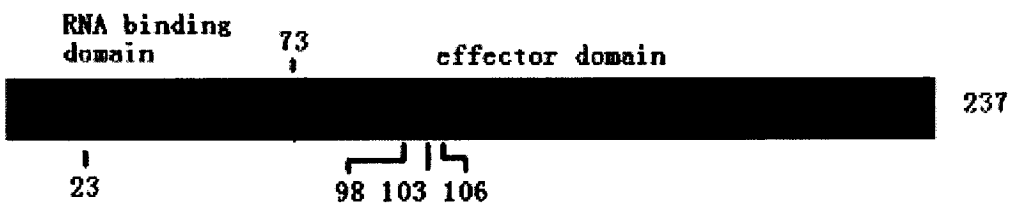

Then IFN resistance and induction were assessed for mouse-adapted variants. In IFN resistance assay, human cells and mouse cells were infected by HK parent virus and five mouse-adapted variants, viral yields were compared between infection, with and without IFN protecting the cells. For IFN induction assays, supernatants from viral infection were tested for their ability to protect cells from vesicular stomatitis virus (VSV) infection, hence indicating the level of IFN production during viral infection.

(B) Production of synthetic recombinant influenza A virus possessing defined NS1 mutations obtained from virulent MA variants.

Second step of this project was to generate an influenza A virus rescuing system leading to generation of recombinant viruses with mouse-adapted NS1 genes inserted in HK wild type backbone genome. This system employs eight RNA expression plasmids containing cDNAs of each individual gene segment, plus four protein expression plasmids producing the polymerase complex and nucleocapsid protein.

(C) Characterization the IFN antagonism functions of mutant NS1 proteins in isogenic genome backgrounds.

Lastly, it was to test and to compare the IFN induction and resistance property of mouse-adapted mutant NS1 proteins in the synthetic influenza A viruses with identical genome background.

MATERIALS AND METHODS

For the components and method of preparation of all solutions and reagents, see Appendix I.

2.1 Cells and Viruses

Madin-Darby canine kidney epithelial cells (MDCK), 293T cells (human embryonic kidney epithelial cell line expressing the temperature-sensitive simian virus 40 T antigen), A549 cells (human lung epithelium, lung carcinoma), MRC5 cells (normal human lung fibroblast), M1 cells (kidney collecting duct epithelium from transgenic mouse containing SV40 early region), mouse embryo fibroblast cells (MEF, BALB/c inbred Mice), Hela cells (human cervix epithelial adenocarcinoma), and L929 cells (mouse connective tissue cells) were grown and maintained at 3.5% CO_2, in minimal essential medium (MEM) supplemented with 8% fetal bovine serum (FBS), 100 u/ml penicillin /100 µg/ml streptomycin (P/S), 2 mM L-glutamine and 0.22% $NaHCO_3$.

The viruses used in this study were the prototype human H3N2 isolate, A/HK/1/68 (HK) and various A/HK/1/68–mouse adapted (HK-MA) variants. Before mouse adaptation experiments, parent HK virus was plaque purified on MDCK cells. A mouse adaptation experiment was carried out by performing 20 passages in mouse lung, resulted in the HKMA20 series of variants. A dose of 1 X 10^6 pfu per mouse of the prototype human isolate, HK, was used to infect a group of 3 mice for 3 days. Serial passage in mouse lung was achieved by subsequent serial cycles of intranasal infection with 50 µl of 1/10 diluted lung extracts under halothane anesthesia. Virus extracts of infected lungs were prepared by sonication of lungs suspended in PBS (1 ml/lung). The sonicated lung extracts were clarified by low

speed centrifugation before dilution (1/10 in PBS) and filter sterilization (0.2 μm filter). Other independent mouse adaptation experiments were employed using the same dosage of virus. Ten sister clones of A/HK/1/68 were derived by plaque isolation on MDCK cells. Each clone was serially passaged in mouse lung starting with10 passages in 1 mouse for 1 day, then 5 passages in 2 mice for 2 days, and finally 6 passages in 2 mice for 3 days. For each of the 10 independent mouse-adapted passage 21st populations, 3 clones were isolated. Both the HK and HK-MA viruses were clonally purified in MDCK cell monolayer by 2 serial plaque-to-plaque isolation, followed by stock preparation in the allantoic cavity of 10-day-old chicken embryos. (See Figure 7) The plaque purified clones were designated as HK (sister clone #) MA (mouse passage #) - (clone #). There are 6 variants used in this study: HKMA20, HKMA20c, HK4MA21-1, HK5MA21-1, HK5MA21-2, and HK5MA21-3 (See Table 2). All the mouse adaptation experiments were done before this project was started.

Vesicular stomatitis virus (VSV) used in this project is Indiana strain which was kindly provided by Dr. Yong Kang, University of Western Ontario. VSV was grown on L929 cells at MOI of 0.1, the supernatant was harvested and these virus samples were titrated on L929 cells.

2.2 Virus Amplification

2.2.1 Virus Amplification in Chicken Embryo

Eggs were incubated for 9-10 days at 39.75°C and then candled to locate the site of inoculation adjacent to the embryo. A 100 μl volume of virus sample was injected into the allantoic cavity of 10-day-old chicken embryos, followed by incubation at

Figure 7: Mouse Adaptation Approach for HKMA20 Series and HKMA21 Series

CD-1 strain mice were utilized for the experiments. They are infected intranasally.

HKMA20(#) series

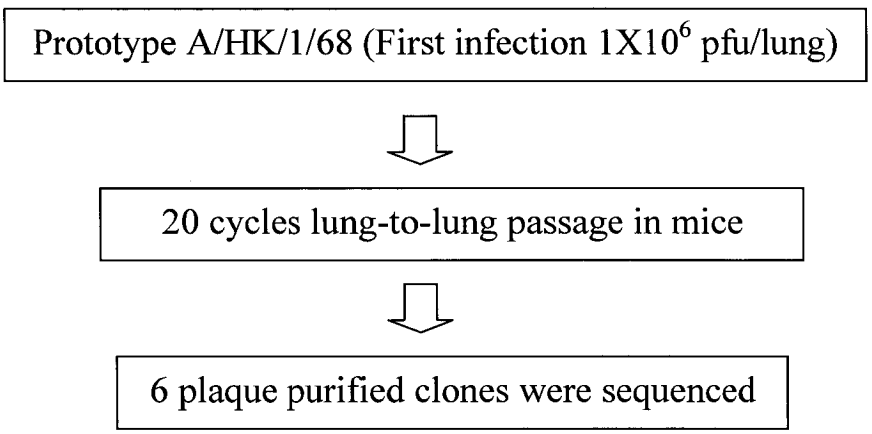

* HKMA20 series have been adapted for 180 mouse days: 3 mice X 3 days X 20 lung-passages.

HK(#)MA21-(#) series

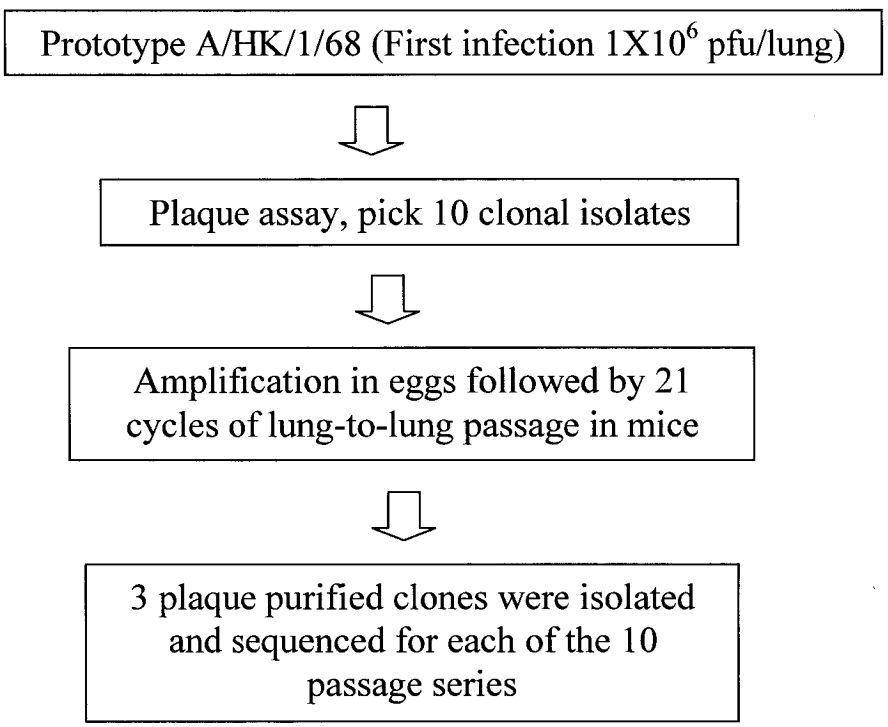

* HKMA21 series have been adapted for 66 mouse days: (1 mouse X 1 day X 10 lung-passages) + (2 mice X 2 days X 5 lung-passages) + (2 mice X 3 days X 6 lung-passages)

34°C for 3 days. Following incubation, eggs were chilled at 4°C for 24 h to prevent bleeding. The allantoic fluid was then collected, followed by centrifugation at 1500 rpm for 15 min at 4°C (IEC DPR-6000 centrifuge, Fisher Scientific Ltd.) to sediment the debris and red blood cells (RBCs). The clarified virus-contained allantoic fluid was stored at -80°C. The amplified virus was designated as E(passage #).

2.2.2 Virus Amplification in MDCK Cells

Confluent monolayers of MDCK cells in each well of a 6-well dish were inoculated with a 100 µl volume of virus sample. After adsorption for 30 min in the CO_2 incubator with rocking the dish every 15 min, serum free 1X MEM supplemented with antibiotics (P/S), glutamine and 1 µg/ml trypsin (crystallized trypsin, Sigma) was incubated with the cells in a CO_2 incubator until more than three quarters of the cells were dead. After collection of the culture medium, the cell debris was spun down by 1500 rpm for 5 min. Then the supernatant was collected and stored at -80°. The amplified virus was designated as P(passage #).

2.3 Quantitation of Virus

2.3.1 Plaque Assay

Confluent monolayer cultures of MDCK cells were used for plaque assay. Cells were grown in 6-well dishes. Viral titre was represented as plaque forming units per ml (pfu/ml). Virus was serially diluted in cold phosphate buffered saline (PBS). The cell monolayer was washed twice with 37°C PBS then inoculated with 0.1 ml of serially diluted virus in duplicate for each dilution. After ½ h adsorption of virus at 37°C, 3 ml of warm overlay (~40°C) containing 1 X MEM supplemented with 0.6 g/ml agarose, 100 µg/ml streptomycin, 100 U/ml penicillin, 2.2 mg/ml sodium bicarbonate, 2 mM L-glutamine and 1 µg/ml trypsin was added to each well, and

allowed to solidify at room temperature. The plates were then incubated at 37°C for approximately 3 days. At this time, the plaques were fixed with Carnoy's fixative for 45 min, the overlay then was flushed off in a stream of tap water and the plates were allowed to dry for counting.

2.3.2 Hemagglutination Assay (HA Assay)

HA assays were done in 96-well round bottom microtiter plates. After loading 100 µl of virus samples with desired concentration in the first row, serial 2-fold dilutions were carried out in cold PBS using a semi-automatic 50 µl minidiluter (Cooke Engineering Co.). Then 50 µl of washed chicken erythrocytes at a concentration of 0.5% (v/v) were added to each well, followed by shaking for 1 min and incubation at room temperature for at least 45 min. Virus titers were determined according to the titration of end-point dilution that gave agglutination (representing 1 HA unit per 50 µl).

2.4 Isolation and Purification of Virus by Polyethylene Glycol Precipitation

Polyethylene glycol 8000 (PEG 8000) was added to 1.5 ml of virus samples to yield an 8% w/v solution. The solution was mixed to allow complete dissolution of PEG 8000, followed by shaking at 4°C for 1 h. The solution was then centrifuged at 7000 rpm for 20 min at 4°C (Beckman Avanti Centrifuge). Pellets were drained and resuspended in 0.2 ml STE, for storage at -80°C.

2.5 RNA Extraction

Virus samples were suspended in STE buffer with the subsequent addition of 1/20 volume of vanadyl ribonucleoside complex (V-NSD), 1/400 volume of protease K and 1/20 volume of 20% sodium dodecyle sulfate (SDS). The mixture was then incubated at 37°C for 30 min. This was followed by two cycles of phenol : chloroform

(1:1) extraction, with a 10 min centrifugation at 2000 rpm after each extraction. Phenol was removed and the RNA was collected as the aqueous phase. Overnight precipitation was carried out at -20°C after addition of 1/10 volume of 3 M sodium acetate and 2.5 volume of ethanol. The precipitate was harvested by centrifugation at 8000 rpm for 20 min, then resuspended in a mixture of 2% diethyl pyrocarbonate (DEPC) treated water and ethanol at a 1:3 volume ratio, then stored at -80°C.

2.6 Reverse Transcription Polymerase Chain Reaction (RT-PCR)

From the stored RNA sample (as described for RNA extraction), 200 µl was pelleted at 13000 rpm for 15 min at 4°C. To make cDNA, the RNA pellet was dried and then dissolved in a 40 µl DEPC H_2O with 1X First-Strand buffer (Invitrogen), 100 ng of each primer, 10 mM dithiothreitol (DTT), 1 mM each DNTP, 40 units RNAguard Recombinant Ribonuclease Inhibitor (Invitrogen), and 400 units Murine Leukemia reverse transcriptase (Invitrogen). The reaction was performed using an automatic thermal cycler (PROGENE Techne, Mandel) according to the following reaction temperatures: 21°C for 10 min, 33°C for 10 min, 37°C for 10 min and 42°C for 1 h. The cDNA were stored at -20°C. For the PCR reaction, 4 µl of the cDNA mixture, 100 ng of each primers, 0.25 mM of each dNTP, 1.5 mM $MgCl_2$, PCR buffer and 5 units Taq DNA polymerase (Invitrogen) in 100 µl final reaction volume. The reaction was performed according to the following reaction temperature: 1 cycle of 94°C for 4 min; 3 cycles of 94°C for 30 sec, 31°C for 30 sec, 72°C for 2 min; 30 cycles of 94°C for 1 min, 47°C for 30 sec, 72°C for 2 min; and 1 cycle of 72°C for 10 min. The PCR product was purified using QIAquick PCR Purification Kit (Qiagen), before sending a commercial sequencing service (Core DNA Sequencing and Synthesis Facility, University of Ottawa).

2.7 Glycogen Precipitation of DNA

To the DNA sample, 1 volume of water saturated phenol / chloroform / isoamyl alcohol (25:24:1) was added and mixed, followed by centrifugation at 13000 rpm for 2 min at 4°C. The aqueous phase was collected, 1/10 volume of 3 M sodium acetate (PH: 5), 1/10 volume of 1 µg/µl Glycogen and 2.5 volume of ethanol were added, followed by incubation on ice for 5 min and centrifugation at 13000 rpm for 15 min at 4°C. After rinsing with 70% ethanol, the DNA pellet was dried and dissolved in the desired volume of double distilled water and stored at -20°C.

2.8 Gel Extraction of DNA

DNA samples were purified by electrophoresis on agarose gels containing TBE buffer. After 0.8% agarose gel electrophoresis, the band containing the desired DNA was excised with a clean blade under ultra-violet light (hand-held BLAK-RAY long wave ultraviolet lamp 21). Gel extraction was performed using the QIAquick Gel Extraction Kit (Qiagen), according to the manufacturer's protocol.

2.9 Ligation Independent Cloning and Transformation

One vector for this study was pHH21 which contained the human RNA polymerase I promoter and the mouse RNA polymerase I terminator, separated by a KpnI site (See Figure 8). To clone the 8 influenza A virus cDNAs by ligation independent cloning, the pHH21 vector was modified so that the KpnI site was replaced by a StuI site. Another modification was insertion of the 5' and 3' end sequences of the influenza gene segments onto the two ends of the pHH21 vector sequence next to the StuI site (See Table 3). The linearizing reaction of the modified circular vector contains 75 µl of the vector DNA from midi-preparation, 50 units StuI enzyme, 1X reaction buffer in a 100 µl reaction, incubated at 37°C for 3 h ~

Figure 8: The pHH21 Vector (2857 bps) for Expression of Viral RNA via the RNA Polymerase I Promoter.

The vector contains the human RNA polymerase I promoter (P_{Ih}) and the mouse RNA polymerase I terminator (T_{Im}), with a KpnI restriction site situated in between them.

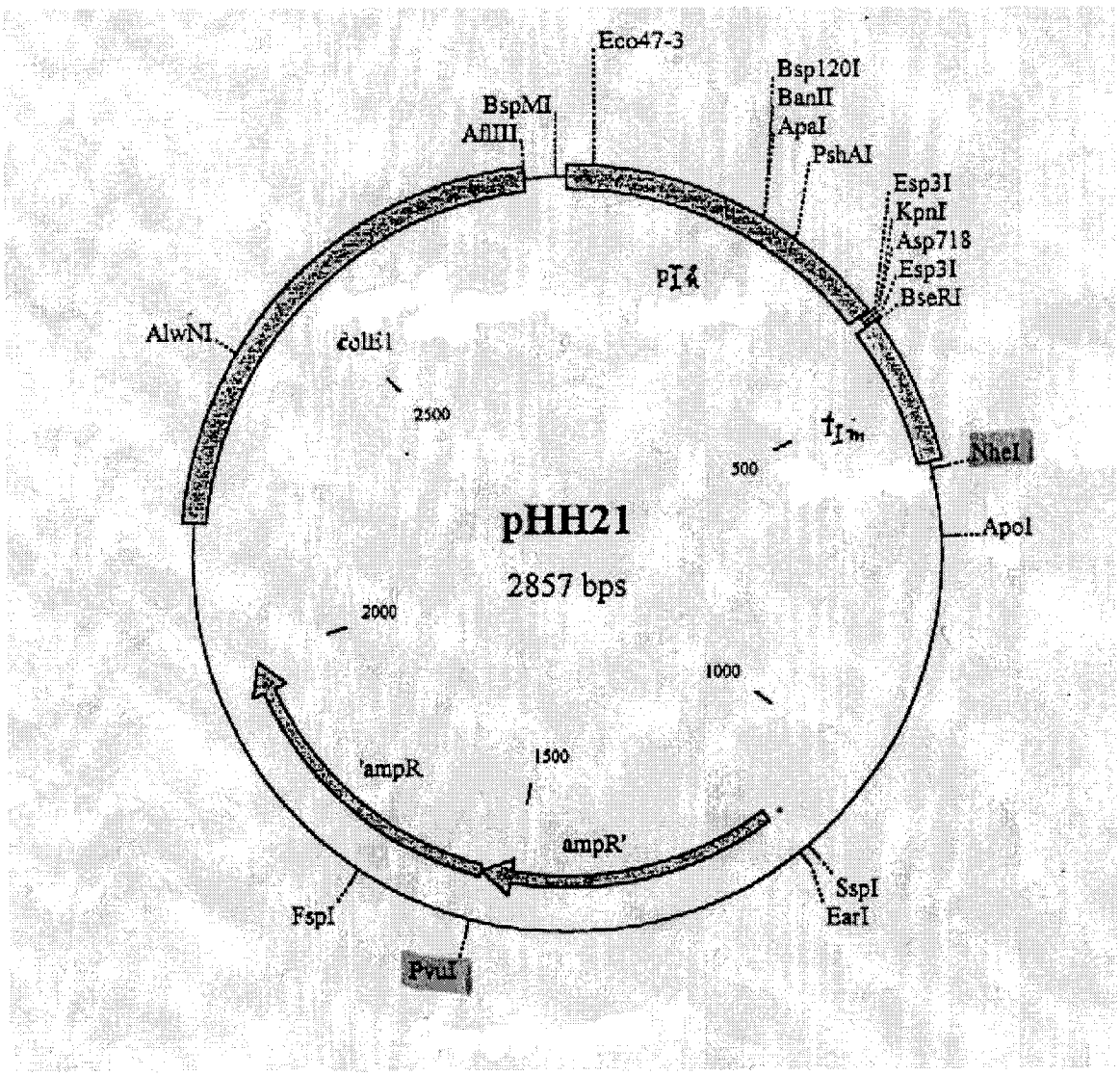
Eco47-3
Bsp120I
BanII
ApaI
PshAI
BspMI
AflIII
Esp3I
KpnI
Asp718
Esp3I
BseRI
AlwNI
ColE1
2500
500
NheI
ApoI
pHH21
2857 bps
2000
1000
1500
'ampR
ampR'
SspI
EarI
FspI
PvuI

overnight. Gel extraction was performed as described before to get the pure StuI cut vector, linear form.

Table 3: Sequence on the two ends of the pHH21 vector next to StuI Site and their corresponding flu gene segments

pHH21 vector	Sequence	corresponding flu gene segments
pHH21(A) 5' end	CCTGCTTTTGCT	HA NS M1 NP
pHH21(G) 5' end	CCTGCTTTCGCT	PB2 PB1 PA NA
3' end	CCTTGTTTCTACT	PB2 PB1 PA HA NP NA M NS

* pHH21 was modified to contain 12 nt sequence complementary to the 5' and 3' ends of the influenza genes. The single nucleotide difference between two 5' end sequences is indicated by underline, and the corresponding influenza gene segments that inserted in that sequence are shown.

To perform the ligation independent cloning and transformation, approximately 500 ng of the desired influenza gene segment and 100 ng of the corresponding pHH21 vector were incubated with 100 µl MAX Efficiency DH5α Competent Cells (Invitrogen) for 30 min on ice. After the cells were heat-shocked for exactly 45 sec at 42°C, they were immediately chilled on ice for 2min. Then 0.9 ml room temperature S.O.C. medium was added to the reaction followed by shaking at 225 rpm at 37°C for 1 h. Finally, the cells were plated on pre-warmed L-B plates containing 100 µg/ml ampicillin and incubated at 37°C overnight.

2.10 Cracking Gel (Clone screening)

This process is to screen large numbers of colonies for colonies that contain desired cDNA sequence. A large amount of cells from each colony were picked and

suspended with 7 µl suspension solution, following by mixing with 10 µl lysis solution and 0.5 µl 6X loading buffer as quickly as possible and immediately loaded into wells of agarose gel, followed by 10 min incubation at room temperature, then TBE buffer was added and the gel run. By comparing with the band of the positive control sample, the colonies with the desired cloned DNA inserts were discovered.

2.11 Purification of plasmid

2.11.1 Small-Scale preparation (Miniprep)

Colonies were picked from L-B plates, for overnight shaking culture in 2.5 ml L-B medium with 200 µg/ml ampicillin. The culture was centrifuged at 14000 rpm for 1 min at 4°C. Miniprep was performed using the OIAquick PCR purification kit (Qigen), according to the manufacturer's protocol.

2.11.2 Medium-Scale preparation (Midiprep)

One ml from a fresh bacterial culture was put into 50 ml L-B medium with 200 µg/ml penicillin, shaken for 4 ~ 5 h at 37°C. A midiprep was performed using the Wizard Plus Midiprep DNA Purification System (Promega), according to the manufacturer's protocol.

2.12 Restriction Digestion

2.12.1 Double Digestion

In order to remove PCR-generated mutations on PB1 gene on plasmid, a double digestion was performed. A fragment of DNA containing the mutations was cut off and replaced by a fragment of mutation-free homologue DNA. In a 40 µl reaction, 5 µg DNA, 10 units of Bsp119I and 10 units of BglII, 2X tango buffer were incubated together in double distilled water at 37°C for overnight. Gel electrophoresis was performed to separate the DNA fragments and isolate the fragment of interest.

2.12.2 Partial Digestion

In order to clean PCR-generated mutations on PB2 gene on plasmid, a partial digestion was performed. A fragment of DNA containing the mutations was cut off and replaced by a fragment of mutations-free homologue DNA. Partial digestion was performed by using small amounts of enzymes or short period of time. In a 20 µl reaction, 2.5 µg DNA, 5 units of NcoI and 1X buffer III were incubated at 37°C overnight, followed by 3 units of PciI addition. Subsequently, 1 µl of the reaction was taken out for gel electrophoresis every hour. After 8 h testing, optimal incubation time for getting desire fragment DNA was obtained. Another partial digestion was performed using the optimal incubation time and enzyme volume. Gel electrophoresis was performed to separate the DNA fragments and isolate the fragment of interest.

2.13 5' Dephosphorylation and Phosphorylation

Dephosphorylation of the 5' phosphates from DNA fragments prevents self-ligation. Following a restriction digestion reaction, 1.5 µl (25 units/µl) of calf intestinal alkaline phosphatase (CIAP) was added to the 40 µl reaction (containing 5 µg DNA) and incubated at 37°C for 1 h. After that, the fragment of interest was isolated. Prior to ligation, DNA fragment was needed to be 5' phosphorylated. The 35.25 µl phosphorylation reaction contained the fragment DNA sample (1.7 µg DNA), 5 units of the T4 polynucleotide kinase (PNK, NEB), 1 mM ATP, and 1X kinase buffer, incubated at 37°C for 30 min. Subsequently, an incubation of 70°C for 10 min was carried out to inactivate the kinase. Samples were stored at -20°C.

2.14 Ligation Reaction

After a piece of mutation-containing DNA was cut out, a homologue mutation-free DNA fragment was introduced back to ligate with the rest part of the plasmid DNA, constructing the circular form. In a 10 µl reaction, two DNA fragments were mixed together with 1 unit of T4 DNA Ligase (Roche), 1X reaction buffer in distilled water. It was incubated at 16ºC overnight.

2.15 Virus Rescue

In order to generate influenza A virus entirely from cloned cDNAs, human embryonic kidney cells (293T) were transfected with eight plasmids, each encoding a viral RNA segment, together with four plasmids encoding viral nucleocapsid protein and polymerase complex proteins (Neumann et al, 1999)). (See Figure 9) Plasmids containing HK virus individual gene segments HA, NP, M and wild type NS were generated and available prior to this project. Plasmids containing WSN individual eight genes segments as well as protein expression plasmids were gifts from Dr. Y. Kawaoka.

2.15.1 Plasmids Mix

The plasmid Mix included eight RNA expression plasmids pHH21 containing cDNAs for the full-length viral RNAs of either A/HK/1/68 or A/WSN/33 virus, together with protein expression plasmids pcDNA (controlled by the cytomegalovirus promoter) containing gene segments PB2, PB1, PA of A/WSN/33 virus, and plasmid pCAGGS (controlled by the chicken β-actin promoter) containing gene segment NP of A/WSN/33 virus. Briefly, 1 µg of each plasmid described before (except that only 0.1 µg of pcDNA-PA) were mixed together, then 1/10 volume of 2.5 M sodium acetate and 2 volume of 95% ethanol were added and incubated on ice for 10 min,

Figure 9: Reverse-Genetics Method for Generating Influenza Viruses entirely from Cloned cDNA.

(Taken from Neumann et al, 1999)

Plasmids containing the RNA polymerase I promoter, a cDNA for each of the eight viral RNA segments, and the RNA polymerase I terminator are transfected into 293T cells together with protein expression plasmids.

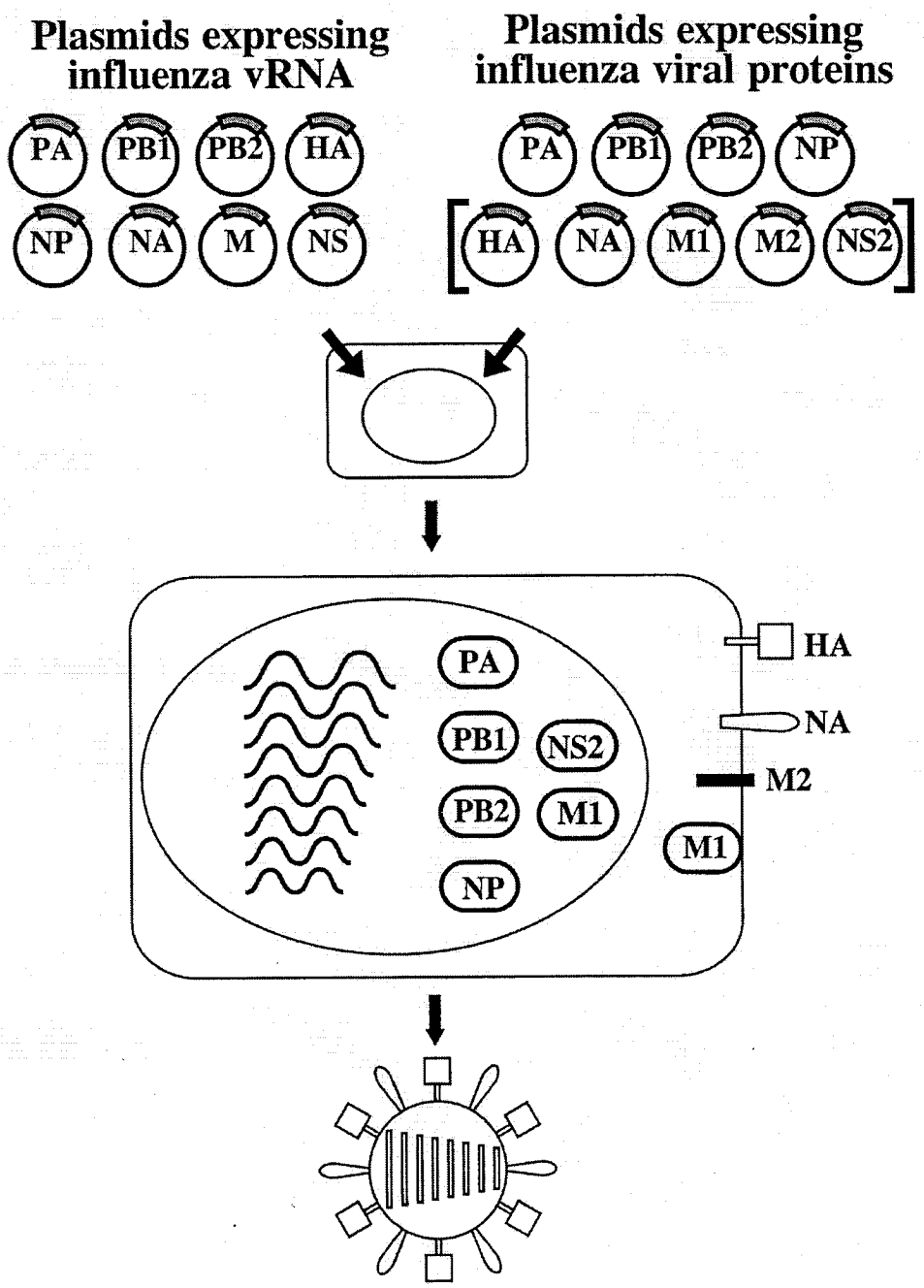
Plasmids expressing influenza vRNA
PA
PB1
PB2
HA
NP
NA
M
NS
Plasmids expressing influenza viral proteins
PA
PB1
PB2
NP
HA
NA
M1
M2
NS2
PA
PB1
NS2
PB2
M1
NP
HA
NA
M2
M1

followed by spinning at 13000 rpm for 15 min at 4°C. After rinsing by 70% ethanol and dried, the pellet was dissolved in 11.1 µl of double distilled water.

2.15.2 Transfection (Generation of Influenza Virus by Plasmid-Driven Expression of Viral RNA Segments, Three Polymerase Subunits, and NP Protein)

Around 60-80% confluent 293T cells and MDCk cell mix (10:1) were transfected with 12 plasmids with the use of lipofectin (Invitrogen) according to the manufacturer's instructions. For solution A, the plasmids DNA mix described before was diluted in 555 µl Opti-MEMI (serum free, GIBCO); for solution B, 22.2 µl lipofectin (1 mg/ml) and 100 µl Opti-MEMI were mixed together and incubated at room temperature for 45 min. After combination of solution A and B, incubation of the DNA-lipid mixture at room temperature for 15 min was carried out, followed by addition of an extra 0.8 ml Opti-MEMI. The cells were then washed once with warm PBS, and overlaid by the lipofectin-DNA complex, incubated for 6 h at 37°C in a CO_2 incubator. Finally, the DNA-containing medium was replaced by 3 ml Opti-MEMI containing 1 µg/ml trypsin, and incubated for 2 days at 37°C in a CO_2 incubator. Recombinant viruses were designated as HK/nsMA# or WSN/nsMA#.

2.16 IFN Resistance

2.16.1 Viral Infection, Infection with IFN Treatment, Infection with Anti-IFN Treatment

Viral yields from infection, infection with IFN antagonism, and infection with anti-IFN antibody synergism were compared. In this study, MEF, M1, MRC5, and A549 cells were utilized. In the first group, confluent cell monolayer in 6-well dish was washed, infected by virus of multiplicity of infection (MOI) of 2 and allowed to adsorb

for 30 min, following by incubation in 1XMEM with 1 μg/ml trypsin for 24 h. In the second group, either 1000 units of human IFN or 100 units of mouse IFN was allowed to incubate with the cells for 24 h before the infection performed as group one. In the third group, either 500 units of anti-human IFN or 1000 units of anti-mouse IFN was allowed to add to the 1XMEM after the virus adsorption. After the cells had been infected for 24 h, supernatant was collected and stored at -80°C until a plaque assay was performed for quantification.

In order to analyze the information of cell damage on this infection assay, another experiment were carried out the same as above except just 0.25 μg/ml trypsin was included in the overlaid MEM as to avoid the cell lifted. After 24 h incubation, cells were stained with Coomassie Brilliant Blue staining solution for 45 min in room temperature.

2.17 IFN induction

The viral infection samples from all the cell types mentioned above as well as an infection on Hela cells were tested to quantitate the amount of induced IFN.

2.17.1 IFN Assay

In order to inactive the virus in the sample, 23 μl of 2 N HCl was added to 1ml sample to achieve approximately PH 2. The mixture was incubated at 4°C overnight. Then the sample was neutralized by adding around 16.6 μl 2 M NaOH, followed by serial two fold dilution in complete MEM. Confluent L929 cells (testing mouse IFN) or A549 cells (testing human IFN) in 96-well dish were overlaid by 100 μl dilution sample in each well, followed by incubation at 37°C in a CO_2 incubator for 24 h. After that, each well was infected by 2000 pfu of vesicular stomatitis virus (VSV), and incubated at 37°C in a CO_2 incubator for 48 h. Finally, the cells were stained by

addition of 200 µl Coomassie Brilliant Blue per each well and waited for 45 min. The IFN amount was determined from the end-point dilution where the cells were protected from VSV infection (representing 10 units per ml).

2.17.2 IFN ELISA

This was performed using the Human IFN-β ELISA Kit (PBL Biomedical Laboratories), according to the manufacturer's instructions. Briefly, 100 µl of the sample containing live virus was tested in duplicate manner.

2.18 Mice

The mice used for this study were 4- to 6-week-old outbred Swiss Webster (CD-1) strain from Charles River Laboratories. All experiments were conducted with the approval of the Animal Care Committee of the University of Ottawa.

2.18.1 Histopathology

Mice were inoculated intranasally with 5 X 10^3 pfu, 5 X 10^4 pfu or 10^6 pfu of virus diluted in PBS in a 50 µl volume, while lightly anesthetized with halothane. On days 3 or 5 of infection, the mice were sacrificed by euthanizing with a 90% CO_2 10% O_2 mixture in duplicate for each virus. The lungs and trachea were then exposed so that an 18 gauge needle attached to tube containing 10% formalin in PBS under 25 cm head pressure could be inserted into the trachea to inflate the lungs with fixative. The lungs were left to fix for at least 10 min before being removed for storage in formalin. The lungs were then sectioned and stained with Hematoxylin-Eosin (HE) in the Department of Pathology and Laboratory Medicine, University of Ottawa. Slides were observed in microscope (BH2 Research Microscope, Olympus America Inc.).

2.18.2 Fluorescent Immunostaining of Frozen Sections

Mice were infected and sacrificed as described for the *Histopathology*. Lungs were exposed and removed, followed by frozen sectioned in the Department of Pathology and Laboratory Medicine, University of Ottawa, as described before. For fluorescent immunostaining, sections of fixed lungs were stained primarily with rabbit serum against A/HK/1/68 at 1: 400 dilution in PBS. After incubated overnight at 4°C, slides were extensively washed in PBS, before the secondary antibody, donkey anti rabbit antibody labeled with Cy3, was added to the sections for 1 h at room temperature at 1:400 dilution in PBS. Slides were observed in invert fluorescent microscope (BMAX Series Microscopes, Olympus America Inc.).

.

RESULTS

3.1 Pathology in Mice infected by parent A/HK/1/68 or progeny HKMA20c

Among HK MA20 and MA21 series, only MA20 series had been determined for their LD_{50} in mouse lung. Among all the viruses that had been tested, HKMA20c is the most virulent strain possessing an mLD_{50} of $10^{2.6}$ pfu/mouse, which is 10^5 fold lower than its parental virus HK (Brown st al, 2001). As an extension experiment of these previous data, an in vivo infection was carried out with HK and HKMA20c in order to compare the differences of their infection sites and pathology in mouse lung. Three different infection dosages and two different infection time points were tested. Two mice were infected for each combination of dosage and time point, lung from one mouse was taken for HE staining while lung from the other one was for immunofluorescent staining. One or two slides from each sample were examined under microscope.

3.1.1 Hematoxylin-Eosin (HE) Staining

In order to see the damage and immune cell infiltration in the mouse lungs due to viral infection with HK wild type prototype or virulent mouse adapted variant HKMA20c, formalin-fixed sections of infected lungs were HE stained. Two mice were infected for each group representing a combination of the specific virus, infection dosage and infection days (See Figure 10). In the control lung, the epithelium lining the bronchioles retained its slightly ridged appearance and there were clear spaces in alveoli. In cases of both HK and HKMA20c infections, in bronchioles, columnar ciliated cells become edematous and desquamated. Dead cells and debris were seen in the airway lumen. Patches of alveoli had thickened

Figure 10: Influenza Infected Mouse Lung Pathology (20X magnification)

infection dose (pfu/mouse)	$5X10^3$	$5X10^3$	$5X10^4$	$5X10^4$
day postinfection	3	5	3	5

The above table shows the infection dosage and days for each mouse. However, only part of the slides is shown.

This composite is made up of photographs taken of formalin fixed HE stained mouse lung sections showing signs of severe damage. The photographs were taken in focal areas of destruction and are not representative of the entire lung sections.

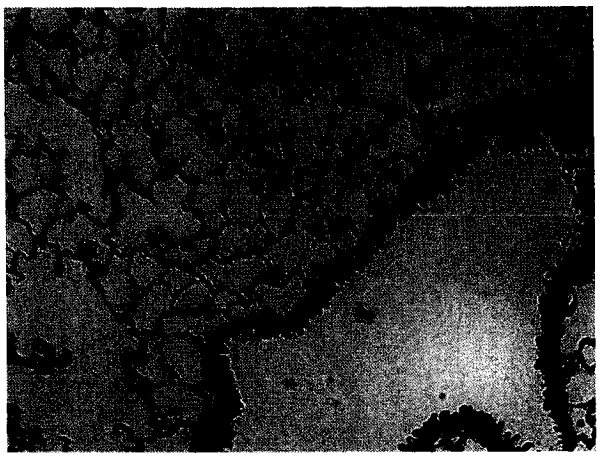

control; mock (PBS) infected

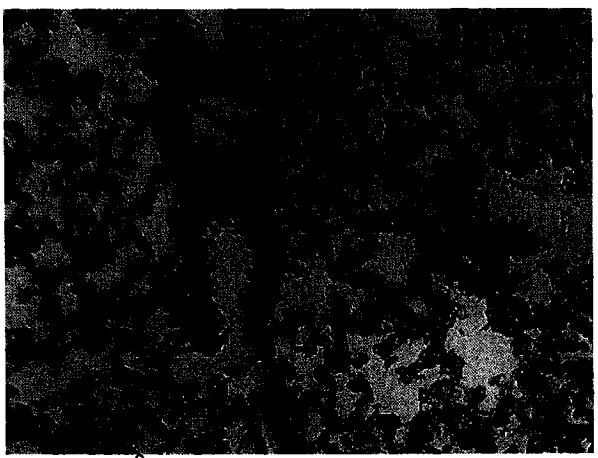

HK;5X10^{3}pfu/mouse;day3 postinfection

MA20c;5X10^{3}pfu/ml;day3 postinfection

HK;5X10^{3}pfu/mouse;day5 postinfection

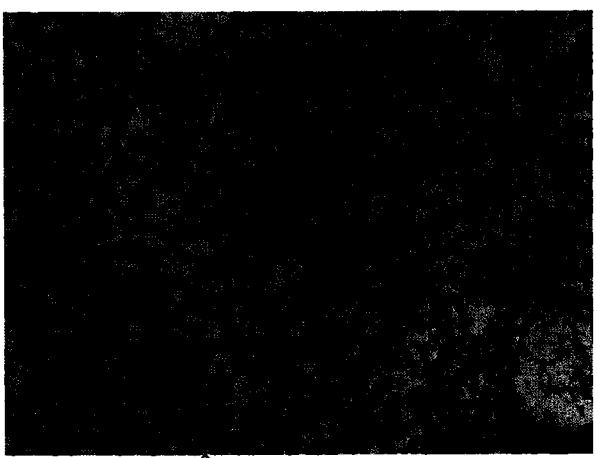

MA20c;5X10^{3}pfu/ml;day5 postinfection

HK;5X10^{4}pfu/mouse;day3 postinfection

MA20c;5X10^{4}pfu/ml;day3 postinfection

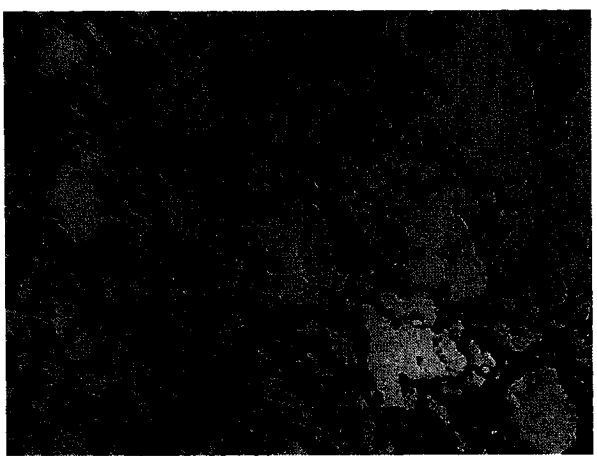

HK;5X10^{4}pfu/mouse;day5 postinfection

MA20c;5X10^{4}pfu/ml;day5 postinfection

walls, hyaline membranes formed inside the alveoli, massive mononuclear leukocyte infiltrated in the interstitium between alveoli. Neighbouring capillary vessels became congested and dilated. Intraalveolar hemorrhage occurred. Comparing infections of the two viruses, in each infection dosage, HKMA20c infection displayed significantly more extensive areas and more intensive severity of alveoli destruction than HK. Comparing the two time points, day 3 and day 5, pathologic manifestation of day 3 were similar or increased on day 5, no sign of cellular repair occurred up to day 5.

3.1.2 Fluorescent Antibody Staining

The next step was to determine the location and extent of lung infection. To do this, frozen lung sections were stained with a rabbit polyclonal anti-influenza immune serum (α-HK) followed by a secondary anti-rabbit IgG antibody labeled with Cy3. Figure 11 is a composite of HK influenza viral antigen stained murine lung sections of 3 infection dosages and 2 time points from infections of parental HK and progeny HKMA20c. The dosages and time points were shown in the table for description of Figure 11. The infection areas for parent HK were basically bronchioles, with few scattered positively stained cells in alveoli. This pattern did not change in higher dosage or in longer times of infection. In contrast to HK, HKMA20c antigen spread throughout bronchioles and alveoli. The pattern did not change for lower dosages or shorter times of infection.

3.2 IFN Resistance of Parent virus HK and Progeny Mouse-Adapted Variants

NS1 mutations that were selected after 20 or 21 passages in murine lung showed that adapted progeny viruses possessed a clustering of mutations within aa 98-106 as well as convergent mutation at aa 106 (See Table 2). This phenomenon

Figure 11: Fluorescent Antibody Staining for Influenza Antigen in Infected Mouse Lung (20X magnification)

infection dose (pfu/mouse)	$5X10^3$	$5X10^3$	$5X10^4$	$5X10^4$	10^6
day postinfection	3	5	3	5	3

The above table shows the infection dosage and days for each mouse. However, only part of the slides is shown.

This composite is made up of photographs of Cy3 conjugated antibodies labeling influenza antigens on frozen sections of mouse lung showing the location of viral infection. The photographs were taken in the most brightly fluorescing areas, and may not be representative of the entire lung section.

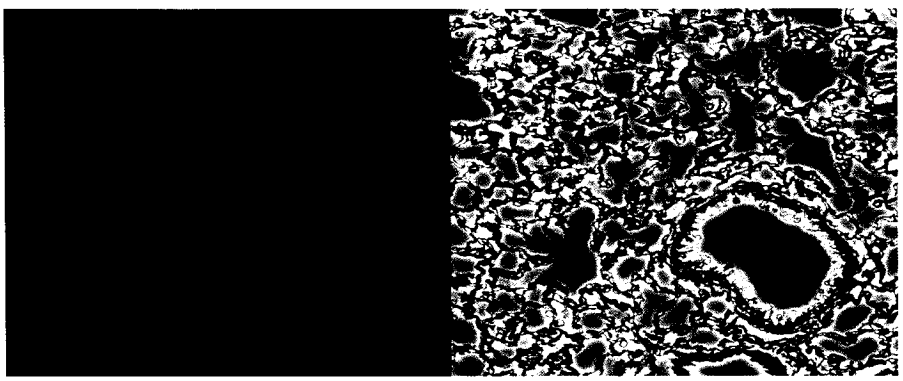

control; mock (PBS) infected

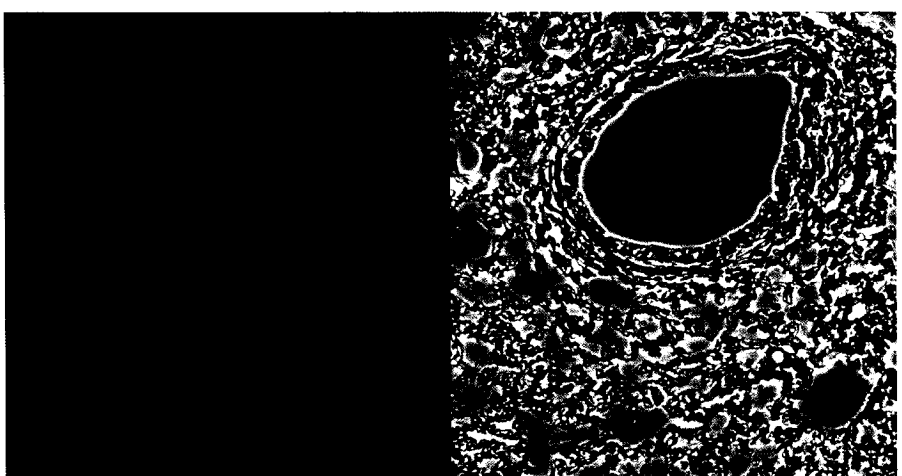

HK;5X10^{3}pfu/mouse;day3 postinfection

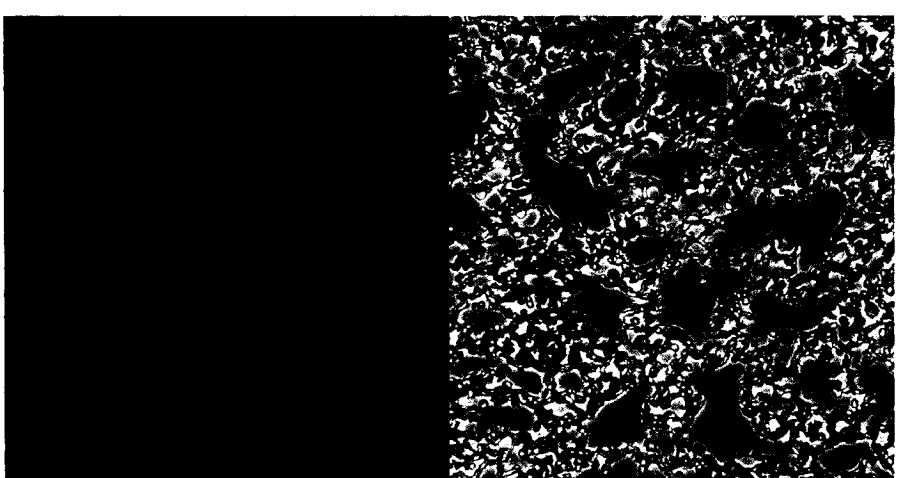

MA20c;5X10^{3}pfu/ml;day3 postinfection

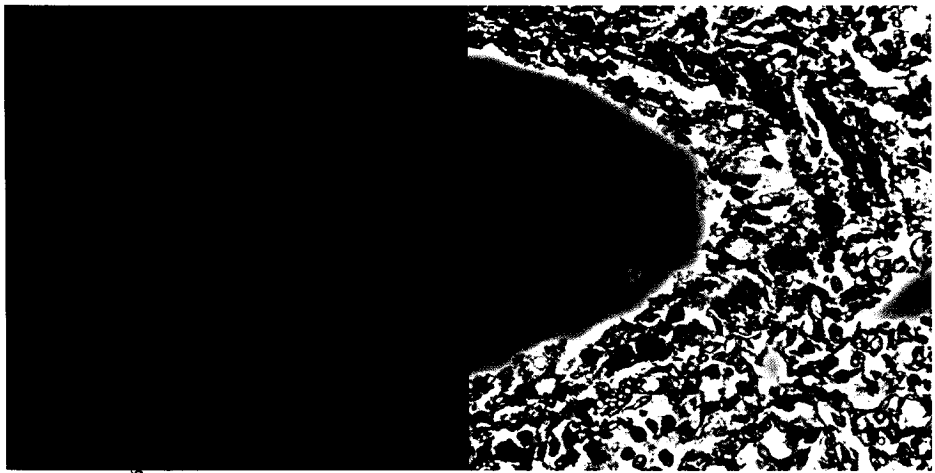

HK;5X10^{3}pfu/mouse;day5 postinfection

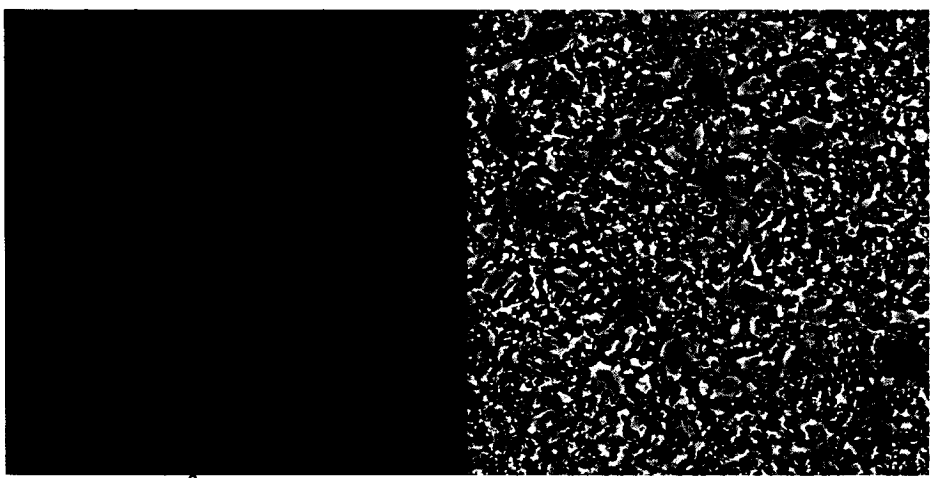

MA20c;5X10^{3}pfu/ml;day5 postinfection

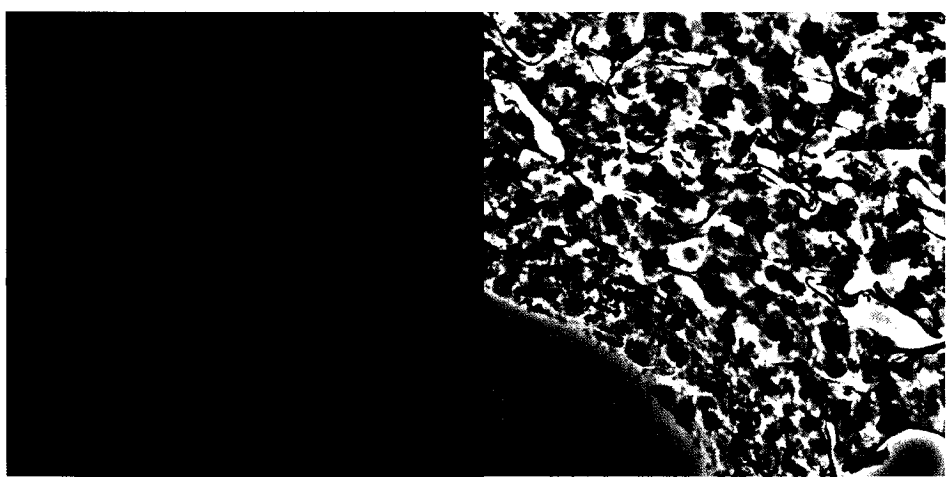

HK 10^6 pfu/mouse day3 postinfection

MA20c 10^6 pfu/mouse day3 postinfection

strongly suggested that these mutations were instrumental in murine adaptation and likely contributed to better replication in the mouse lung. The next step of this project was to examine if these mouse adapted variants had increased their ability of IFN resistance in comparison to their parent virus HK. In total, there were 5 mutant NS1 proteins derived from screening MA clones. The replication abilities of parental and the five NS1 mutant MA viruses were assessed in the presence and absence of IFN at an MOI of 2. Two cell types were tested: human A549 cells and mouse embryo fibroblast MEF cells. The parent HK and progeny MA variants were used to infect cells with (human or mouse) IFN or anti-(human or mouse) IFN treatment. One experiment was carried out with two plaque assays titrating.

The result of infection on A549 cells was shown by coomassie blue staining of fixed cells on Figure 12. Cell damage shown in Figure 12 demonstrated that human IFN protected A549 cells from attack by virus HK and all the MA variants except HK4MA21-1. All the MA variants caused more cell death than virus HK on infection in the absence of IFN. In the presence of human IFN, HK4MA21-1 still caused comparable amounts of cell death, suggesting a greater ability to resist human IFN.

From infection on A549 cell, viral titre reached 10^5 to 10^7 pfu/ml (See Figure 13a). Viral replication of most of the MA variants was similar to or greater than HK parental virus with the exception of HKMA20c that had a ten fold lower yield. Most of the variants showed slightly reduced IFN resistant than parental HK virus except for HK5MA21-3 that was more resistant. Interestingly, the HK5MA21-1 variant was significantly more IFN sensitive than HK or the closely related MA variant HK5MA21-3 that owns the same M106I mutation but not the L98S mutation.

Figure 12: Cell Damage Caused by Parent HK and Mouse Adapted Variants on A549 Cells under the Treatment of Human IFN and No Treatment.

A549 cells were infected by wt HK and MA variants with a MOI of 2 for 24 h. C plate received no treatment other than infection, B plate was treated with 1000 unit/well human IFN 24 h before infection, and the control well received no treatment.

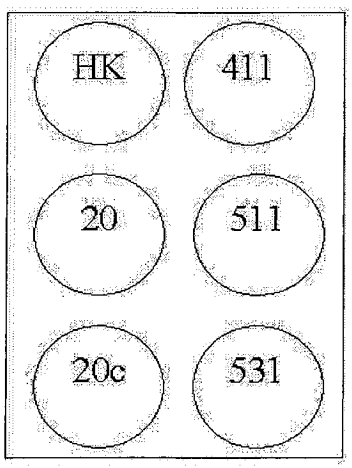

A 6-well dish layout for wt HK and MA variants infection

HK: parent HK
20: HKMA20
20c: HKMA20c
411: HK4MA21-1
511: HK5MA21-1
531: HK5MA21-3

A: control

B: infection with human IFN treatment 24 hour ahead

C: infection

(A) A549 cell, control

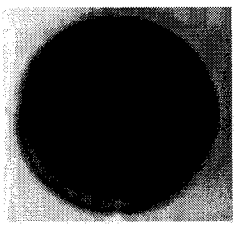

(B) human IFN treated

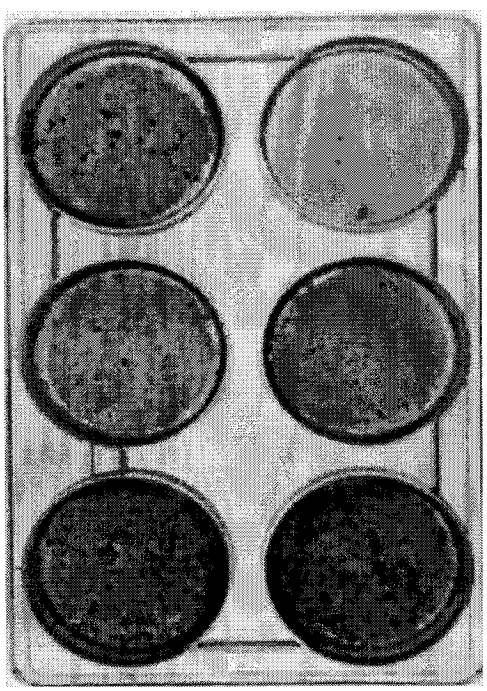

(C) infection, no treatment

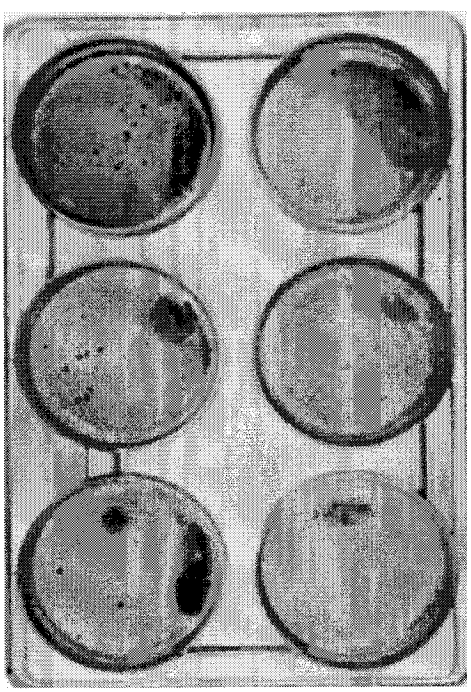

Figure 13a: Replication Titres of Parent HK and Mouse Adapted Variants on A549 Cells with or without Treatment of Human IFN.

Each bar represents average from two plaque assay titrations of one infection experiment on A549 cells, with error bars showing standard deviation. The wild type HK and MA variants are all shown. Titres are expressed as common logarithm.

Infection with human IFN treatment: blue

Infection without treatment (no treatment -n/t): pink

Figure 13b: Difference in Titres of Parent HK and Mouse Adapted Variants on A549 Cells with and without Treatment of Human IFN.

Each bar represents difference of titres between IFN treated infection and no treatment infection for each virus. The numbers are derived by dividing between the two titres.

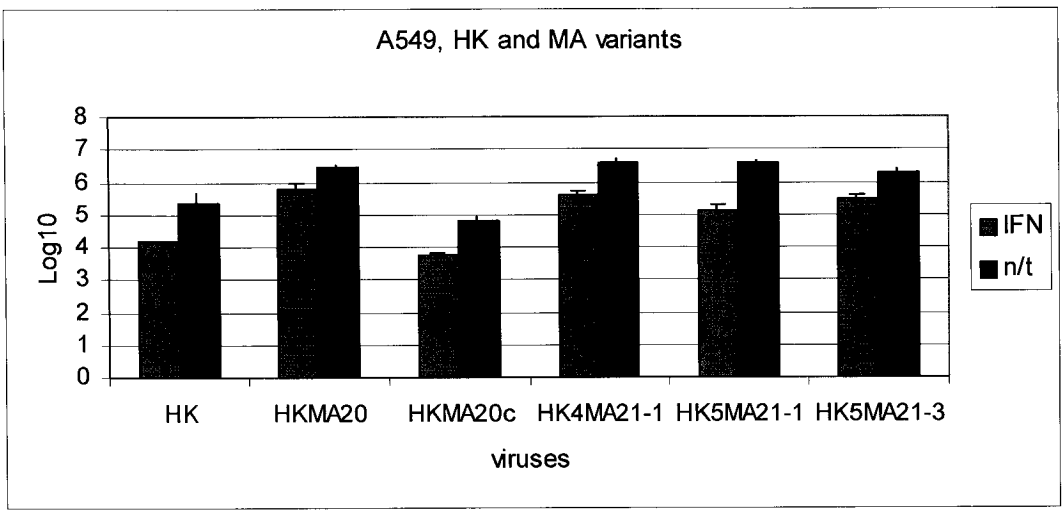
A549, HK and MA variants
Log10
8
7
6
5
4
3
2
1
0
HK
HKMA20
HKMA20c
HK4MA21-1
HK5MA21-1
HK5MA21-3
viruses
IFN
n/t

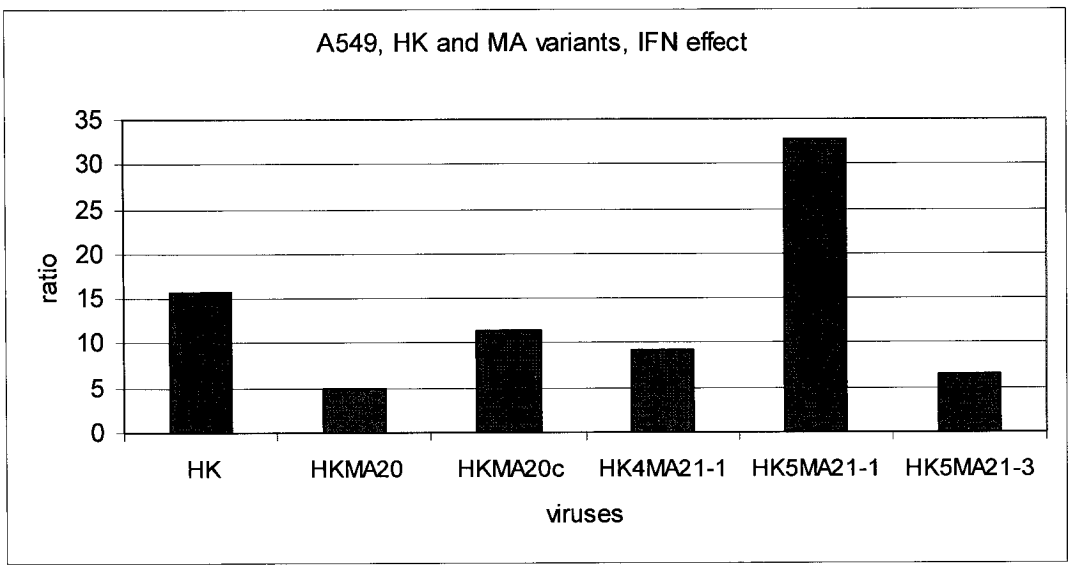
A549, HK and MA variants, IFN effect
ratio
35
30
25
20
15
10
5
0
HK
HKMA20
HKMA20c
HK4MA21-1
HK5MA21-1
HK5MA21-3
viruses

Together these data indicated that mouse-adaptation produced decreases in variable IFN resistance in human lung epithelium.

Next, IFN sensitivity of virus HK and MA variants were compared in mouse cells. Information of infection assay on MEF cells is shown in Figure 14 and 15. The parent virus HK and progeny MA variants were used to infect MEF culture with and without mouse IFN as well as in the presence of mouse anti-IFN. Figure 14 shows the extent of cell damage as assessed by coomassie staining for each of the treatments. HK parent virus had the lowest ability to kill MEF cells relative to the MA variants that produce complete or extensive cell destruction. Among the MA variants, mouse IFN treated HK5MA21-1 infection had the greatest cell viability. Anti-IFN treatment produced little change as to cell survival for most MA variants.

Infection of MEF showed that all the MA variants had increased replication ability in mouse cells (See Figure 15a). In contrast to the response in human A549 cells, all the MA variants were more resistant to IFN in mouse cells than parental HK virus with 5 to 15 folds less inhibition reduction respectively. IFN reduced parental HK virus replication titre to 10^3 pfu/ml but only reduced MA variants to $10^{4.2}$ to 10^6 pfu/ml. Anti-IFN had little effect on viral yield except for HK4MA21-1 and HK5MA21-1 that both possess mutations at NS1 protein aa 106.

These initial experiments showed that MA variants with NS1 mutations are more resistant to IFN in mouse cells but not as uniformly resistant in human cells. This is consistent with the hypothesis that the NS1 mutations increased IFN resistance on adaptation to mice lung tissue. These data cannot be taken as proof that only the NS1 mutations are responsible for increased IFN resistance at this time because

Together these data indicated that mouse-adaptation produced decreases in variable IFN resistance in human lung epithelium.

Next, IFN sensitivity of virus HK and MA variants were compared in mouse cells. Information of infection assay on MEF cells is shown in Figure 14 and 15. The parent virus HK and progeny MA variants were used to infect MEF culture with and without mouse IFN as well as in the presence of mouse anti-IFN. Figure 14 shows the extent of cell damage as assessed by coomassie staining for each of the treatments. HK parent virus had the lowest ability to kill MEF cells relative to the MA variants that produce complete or extensive cell destruction. Among the MA variants, mouse IFN treated HK5MA21-1 infection had the greatest cell viability. Anti-IFN treatment produced little change as to cell survival for most MA variants.

Infection of MEF showed that all the MA variants had increased replication ability in mouse cells (See Figure 15a). In contrast to the response in human A549 cells, all the MA variants were more resistant to IFN in mouse cells than parental HK virus with 5 to 15 folds less inhibition reduction respectively. IFN reduced parental HK virus replication titre to 10^3 pfu/ml but only reduced MA variants to $10^{4.2}$ to 10^6 pfu/ml. Anti-IFN had little effect on viral yield except for HK4MA21-1 and HK5MA21-1 that both possess mutations at NS1 protein aa 106.

These initial experiments showed that MA variants with NS1 mutations are more resistant to IFN in mouse cells but not as uniformly resistant in human cells. This is consistent with the hypothesis that the NS1 mutations increased IFN resistance on adaptation to mice lung tissue. These data cannot be taken as proof that only the NS1 mutations are responsible for increased IFN resistance at this time because

(A) MEF cell, control

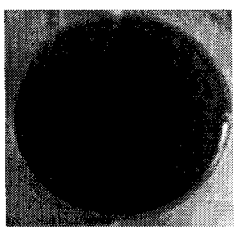

(B) infection, no treatment

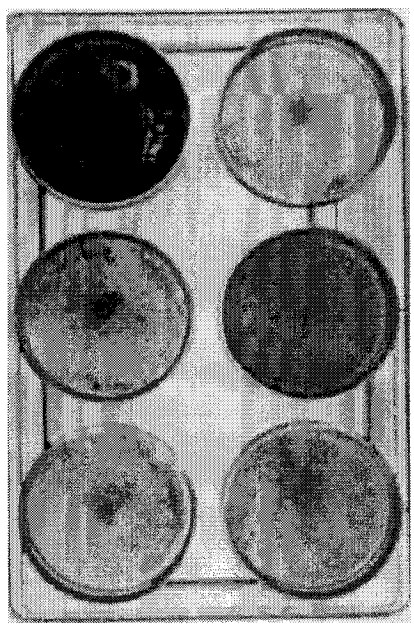

(C) mouse IFN treated

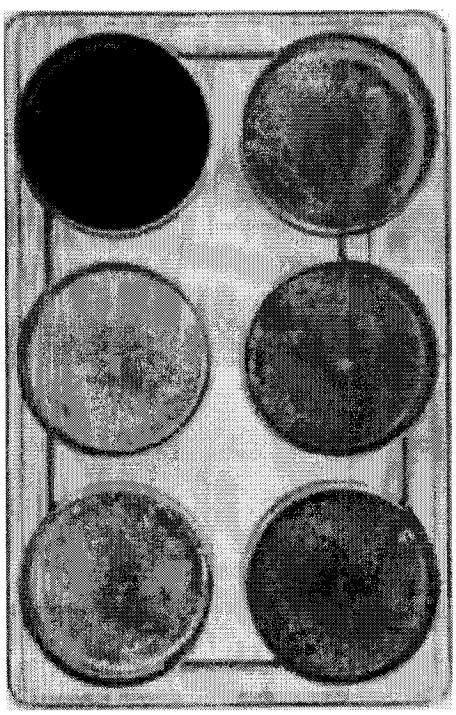

(D) anti-mouse IFN treated

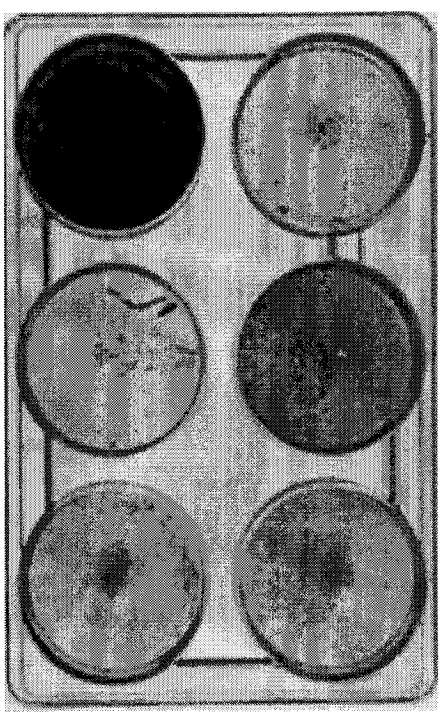

Figure 15a: Replication Titres of Parent HK and Mouse Adapted Variants on MEF Cells with or without Treatment of Mouse IFN, or in the presence of Anti-Mouse IFN Antibody.

Each bar represents average from two plaque assay titrations of one infection experiment on MEF cells, with error bars showing standard deviation. The wild type HK and MA variants are all shown. Titres are expressed as common logarithm.

Infection with mouse IFN treatment: blue

Infection without treatment (no treatment -n/t): pink

Infection with anti-mouse IFN treatment: light yellow

Figure 15b: Difference in Titres of Parent HK and Mouse Adapted Variants on MEF Cells with and without Treatment of Mouse IFN.

Each bar represents difference of titres between IFN treated infection and no treatment infection for each virus. The numbers are derived by dividing between the two titres

Figure 15c: Difference in Titres of Parent HK and Mouse Adapted Variants on MEF Cells without and with Treatment of Anti-Mouse IFN.

Each bar represents difference of titres between no treatment infection and anti-mouse IFN treated infection for each virus. The numbers are derived by dividing between the two titres

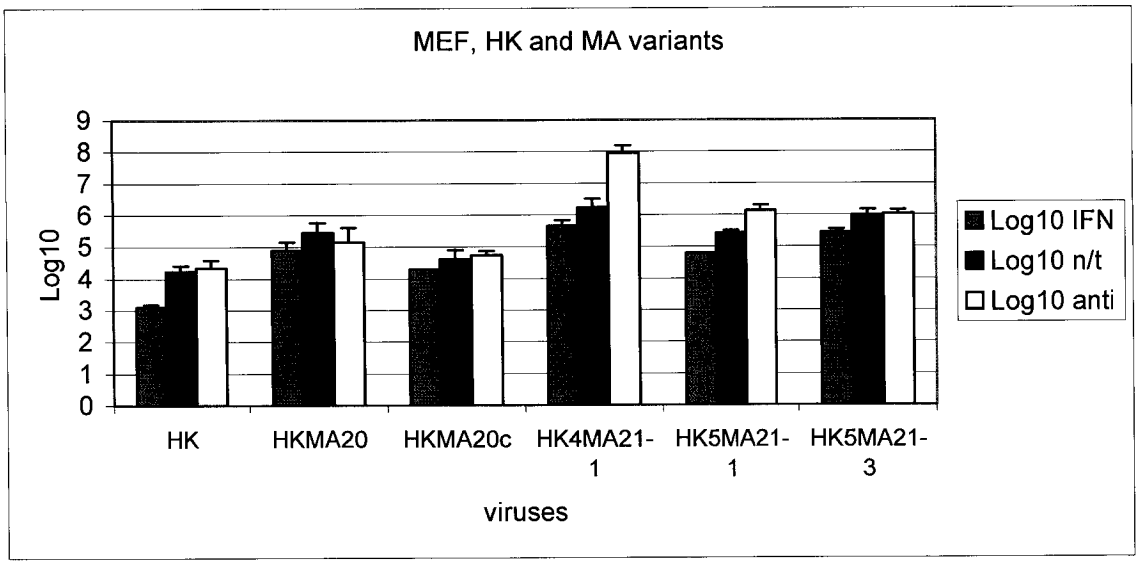
MEF, HK and MA variants
Log10
9
8
7
6
5
4
3
2
1
0
HK
HKMA20
HKMA20c
HK4MA21-1
HK5MA21-1
HK5MA21-3
viruses
Log10 IFN
Log10 n/t
Log10 anti

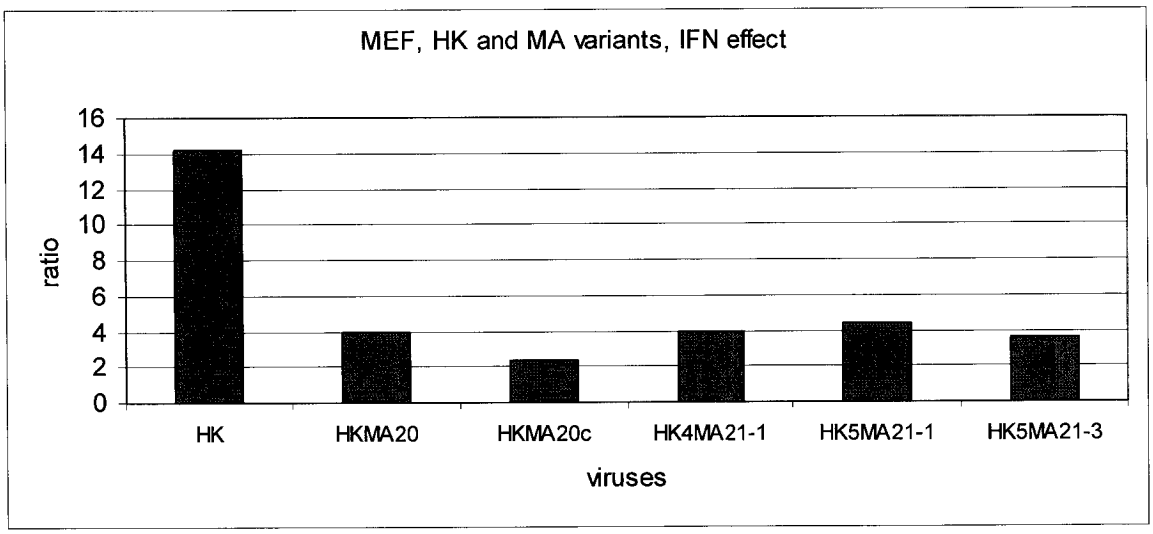
MEF, HK and MA variants, IFN effect
ratio
16
14
12
10
8
6
4
2
0
HK
HKMA20
HKMA20c
HK4MA21-1
HK5MA21-1
HK5MA21-3
viruses

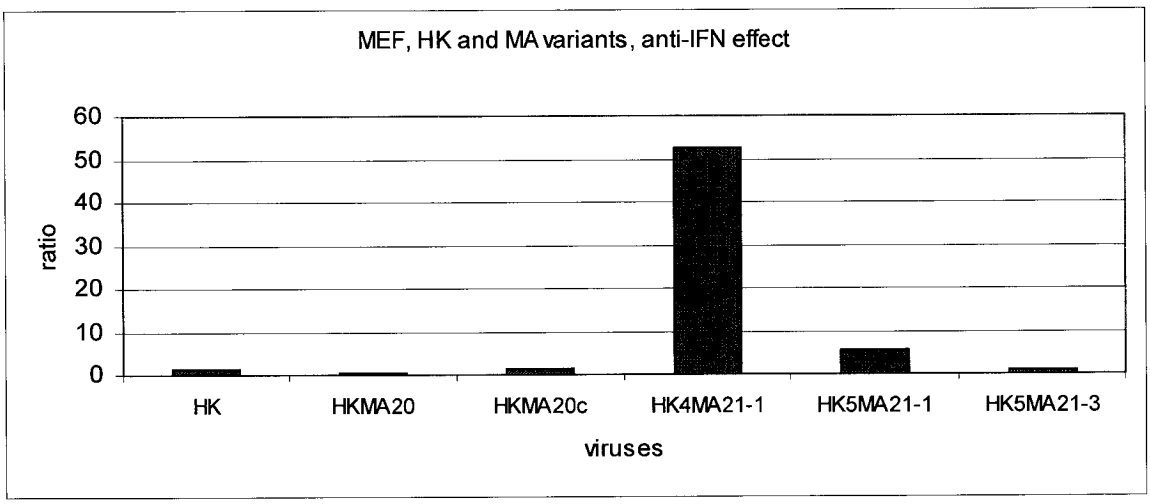
MEF, HK and MA variants, anti-IFN effect
ratio
60
50
40
30
20
10
0
HK
HKMA20
HKMA20c
HK4MA21-1
HK5MA21-1
HK5MA21-3
viruses

these MA variants possess mutations on other genome segments that might affect IFN resistance.

3.3 IFN Induction by Parental Virus HK and Progeny Mouse-Adapted Variants

Inhibition or promotion of host IFN production is employed by different virulent virus strains. In this project, amount of IFN induction was also tested for parent virus HK and progeny MA variants to get a full picture of the interaction between the host IFN and viruses. In order to assess the amounts of IFN induced during infection, IFN bioassay was performed using supernatants collected 24 hours post infection. Only one experiment was done for each cell type. In this Assay, 10 unit/ml is the lowest limit of sensitivity in measurement as the assay employs 0.1 ml of sample with a detection limit of I unit of IFN.

The infection of A549 cells by HK parental virus and MA variants induced very small amount of IFN (see Figure 16). HK parent infection induced 20 unit/ml while all the MA variants induced less than 10 unit/ml. Induction of IFN during infection of MEF cells was much higher, yielding 80 u/ml for the HK parental virus and MA variants with the exception of HKMA20c and HK5MA21-1 that produced 40 and 20 u/ml (see Figure 17). Thus MA variants induced similar or reduced levels of IFN in MEF cells.

3.4 Plasmid Construction

In order to analyze NS1 mutations in an isogenic background, the next objective of this project was to use an influenza A virus rescue system to engineer mutant NS1 genes onto a defined genetic background (Neumann, 1999). This system requires eight plasmids encoding cDNA for the complete influenza A virus genome

Figure 16: Induction of Human IFN of Parent HK and Mouse Adapted Variants on A549 Cells.

Induced IFN amount were tested by IFN assay for one infection experiment on A549 cells of wt HK and MA variants. Each bar represents specific units induced by each virus. Ten units is the lowest amount of IFN that can be accurately detected in this assay.

Figure 17: Induction of Mouse IFN of Parent HK and Mouse Adapted Variants on MEF cells.

Induced IFN amount were tested by IFN assay for one infection experiment on MEF cells of wt HK and MA variants. Each bar represents specific units induced by each virus. Ten units is the lowest amount of IFN that can be accurately detected in this assay.

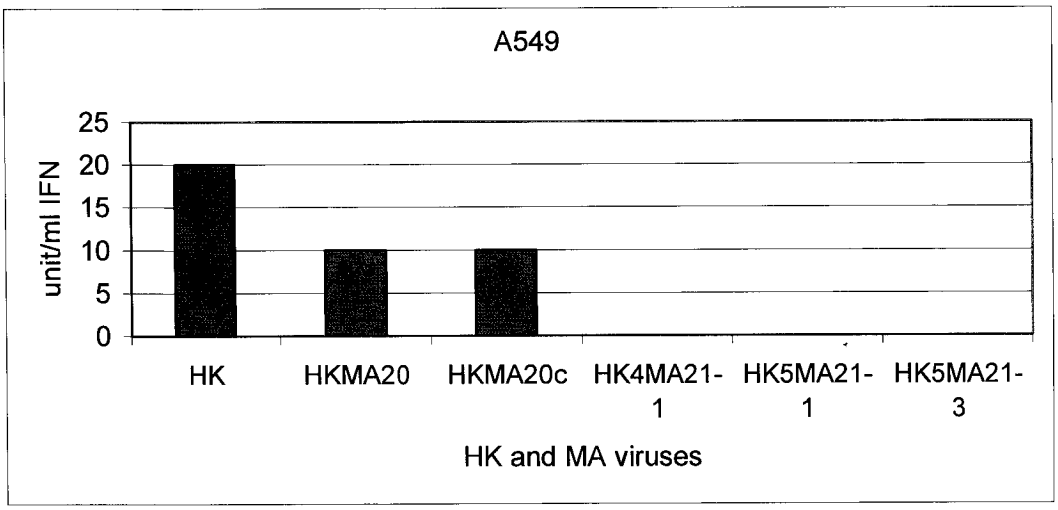
A549
unit/ml IFN
25
20
15
10
5
0
HK
HKMA20
HKMA20c
HK4MA21-1
HK5MA21-1
HK5MA21-3
HK and MA viruses

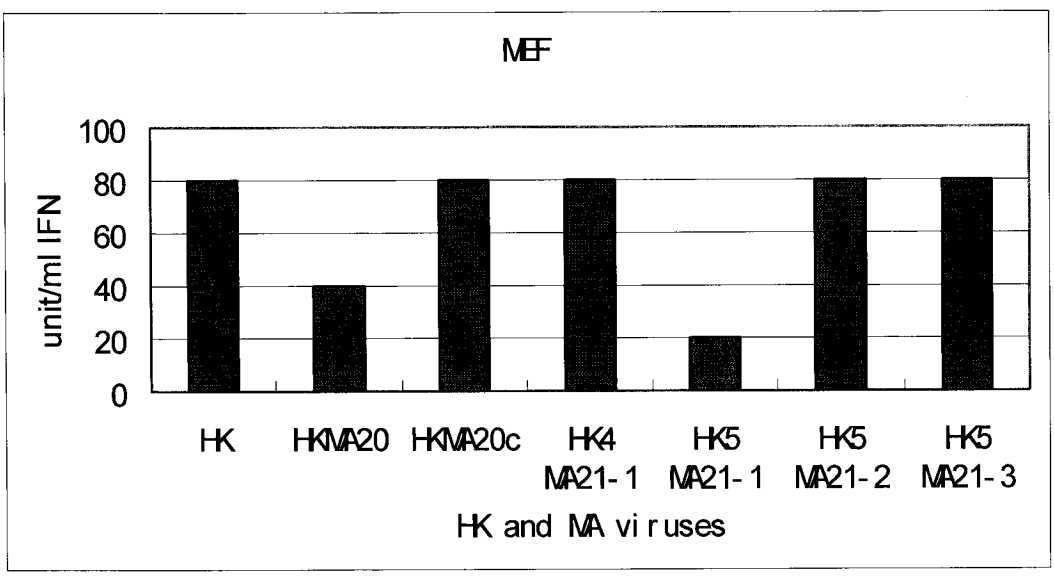
MEF
unit/ml IFN
100
80
60
40
20
0
HK
HKMA20
HKMA20c
HK4 MA21-1
HK5 MA21-1
HK5 MA21-2
HK5 MA21-3
HK and MA viruses

(wild type HK genome), and plasmids encoding the NP and polymerase complex proteins (described in "Materials and Methods").

3.4.1 Cloning and Screening

HK-HA, HK-NP, HK-M, and wild type HK-NS had been previously inserted into pHH21 in our lab. The plasmids that derived and sequenced within this project include vector pHH21 inserted with PB2-17 (HK-PB2), PB1-5 (HK-PB1), PA-5 (HK-PA), NA-1 (HK-NA), MA20-1 (HK-NSMA20), MA20c-3 (HK-NSMA20c), MA411-3 (HK-NSMA411), MA511-11 (HK-NSMA511) and MA531-6 (HK-NSMA531). Because HK-NSMA521 and HK-NSMA531 were identical (see Table 2), HK-NSMA521 was not cloned. Mutation artifacts from cloning were identified on clones PB2-17, PB1-5 and NA-1 (see Table 4). These mutations were corrected and the plasmids with HK wild type gene sequence were PB1-n4 (PB1) and NA-n11 (NA). PB2-n11 (PB2) still had the point mutation I585V, but because Valine on 585 was also present on a contemporary strain of A/HK/1/68: influenza A/Northern territory/60/68, it was presumed that this mutation would not inhibit replication and was employed in rescue experiments.

3.4.2 Verification of Plasmid Construct

The pHH21 plasmid set containing cDNA for each of the eight viral RNA segments of WSN strain was provided by Dr. Y. Kawaoka. Recombinant viruses can be obtained by transfecting all of these plasmids along with protein expression plasmids expressing PB2, PB1, PA and NP into 293T cells. To test if pHH21 plasmid containing an individual HK segment is effective for viral rescuing, each one was mixed with seven other gene segments from WSN set and transfected for virus rescue. Synthetic recombinant virus was detected by cytopathological effect (CPE)

Table 4: Summary of Mutations in HK Segments 1, 2, and 6 on Plasmids

gene segment	clone	mutations on AA sequence	mutation correction	clone with clean gene	mutation on AA sequence
PB2	PB2-17	Q237R, K332R, I585V	+	PB2-n11	I585V
PB1	PB1-5	A462T, M535T	+	PB1-n4	n/a
PA	PA-5	n/a			
NA	NA-1	G415S	+	NA-n11	n/a
NS-MA20	MA20-1	n/a			
NS-MA20c	MA20C-3	n/a			
NS-MA411	MA411-3	n/a			
NS-MA511	MA511-11	n/a			
NS-MA531	MA531-6	n/a			

on MDCK cells that were incubated with the transfection supernatant in the presence of trypsin (See Table 5). Also trials of pHH21 containing individual segment from WSN mixed with seven other genes on HK backbone were performed (See Table 5). The plasmids that were effective for virus rescue are showed in Table 6. Plasmid PB1-4 (PB1) contains mutations I300T and S706P. Two separate efforts were made to correct these mutations by restriction digestion, agarose gel separation, isolation and ligation. However, technical difficulties were encountered and the repairs were unsuccessful. This mutant HK-PB1 gene was competent for

Table 5: Trial of Each Plasmid for Virus Rescue

segment(s) from HK	segment(s) from WSN	success
NS	*7 genes on WSN backbone*	yes
NP	*7 genes on WSN backbone*	no
NP(a)	*7 genes on WSN backbone*	yes
NA(n11)	*7 genes on WSN backbone*	no
NA(37,43,45,46,48)	*7 genes on WSN backbone*	yes
7 genes on HK backbone	PB2	no
7 genes on HK backbone	PB1	yes
7 genes on HK backbone	PA	no
7 genes on HK backbone	HA	no
7 genes on HK backbone	NP	no
7 genes on HK backbone	NA	no
7 genes on HK backbone	M	no
7 genes on HK backbone	NS	no
HA	*7 genes on WSN backbone*	yes
PB2(n11)	*7 genes on WSN backbone*	yes
PA((5)	*7 genes on WSN backbone*	yes
M	*7 genes on WSN backbone*	yes
PB1(n1,n2,n3,n4)	*7 genes on WSN backbone*	no
PB1(4)**not clean**	*7 genes on WSN backbone*	yes
PB1(6)**not clean**	*7 genes on WSN backbone*	no

Table 6: Summary of Mutations in HK Segments 1 and 2 on Plasmids

gene segment	plasmid	mutations on AA sequence
PB2	PB2_N11	I585V
PB1	PB1_4	I300T S706P
PA	PA5	n/a
NA	NA48	n/a
NSMA20	NS20(1)	n/a
NSMA20c	NS20c(3)	n/a
NSMA411	NS411(3)	n/a
NSMA511	NS511(11)	n/a
NSMA531	NS531(6)	n/a

virus rescue and was employed for generating viruses that differed solely to NS1 mutations.

3.5 Virus Rescue

3.5.1 Initial Rescue Attempts

In theory, transfection of the eight plasmids that contain cDNA for the full-length viral RNAs of the influenza A virus into eukaryotic cells should result in the production of all eight influenza vRNAs. The RNA polymerase complex proteins and NP protein, if co-expressed in the same cell, should be able to assemble the vRNAs into functional vRNPs that are replicated and transcribed to form infectious influenza viruses. The plan was to produce recombinant viruses that differed solely due to the presence of the wild type HK NS gene and each of the 5 mutant MA NS genes.

Attempts were performed to rescue recombinant viruses containing these NS genes into the backbone of wild type HK genome (See Table 7). Synthetic recombinant viruses were designated as HK/nsMA#. However, virus rescuing into the HK backbone did not occur on every attempt. Rescue of viruses containing NSHKwt, NSMA511 and NSMA531 into the HK backbone gave around 50% success rate, while there was no synthetic virus generated for NSMA20, NSMA20c or NSMA411 in HK backbone among 7 rescue attempts. It appears that some of the NS mutations selected in mouse decreased replication ability in human 293T cells. To overcome the attenuation of NS1 protein mutations, constructions of the NS series into the mouse- and lab-adapted A/WSN/33 (H1N1) virus were attempted. WSN has an extensive passage history in eggs and animals and replicates to high yield in many cell types. The virus rescue experiments in backbone of WSN genome were uniformly successful on the first trial (See Table 8). Synthetic recombinant viruses were designated as WSN/nsMA#.

3.5.2 Characterization of Synthetic Recombinant Viruses

In order to test the synthetic recombinant viruses in the upcoming bioassays, high titre of these viruses needed to be obtained. The commonly used hosts to propagate influenza A virus are MDCK cells and chicken embryos. Normally passage of viruses for stock preparation was limited within one or two passages to avoid selecting mutations that occur during cross species propagation.

These synthetic viruses were passed on MDCK cells followed by another passage on MDCK, or on 10-day or 7-day old chicken embryos. All propagation approaches have only been performed once for each virus and only one plaque assay was done for titration. Viral titres got from different propagation approaches

Table 7: Summary of rescue attempt on HK backbone

HK backbone	number of rescue attempt	times of success	rate
HK/nsHKwt	9	5	55%
HK/nsMA20	7	0	0
HK/nsMA20c	7	0	0
HK/nsMA411	7	0	0
HK/nsMA511	7	3	42%
HK/nsMA531	7	5	71%

Table 8: Summary of rescue attempt on WSN backbone

WSN backbone	number of rescue attempt	times of success	rate
WSN	12	12	100%
WSN/nsHKwt	1	1	100%
WSN/nsMA20	1	1	100%
WSN/nsMA20c	1	1	100%
WSN/nsMA411	1	1	100%
WSN/nsMA511	1	1	100%
WSN/nsMA531	1	1	100%

were compared. The 7-day-old embryo has an immature IFN response. Viral replication was measure by plaque assay on MDCK cells (See Figure 18). Most of the rescued viruses yielded similar titres as around 10^8 pfu/ml from P2 stock, except WSN/nsMA20c had a slightly lower titre (10 fold lower) and WSN/nsMA411 was severely attenuated with a maximum yield of 10^5 pfu/ml. Two passages (P2) on MDCK cells gave the highest titre among the different propagation approaches: P1 (one passage on MDCK), P2 (two passages on MDCK), P1E(10d)1 (one passage on MDCK followed by one passage on 10-day-old chicken embryo), and P1E(7d)1 (one passage on MDCK followed by one passage on 7-day-old chicken embryo).

Each virus formed plaques on MDCK cells with two significantly different sizes. Basically, for all the synthetic recombinant viruses, titre of the population of large-size-plaque-forming virus was higher than titre of the population of small-size-plaque-forming virus. Viral yield and Plaque size are determined for all different stock preparations from the MDCK and embryonated egg and are described in appendix III.

3.6 IFN Resistance of Synthetic Recombinant Viruses

If the initial hypothesis is correct it is expected that recombinant influenza virus possessing the MA mutant NS1 proteins would have improved viral replication ability in the presence of mouse IFN when compared to wild type (wt) HK NS1 protein. One of the last objectives was to pinpoint the effect of IFN resistance of each individual MA mutation on NS1 protein contributed to the whole virus. First, the synthetic recombinant viruses were tested for their replication ability in the presence of IFN, or anti-IFN antibody. Four cell types were utilized: A549 (human epithelium), MRC5 (human fibroblast), M1 (murine epithelium), and MEF (murine fibroblast).

Figure 18: Replication Titres of Synthetic Recombinant Viruses (WSN/nsHK or MA#).

Each bar represents one plaque assay titration of one growth experiment. The rescued wild type WSN (as control), all synthetic recombinant viruses in WSN backbone are shown. Titres are expressed as common logarithm.

P1: one passage on MDCK cells; blue

P2: two passages on MDCK cells; pink

P1E(10D)1: one passage on MDCK cells followed by one passage in 10-day old embryonated eggs; light yellow

P1E(7D)1: one passage on MDCK cells followed by one passage in 7-day old embryonated eggs; light green

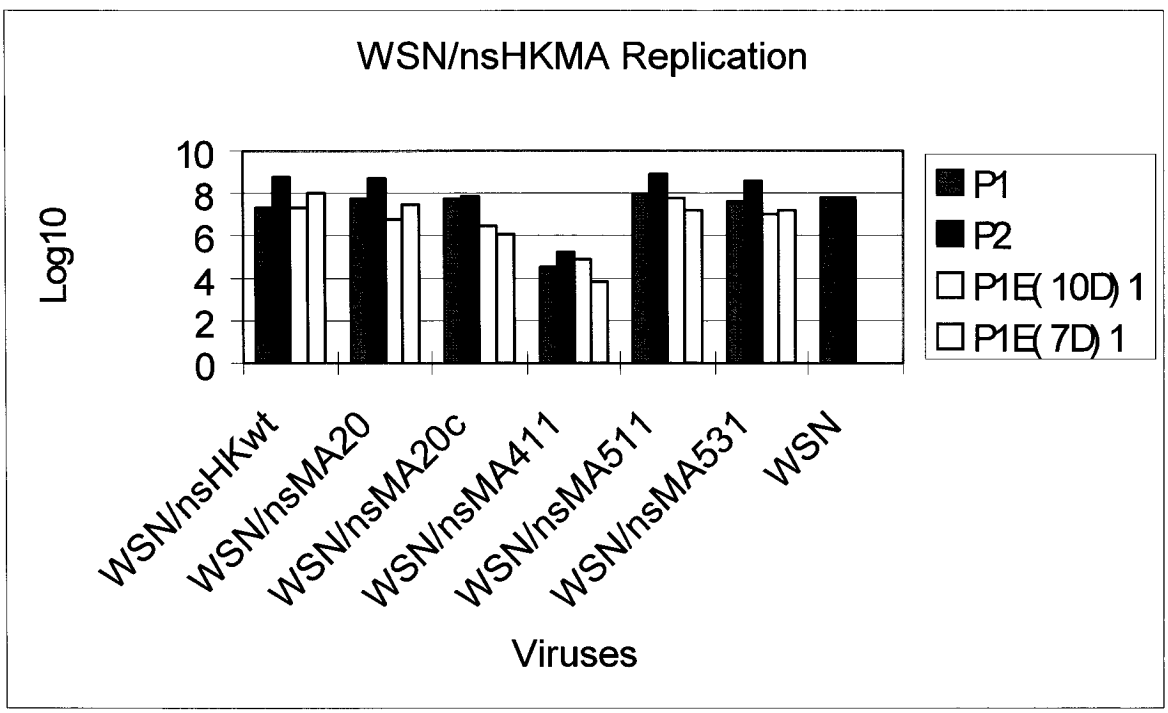
WSN/nsHKMA Replication
Log10
10
8
6
4
2
0
P1
P2
P1E(10D) 1
P1E(7D) 1
WSN/nsHKwt
WSN/nsMA20
WSN/nsMA20c
WSN/nsMA411
WSN/nsMA511
WSN/nsMA531
WSN
Viruses

This infection assay along with one plaque assay titration was repeated in each cell type respectively. Each graph represents data averaged from one cell type.

The synthetic recombinant viruses WSN/nsMA# were used to infect cells with or without (human or mouse) IFN treatment, or with anti-(human or mouse) IFN treatment. The MOI was 2 except for WSN/nsMA411 (MOI: 0.02) since the titre of this viral stock was only sufficient for this level of infection. For this reason, infection of WSN/nsMA411 was not directly comparable with the results of the other synthetic recombinant viruses.

Cell damage profiles on infection of A549 cells were shown by coomassie blue staining in Figure 19. Where both wt HK and MA mutants NS recombinant viruses destroyed untreated A549 monolayers, human IFN protected cells from infection and anti-human IFN antibody caused more extensive cell lysis with reduced staining. WSN/nsMA20c had the highest ability to cause cell death with IFN treatment, suggesting that it possessed the strongest IFN antagonist action. Viral replication titres in A549 cells were around 10^5 pfu/ml (See Figure 20a). According to the titre difference between infection and infection in the presence of human IFN, WSN/nsMA20, WSN/nsMA511 and WSN/nsMA531 were inhibited around 1000 fold, which was greater than seen for WSN/nsHKwt. IFN inhibited WSN/nsMA20c by 100 fold, which is less inhibition than seen for WSN/nsHKwt (See Figure 20b). None of the recombinant viruses gained a replication advantage by adding anti-human IFN (See Figure 20c).

Cell damage profiles on infection of MRC5 cells is shown in Figure 21 and was similar to that of A549 cells, where WSN/nsMA20c had the highest ability to cause cell death. Both human IFN and anti-human IFN antibody did not affect cell damage

Figure 19: Cell Damage Caused by Synthetic Recombinant Viruses (WSN/nsHK or MA#) on A549 Cells under the Treatment of Human IFN, No Treatment (n/t), or the Treatment of Anti-Human IFN.

A549 cells were infected by synthetic recombinant viruses (WSN/nsHK or MA#) with a MOI of 2 for 24 h. B plate received no treatment other than infection, C plate was treated with 1000 unit/well human IFN 24 h before infection, D plate was treated with 500 unit/well anti-human IFN after viral absorption to the cells, and the control well received no treatment.

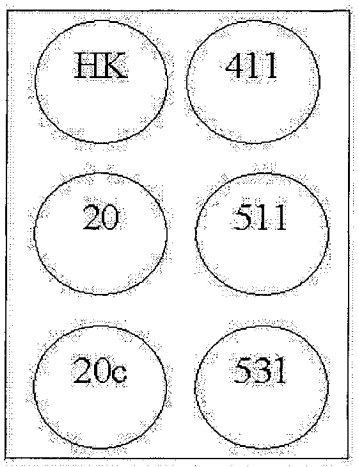

A 6-well dish layout for WSN series recombinant viruses infection

HK: WSN/nsHK	411: WSN/MA411
20: WSN/nsMA20	511: WSN/nsMA511
20c: WSN/nsMA20c	531: WSN/nsMA531

A: control

B: infection

C: infection with human IFN treatment 24 hour ahead

D: infection with anti-human IFN treatment

(A) A549 cell, control

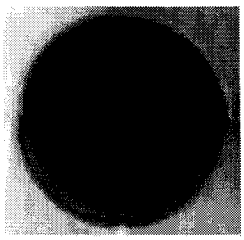

(B) infection, no treatment

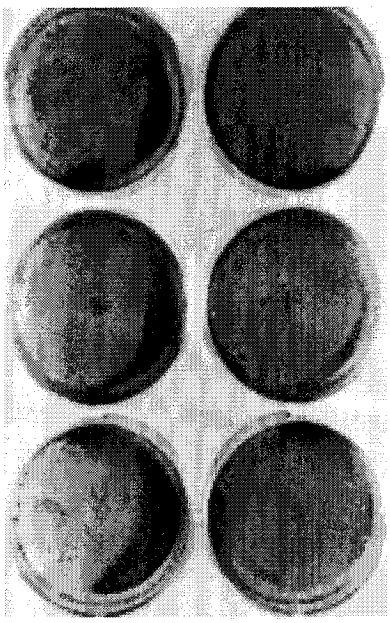

(C) human IFN treated

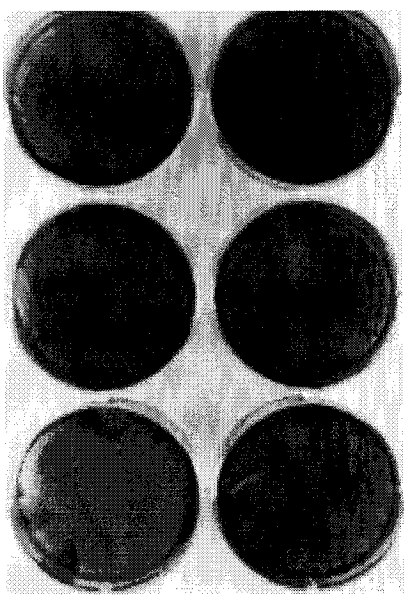

(D) anti-human IFN treated

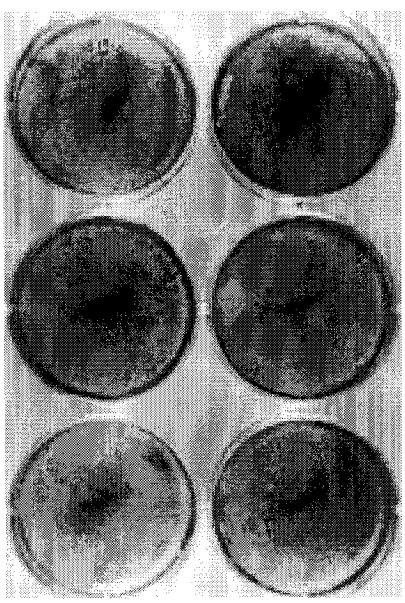

Figure 20a: Replication Titres of Synthetic Recombinant Viruses (WSN/nsHK or MA#) on A549 Cells with or without Treatment of Human IFN, or in the presence of Anti-Human IFN Antibody.

Each bar represents average from plaque assay titrations of two infection experiments on A549 cells, with error bars showing standard deviation. The WSN series recombinant viruses are all shown. Titres are expressed as common logarithm.

Infection with human IFN treatment: blue

Infection without treatment (no treatment –n/t): pink

Infection with anti-human IFN treatment: light yellow

Figure 20b: Difference in Titres of Synthetic Recombinant Viruses (WSN/nsHK or MA#) on A549 Cells with and without Treatment of Human IFN.

Each bar represents difference of titres between IFN treated infection and no treatment infection for each virus. The numbers are derived by dividing between the two titres.

Figure 20c: Difference in Titres of Synthetic Recombinant Viruses (WSN/nsHK or MA#) on A549 Cells without and with Treatment of Anti-Human IFN.

Each bar represents difference of titres between no treatment infection and anti-human IFN treated infection for each virus. The numbers are derived by dividing between the two titres.

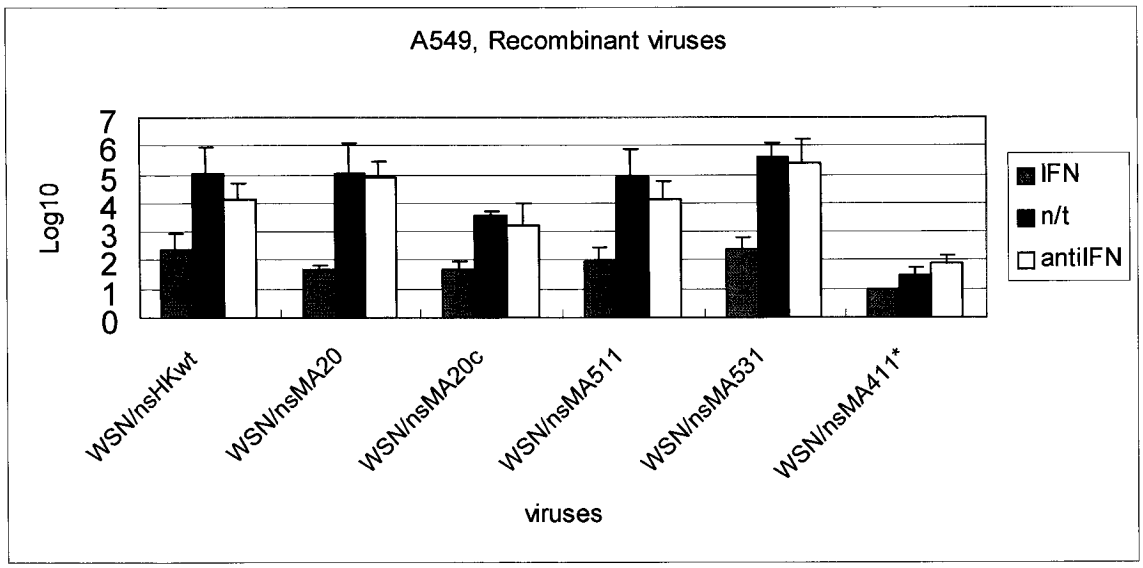
A549, Recombinant viruses
Log10
7
6
5
4
3
2
1
0
IFN
n/t
antiIFN
WSN/nsHKwt
WSN/nsMA20
WSN/nsMA20c
WSN/nsMA511
WSN/nsMA531
WSN/nsMA411*
viruses

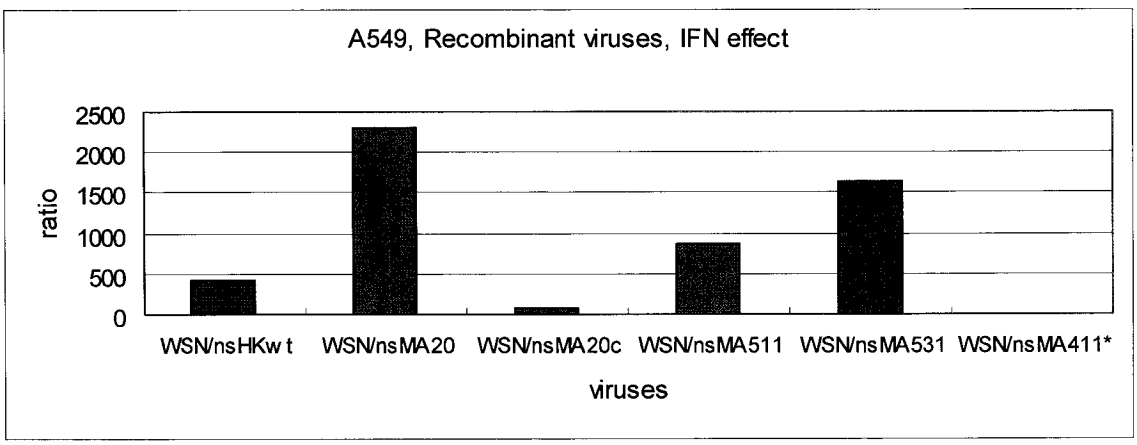
A549, Recombinant viruses, IFN effect
ratio
2500
2000
1500
1000
500
0
WSN/nsHKwt
WSN/nsMA20
WSN/nsMA20c
WSN/nsMA511
WSN/nsMA531
WSN/nsMA411*
viruses

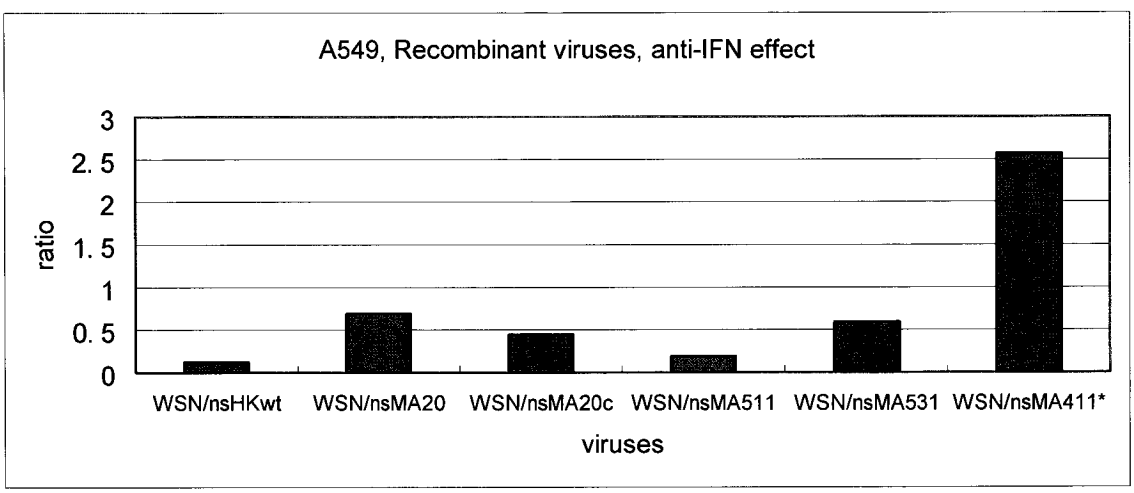
A549, Recombinant viruses, anti-IFN effect
ratio
3
2. 5
2
1. 5
1
0. 5
0
WSN/nsHKwt
WSN/nsMA20
WSN/nsMA20c
WSN/nsMA511
WSN/nsMA531
WSN/nsMA411*
viruses

relative to the untreated infection (See Figure 21). Viral replication titres in MRC5 cells were around 10^5 pfu/ml (See Figure 22a). According to the titre difference between infection in the presence and absence of human IFN, the WSN with MA mutant NS genes had similar difference as the WSN with HK NS wt gene which was around 500 fold difference, except WSN/nsMA20c, which was more resistant and had around 30 fold inhibition (See Figure 22b). Also similar to A549 cell, none of these viruses had improved replication in the presence of anti-human IFN (See Figure 22c).

Cell damage profiles on infection of M1 cells are shown in Figure 23. WSN/nsMA20c had the highest ability to cause cell death. Mouse IFN protected cells from infection. WSN/nsMA20c overcame the IFN response and caused comparable amounts of cell death as in the untreated infection. On the other hand, anti-mouse IFN antibody did not show a detectable affect on cell damage in comparison with the untreated infection. Replication titres on M1 cells were around 10^5 pfu/ml, except that WSN/nsMA20c had a very low titre, 10^3 pfu/ml, indicating that this mutatioin attenuated replication (See Figure 24a). According to the viral titre difference between infection and infection in the presence of mouse IFN, WSN/nsHKwt was the most IFN sensitive (See Figure 24b). All synthetic recombinant viruses possessing MA mutant NS1 gained more IFN resistance although WSN/nsMA511 had the smallest decrease in inhibition. All of these viruses demonstrated small increases in replication in the presence of anti-mouse IFN (See Figure 24c).

Cell damage profiles on infection of MEF cells are shown on Figure 25. In

Figure 21: Cell Damage Caused by Synthetic Recombinant Viruses (WSN/nsHK or MA#) on MRC5 Cells under the Treatment of Human IFN, No Treatment (n/t), or the Treatment of Anti-Human IFN.

MRC5 cells were infected by synthetic recombinant viruses (WSN/nsHK or MA#) with a MOI of 2 for 24 h. B plate received no treatment other than infection, C plate was treated with 1000 unit/well human IFN 24 h before infection, D plate was treated with 500 unit/well anti-human IFN after viral absorption to the cells, and the control well received no treatment.

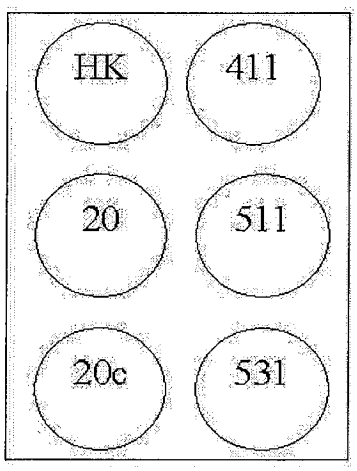

A 6-well dish layout for WSN series recombinant viruses infection

HK: WSN/nsHK	411: WSN/MA411
20: WSN/nsMA20	511: WSN/nsMA511
20c: WSN/nsMA20c	531: WSN/nsMA531

A: control

B: infection

C: infection with human IFN treatment 24 hour ahead

D: infection with anti-human IFN treatment

(A) MRC5 cell, control

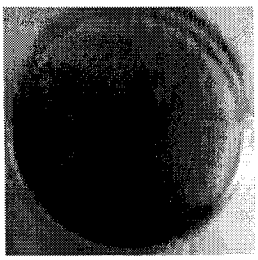

(B) infection, no treatment

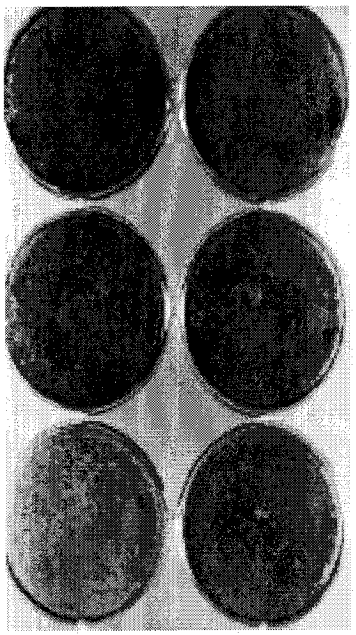

(C) human IFN treated

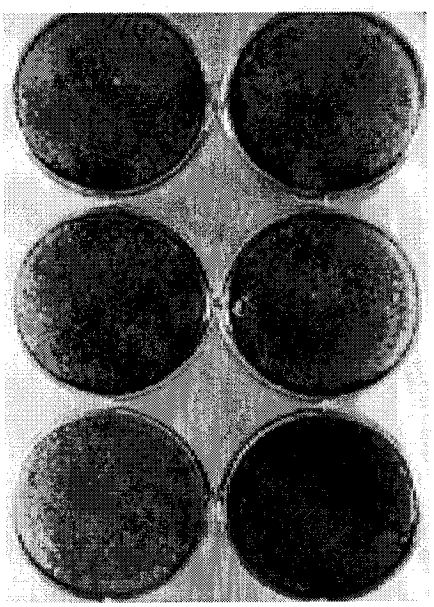

(D) anti-human IFN treated

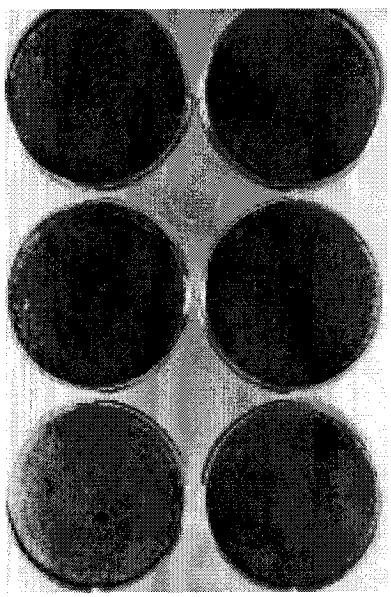

Figure 22a: Replication Titres of Synthetic Recombinant Viruses (WSN/nsHK or MA#) on MRC5 Cells with or without Treatment of Human IFN, or in the presence of Anti-Human IFN Antibody.

Each bar represents average from plaque assay titrations of two infection experiments on MRC5 cells, with error bars showing standard deviation. The WSN series recombinant viruses are all shown. Titres are expressed as common logarithm.

Infection with human IFN treatment: blue

Infection without treatment (no treatment –n/t): pink

Infection with anti-human IFN treatment: light yellow

Figure 22b: Difference in Titres of Synthetic Recombinant Viruses (WSN/nsHK or MA#) on MRC5 Cells with and without Treatment of Human IFN.

Each bar represents difference of titres between human IFN treated infection and no treatment infection for each virus. The numbers are derived by dividing between the two titres.

Figure 22c: Difference in Titres of Synthetic Recombinant Viruses (WSN/nsHK or MA#) on MRC5 Cells without and with Treatment of Anti-Human IFN.

Each bar represents difference of titres between no treatment infection and anti-human IFN treated infection for each virus. The numbers are derived by dividing between the two titres.

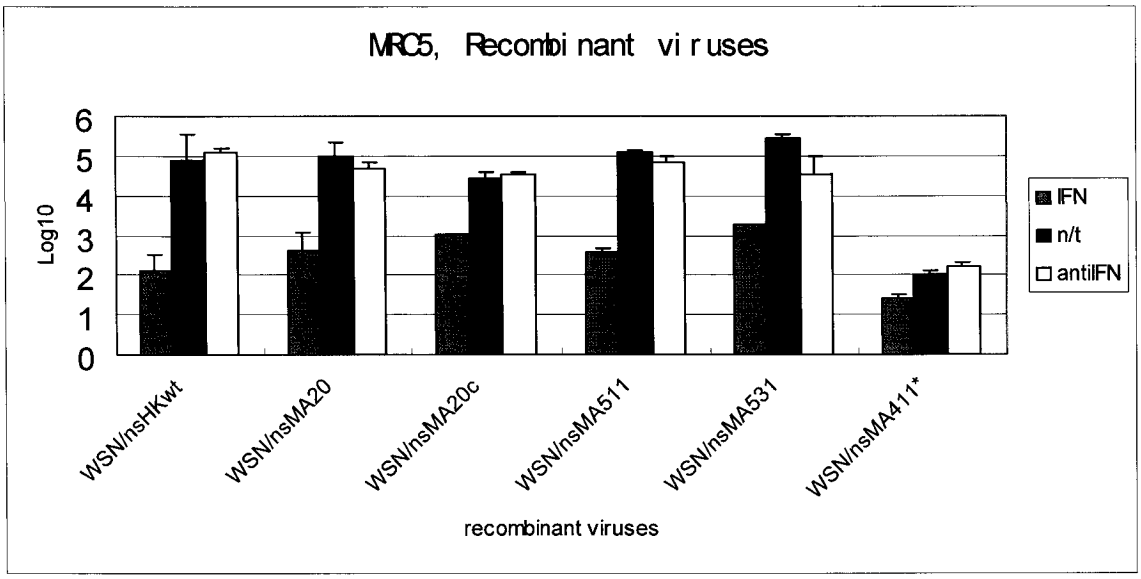
MRC5, Recombinant viruses
Log10
6
5
4
3
2
1
0
IFN
n/t
antiIFN
WSN/nsHKwt
WSN/nsMA20
WSN/nsMA20c
WSN/nsMA511
WSN/nsMA531
WSN/nsMA411*
recombinant viruses

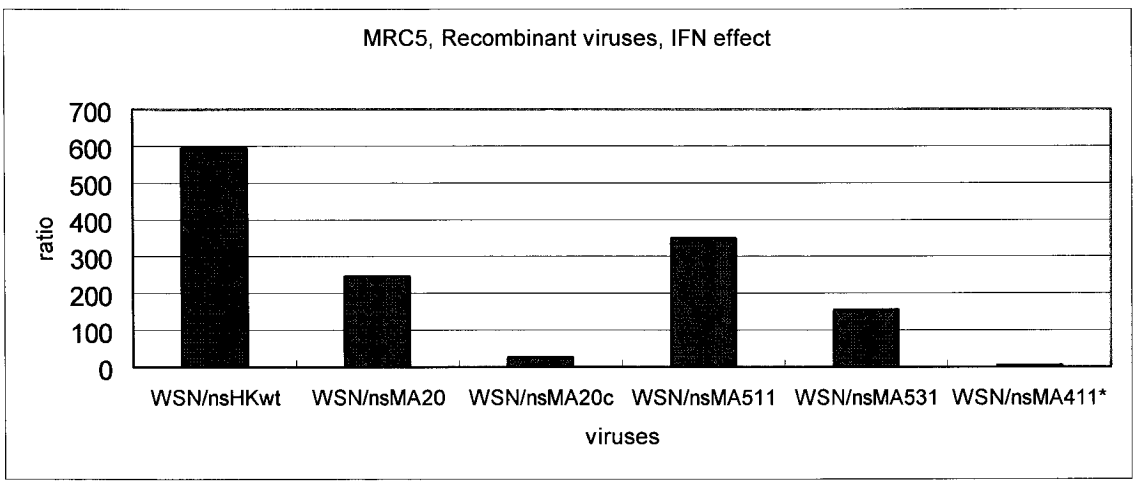
MRC5, Recombinant viruses, IFN effect
ratio
700
600
500
400
300
200
100
0
WSN/nsHKwt
WSN/nsMA20
WSN/nsMA20c
WSN/nsMA511
WSN/nsMA531
WSN/nsMA411*
viruses

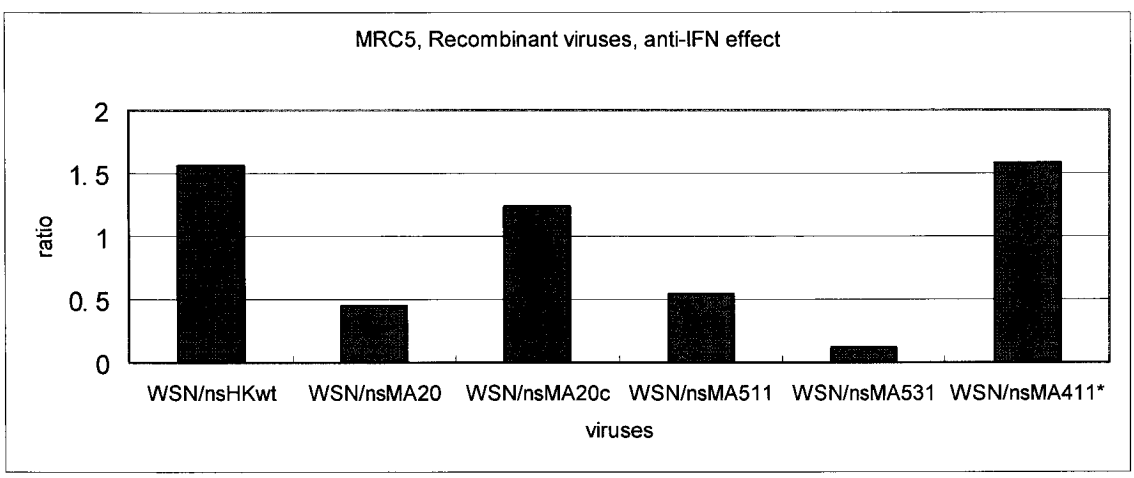
MRC5, Recombinant viruses, anti-IFN effect
ratio
2
1.5
1
0.5
0
WSN/nsHKwt
WSN/nsMA20
WSN/nsMA20c
WSN/nsMA511
WSN/nsMA531
WSN/nsMA411*
viruses

Figure 23: Cell Damage Caused by Synthetic Recombinant Viruses (WSN/nsHK or MA#) on M1 Cells under the Treatment of Mouse IFN, No Treatment (n/t), or the Treatment of Anti-Mouse IFN.

M1 cells were infected by synthetic recombinant viruses (WSN/nsHK or MA#) with a MOI of 2 for 24 h. B plate received no treatment other than infection, C plate was treated with 100 unit/well mouse IFN 24 h before infection, D plate was treated with 1000 unit/well anti-mouse IFN after viral absorption to the cells, and the control well received no treatment.

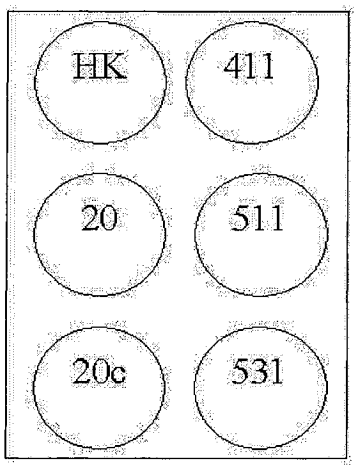

A 6-well dish layout for WSN series recombinant viruses infection

HK: WSN/nsHK 411: WSN/nsMA411
20: WSN/nsMA20 511: WSN/nsMA511
20c: WSN/nsMA20c 531: WSN/nsMA531

A: control

B: infection

C: infection with mouse IFN treatment 24 hour ahead

D: infection with anti-mouse IFN treatment

(A) M1cell, control

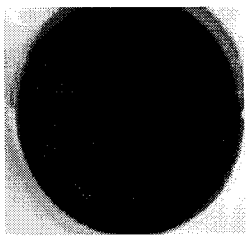

(B) infection, no treatment

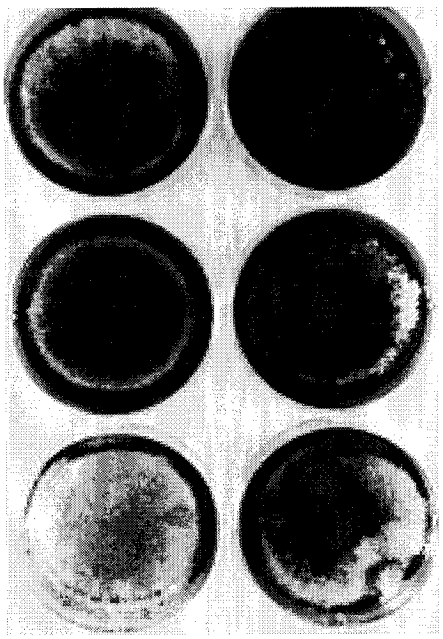

(C) mouse IFN treated

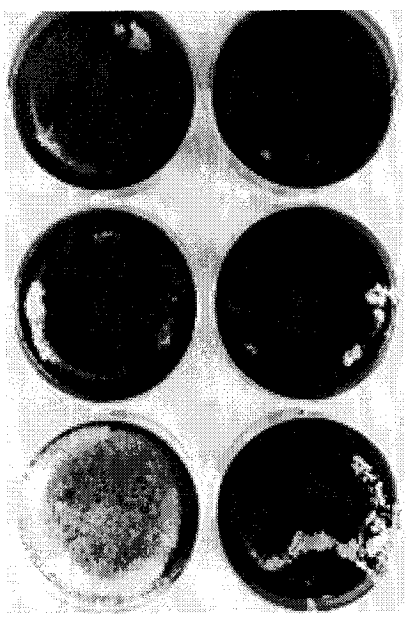

(D) anti-mouse IFN treated

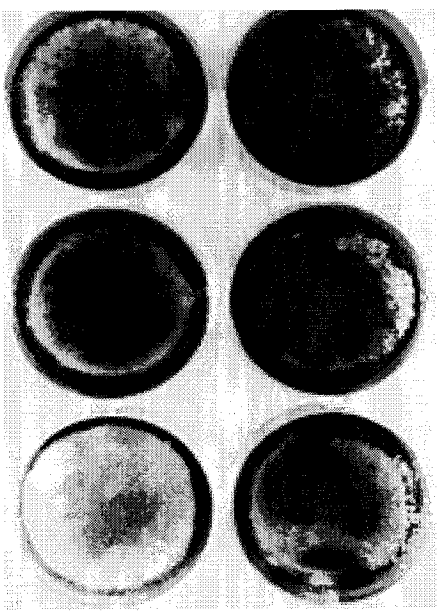

Figure 24a: Replication Titres of Synthetic Recombinant Viruses (WSN/nsHK or MA#) on M1 Cells with or without Treatment of Mouse IFN, or in the presence of Anti-Mouse IFN Antibody.

Each bar represents average from plaque assay titrations of two infection experiments on M1 cells, with error bars showing standard deviation. The WSN series recombinant viruses are all shown. Titres are expressed as common logarithm.

Infection with human IFN treatment: blue

Infection without treatment (no treatment –n/t): pink

Infection with anti-human IFN treatment: light yellow

Figure 24b: Difference in Titres of Synthetic Recombinant Viruses (WSN/nsHK or MA#) on M1 Cells with and without Treatment of Mouse IFN.

Each bar represents difference of titres between mouse IFN treated infection and no treatment infection for each virus. The numbers are derived by dividing between the two titres.

Figure 24c: Difference in Titres of Synthetic Recombinant Viruses (WSN/nsHK or MA#) on M1 Cells without and with Treatment of Anti-Mouse IFN.

Each bar represents difference of titres between no treatment infection and anti-mouse IFN treated infection for each virus. The numbers are derived by dividing between the two titres.

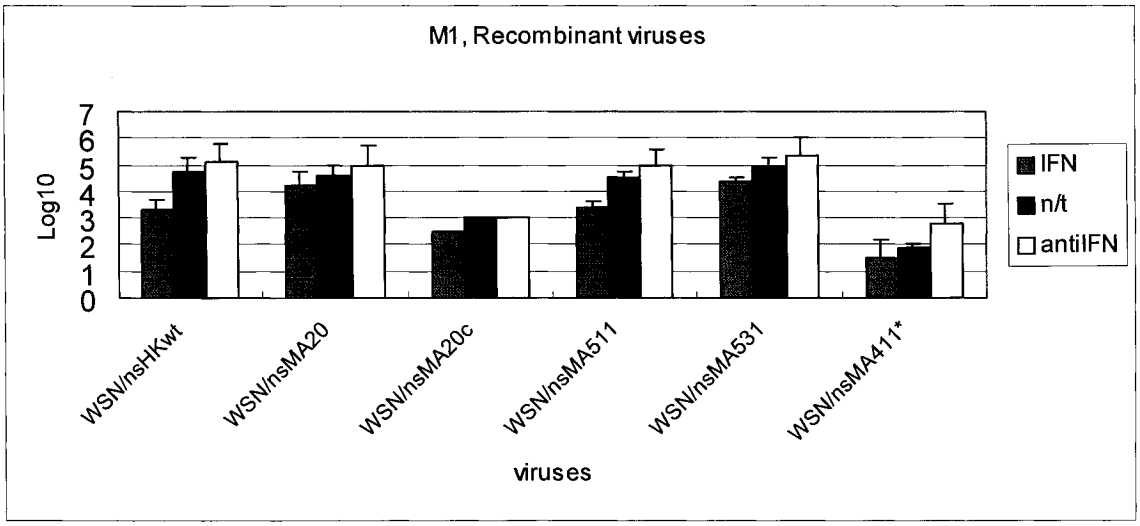
M1, Recombinant viruses
Log10
7
6
5
4
3
2
1
0
IFN
n/t
antiIFN
WSN/nsHKwt
WSN/nsMA20
WSN/nsMA20c
WSN/nsMA511
WSN/nsMA531
WSN/nsMA411*
viruses

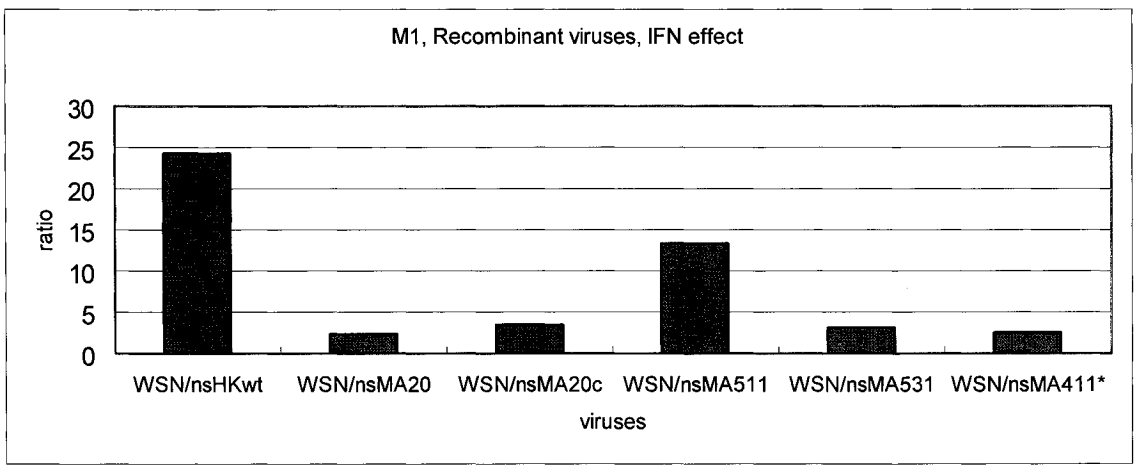
M1, Recombinant viruses, IFN effect
ratio
30
25
20
15
10
5
0
WSN/nsHKwt
WSN/nsMA20
WSN/nsMA20c
WSN/nsMA511
WSN/nsMA531
WSN/nsMA411*
viruses

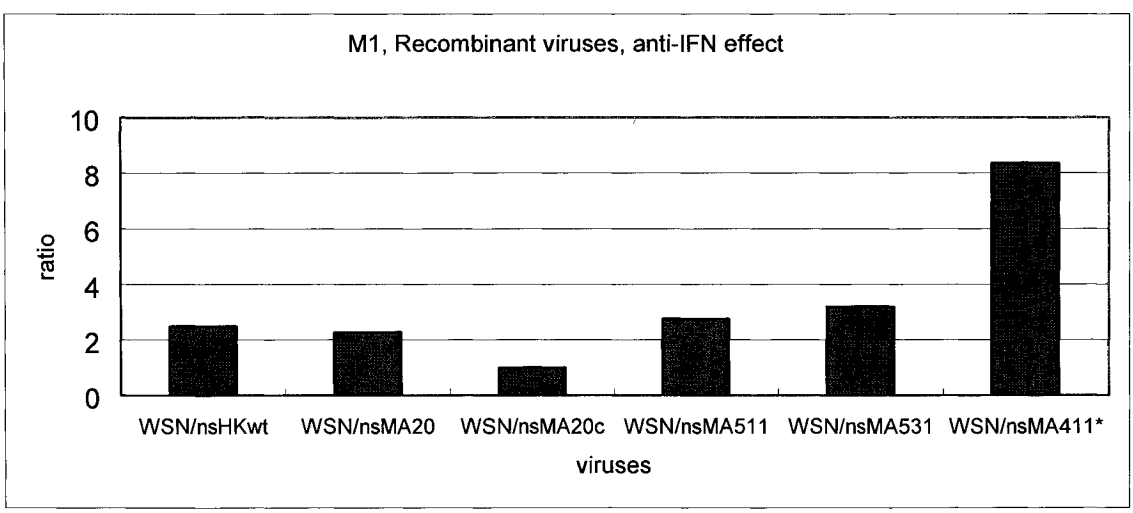
M1, Recombinant viruses, anti-IFN effect
ratio
10
8
6
4
2
0
WSN/nsHKwt
WSN/nsMA20
WSN/nsMA20c
WSN/nsMA511
WSN/nsMA531
WSN/nsMA411*
viruses

infection without IFN or anti-IFN, WSN/nsMA20c infection had the least amount of cell viability, with WSN/nsMA20 and WSN/nsMA531 causing more cell destruction than the other infections. Mouse IFN showed protection on infections of WSN/nsMA20, and WSN/nsMA531. Except in WSN/nsMA411 infection, anti-mouse IFN antibody enhanced the viruses' ability to kill cells in infection. Viral replication titres on MEF cells were around 10^4 to 10^5 pfu/ml, except that WSN/nsMA20c had 10^3 pfu/ml (See Figure 26a). With respect to IFN resistance, most of the MA mutant NS gene variants were similar to HKwt that was inhibited 40 fold. Two of the MA mutant NS variants, 20c and 531 were more resistant to IFN and showed less than 10 fold inhibition (See Figure 26b). None of the viruses produced significantly more infectious yield in the presence of anti-mouse IFN (See Figure 26c).

3.7 IFN Induction of Synthetic Recombinant Viruses

Regulation of host IFN production is another way that the virus can demonstrate its anti-IFN mechanism. Influenza viruses as described earlier have mechanisms that inhibit host IFN production. However, some virulent viruses, like HPAI H5N1, have been reported to enhance expression of proinflammatory cytokines including IFN. The pathology of those viruses involved proinflammatory - anti-inflammatory cytokine imbalance (Cheung et al, 2002; Fisman, 2000; Headley et al, 1997; To et al, 2001). The last step of this project was to clarify the ability of the synthetic recombinant viruses containing the MA mutant NS1 proteins to induce IFN production.

3.7.1 IFN Assay

The principle of IFN assay is the biology of vesicular stomatitis virus (VSV) of highly sensitivity to IFN. Cells synthesize and secrete IFN into cell culture

Figure 25: Cell Damage Caused by Synthetic Recombinant Viruses (WSN/nsHK or MA#) on MEF Cells under the Treatment of Mouse IFN, No Treatment (n/t), or the Treatment of Anti-Mouse IFN.

MEF cells were infected by synthetic recombinant viruses (WSN/nsHK or MA#) with a MOI of 2 for 24 h. B plate received no treatment other than infection, C plate was treated with 100 unit/well mouse IFN 24 h before infection, D plate was treated with 1000 unit/well anti-mouse IFN after viral absorption to the cells, and the control well received no treatment.

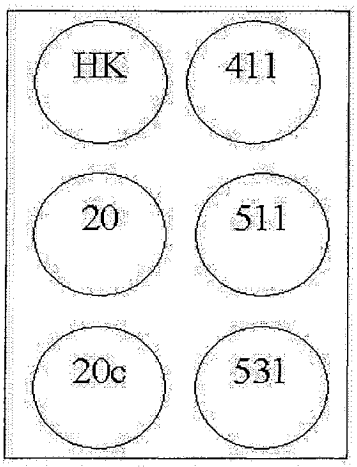

A 6-well dish layout for WSN series recombinant viruses infection

HK: WSN/nsHK 411: WSN/nsMA411
20: WSN/nsMA20 511: WSN/nsMA511
20c: WSN/nsMA20c 531: WSN/nsMA531

A: control

B: infection

C: infection with mouse IFN treatment 24 hour ahead

D: infection with anti-mouse IFN treatment

(A) MEF cell, control

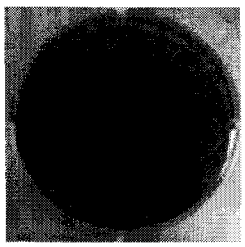

(B) infection, no treatment

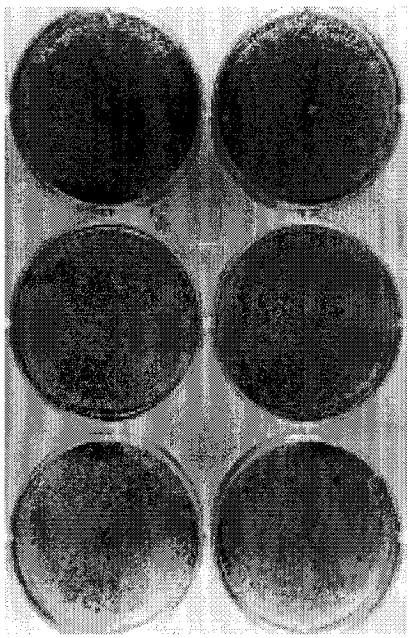

(C) mouse IFN treated

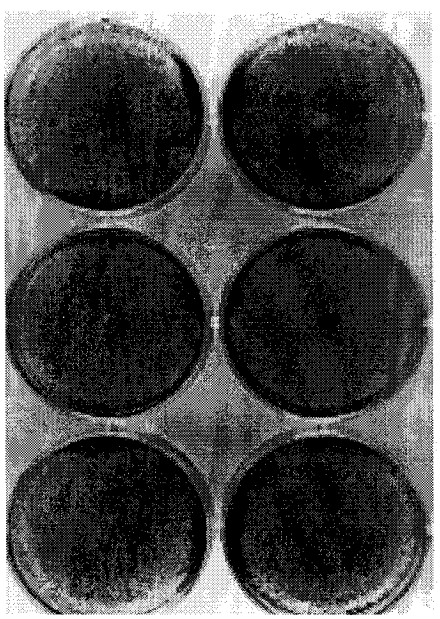

(D) anti-mouse IFN treated

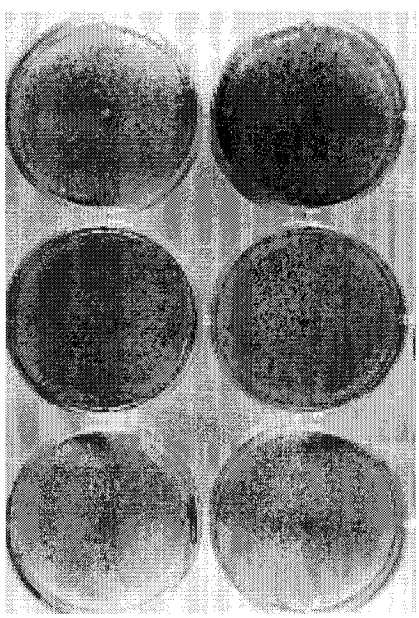

Figure 26a: Replication Titres of Synthetic Recombinant Viruses (WSN/nsHK or MA#) on MEF Cells with or without Treatment of Mouse IFN, or in the presence of Anti-Mouse IFN Antibody.

Each bar represents average from plaque assay titrations of two infection experiments on M1 cells, with error bars showing standard deviation. The WSN series recombinant viruses are all shown. Titres are expressed as common logarithm.

Infection with human IFN treatment: blue

Infection without treatment (no treatment –n/t): pink

Infection with anti-human IFN treatment: light yellow

Figure 26b: Difference in Titres of Synthetic Recombinant Viruses (WSN/nsHK or MA#) on MEF Cells with and without Treatment of Mouse IFN.

Each bar represents difference of titres between no treatment infection and anti-mouse IFN treated infection for each virus. The numbers are derived by dividing between the two titres.

Figure 26c: Difference in Titres of Synthetic Recombinant Viruses (WSN/nsHK or MA#) on MEF Cells without and with Treatment of Anti-Mouse IFN.

Each bar represents difference of titres between no treatment infection and anti-mouse IFN treated infection for each virus. The numbers are derived by dividing between the two titres.

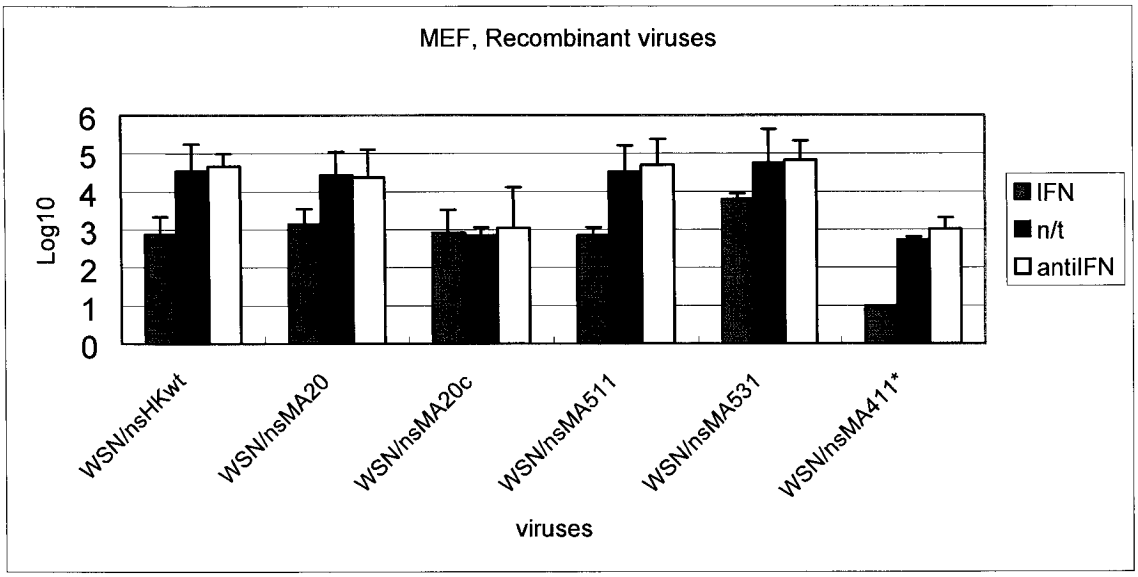
MEF, Recombinant viruses
Log10
6
5
4
3
2
1
0
IFN
n/t
antiIFN
WSN/nsHKwt
WSN/nsMA20
WSN/nsMA20c
WSN/nsMA511
WSN/nsMA531
WSN/nsMA411*
viruses

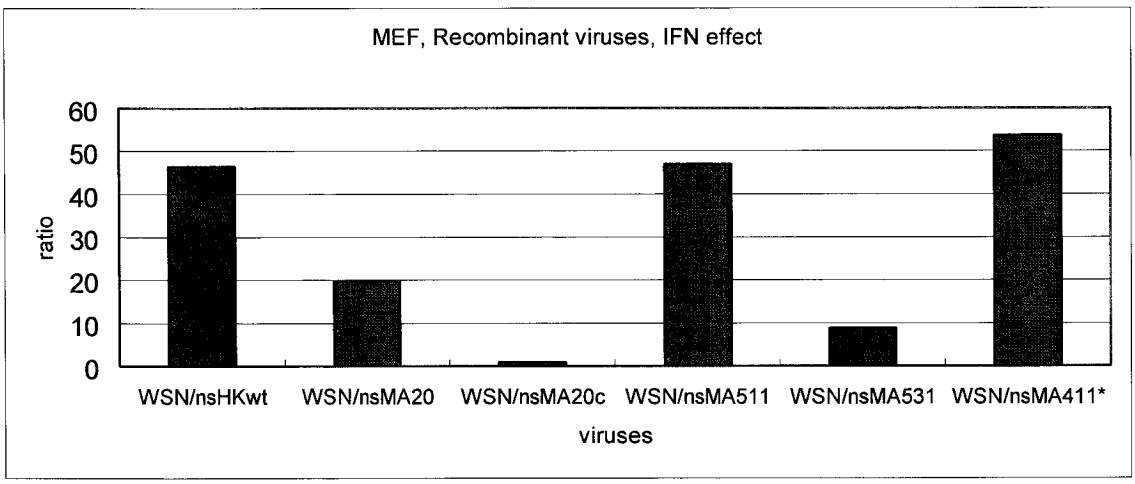
MEF, Recombinant viruses, IFN effect
ratio
60
50
40
30
20
10
0
WSN/nsHKwt
WSN/nsMA20
WSN/nsMA20c
WSN/nsMA511
WSN/nsMA531
WSN/nsMA411*
viruses

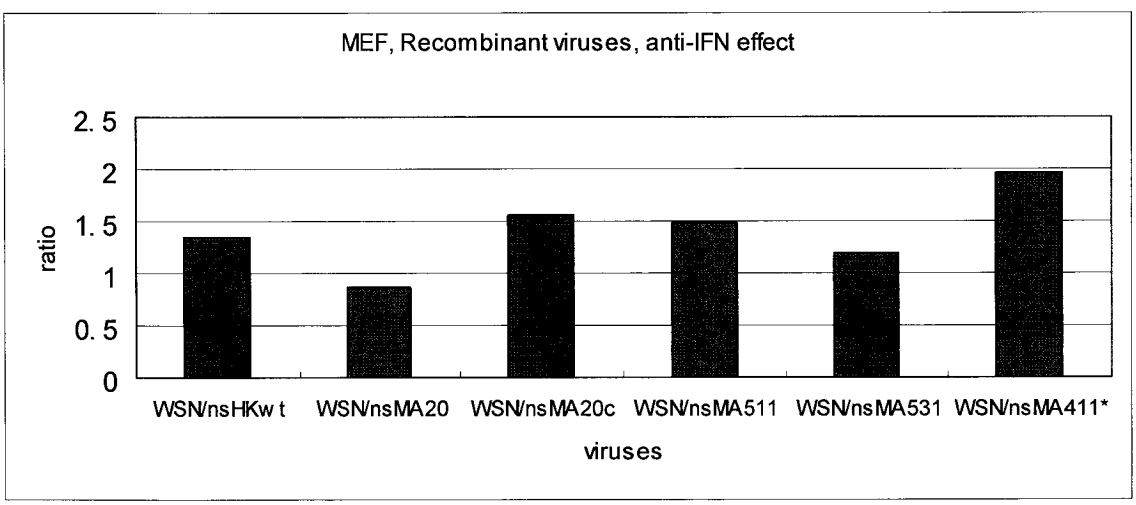
MEF, Recombinant viruses, anti-IFN effect
ratio
2.5
2
1.5
1
0.5
0
WSN/nsHKwt
WSN/nsMA20
WSN/nsMA20c
WSN/nsMA511
WSN/nsMA531
WSN/nsMA411*
viruses

supernatant when they are infected by viruses. Cells should be protected from VSV infection if they are incubated with IFN containing supernatant. IFN assays of each cell type were performed twice testing samples from different infections. Assays got same trend in the repeated one for each cell type respectively. Each graph represents only one assay. In this Assay, 10 unit/ml is the lowest limit of sensitivity in measurement.

The amounts of IFN generated from infection of synthetic recombinant viruses were measured. Infection of A549 cells, consistent with the earlier results from infection of HK and MA variants, produced poor amounts of IFN (See Figure 27a), which was consistent with other document (Ronni T., 1997). On two other human cell lines, Hela and MRC5, WSN/nsMA20c induced 20 unit/ml of IFN, while the other synthetic recombinant viruses all induced less than 10 unit/ml (See Figure 27b and c). For infection of M1 cells, two assays were performed and WSN/nsMA20c induced over 1000 unit/ml mouse IFN, being 5 fold higher than all other synthetic recombinant viruses, which induced two to several hundred units/ml (See Figure 28). WSN/nsHKwt induced similar amounts of mouse IFN as the synthetic recombinant viruses containing MA mutant NS1 proteins other than 20c. Infection on MEF cells, yielded similar amounts of IFN as seen for the M1 cells with WSN/nsMA20c inducing the highest titre of mouse IFN (See Figure 29).

3.7.2 IFN ELISA

To confirm that the synthetic recombinant viruses induced low amount of IFN in the human cell assays, all the infected cell supernatants from human cells were tested utilizing an ELISA kit detecting human IFN-β. All samples were tested in duplicate manner. The ELISA detection range was from 250 pg/ml to 10,000 pg/ml

(See Figure 30a). The absorptions of all the samples from A549 cells, Hela cells, and MRC5 cells were less than the reading for 250 pg/ml IFN-β which represents 10 to 25 units/ml of IFN-β (10~25 pg/unit) (See Figure 30b, c, and d). This result confirmed that these viruses induced low amount of IFN in these human cells.

Figure 27a: Induction of Human IFN by Synthetic Recombinant Viruses (WSN/nsHK or MA#) on A549 Cells.

IFN quantities were tested by IFN assay for two infection experiments on A549 cells of WSN series recombinant viruses. Each bar represents the average of specific units induced by each virus average in two experiments. Ten units is the lowest amount of IFN that can be accurately detected in this assay.

Figure 27b: Induction of Human IFN by Synthetic Recombinant Viruses (WSN/nsHK or MA#) on Hela Cells.

Induced IFN amount were tested by IFN assay for two infection experiments on Hela cells of WSN series recombinant viruses. Each bar represents specific units induced by each virus average from two experiments. Ten units is the lowest amount of IFN that can be accurately detected in this assay.

Figure 27c: Induction of Human IFN by Synthetic Recombinant Viruses (WSN/nsHK or MA#) on MRC5 Cells.

Induced IFN amount were tested by IFN assay for two infection experiments on MRC5 cells of WSN series recombinant viruses. Each bar represents specific units induced by each virus average from two experiments. Ten units is the lowest amount of IFN that can be accurately detected in this assay.

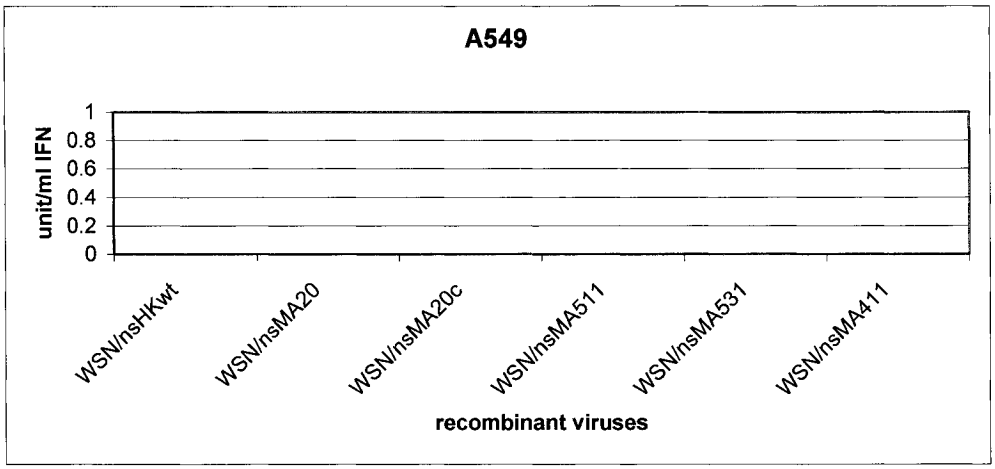
A549
unit/ml IFN
1
0.8
0.6
0.4
0.2
0
WSN/nsHKwt
WSN/nsMA20
WSN/nsMA20c
WSN/nsMA511
WSN/nsMA531
WSN/nsMA411
recombinant viruses

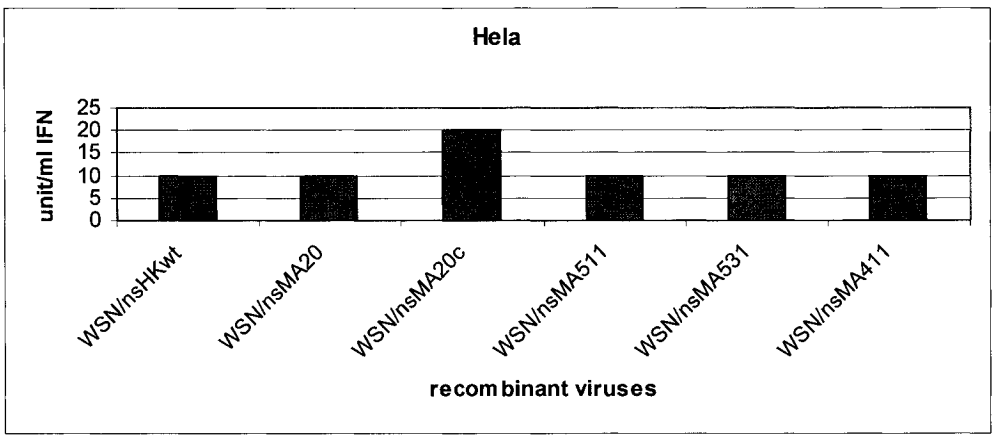
Hela
unit/ml IFN
25
20
15
10
5
0
WSN/nsHKwt
WSN/nsMA20
WSN/nsMA20c
WSN/nsMA511
WSN/nsMA531
WSN/nsMA411
recombinant viruses

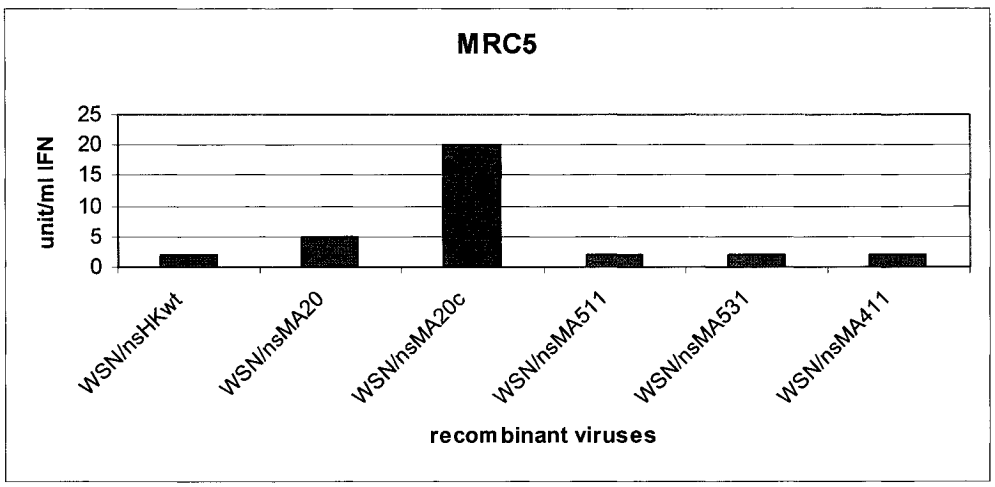
MRC5
unit/ml IFN
25
20
15
10
5
0
WSN/nsHKwt
WSN/nsMA20
WSN/nsMA20c
WSN/nsMA511
WSN/nsMA531
WSN/nsMA411
recombinant viruses

Figure 28a: Induction of Mouse IFN by Synthetic Recombinant Viruses (WSN/nsHK or MA#) on M1 cells.

Induced IFN amount were tested by IFN assay for one infection experiment on M1 cells of WSN series recombinant viruses. Each bar represents specific units induced by each virus. Ten units is the lowest amount of IFN that can be accurately detected in this assay.

Figure 28b: Induction of Mouse IFN by Synthetic Recombinant Viruses (WSN/nsHK or MA#) on M1 cells, a duplicate experiment as the previous one.

Induced IFN amount were tested by IFN assay for a separate infection experiment from the previous one on M1 cells of WSN series recombinant viruses. Each bar represents specific units induced by each virus. Ten units is the lowest amount of IFN that can be accurately detected in this assay.

Figure 29: Induction of Mouse IFN by Synthetic Recombinant Viruses (WSN/nsHK or MA#) on MEF cells.

Induced IFN amount were tested by IFN assay for one infection experiment on MEF cells of WSN series recombinant viruses. Each bar represents specific units induced by each virus. Ten units is the lowest amount of IFN that can be accurately detected in this assay.

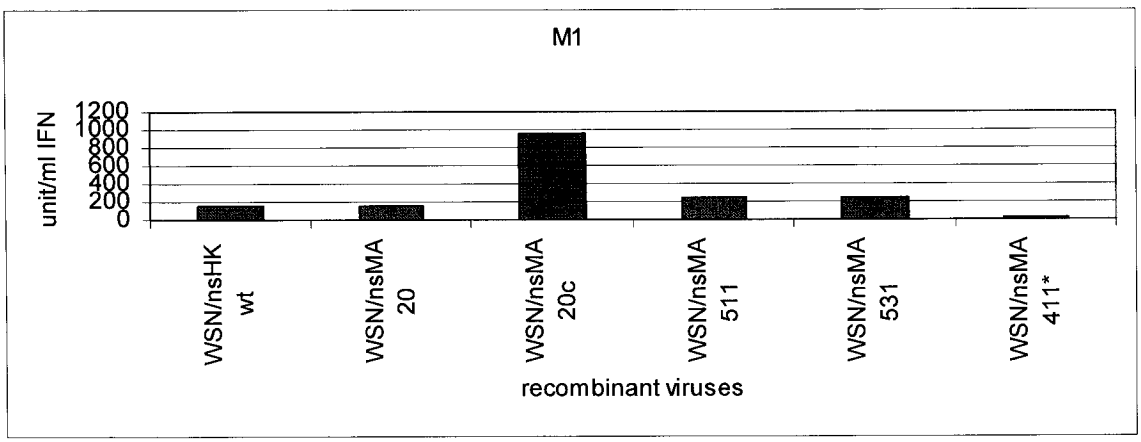
M1
unit/ml IFN
1200
1000
800
600
400
200
0
WSN/nsHK wt
WSN/nsMA 20
WSN/nsMA 20c
WSN/nsMA 511
WSN/nsMA 531
WSN/nsMA 411*
recombinant viruses

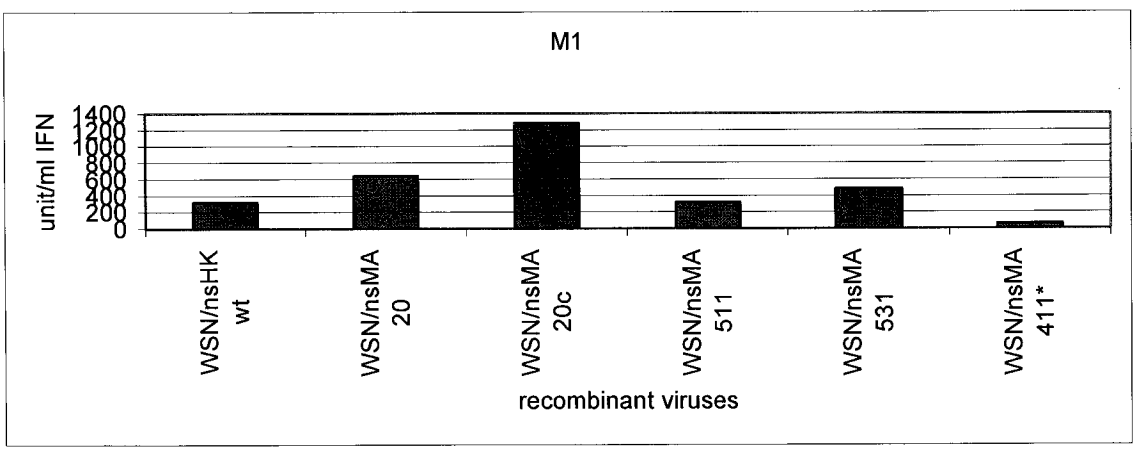
M1
unit/ml IFN
1400
1200
1000
800
600
400
200
0
WSN/nsHK wt
WSN/nsMA 20
WSN/nsMA 20c
WSN/nsMA 511
WSN/nsMA 531
WSN/nsMA 411*
recombinant viruses

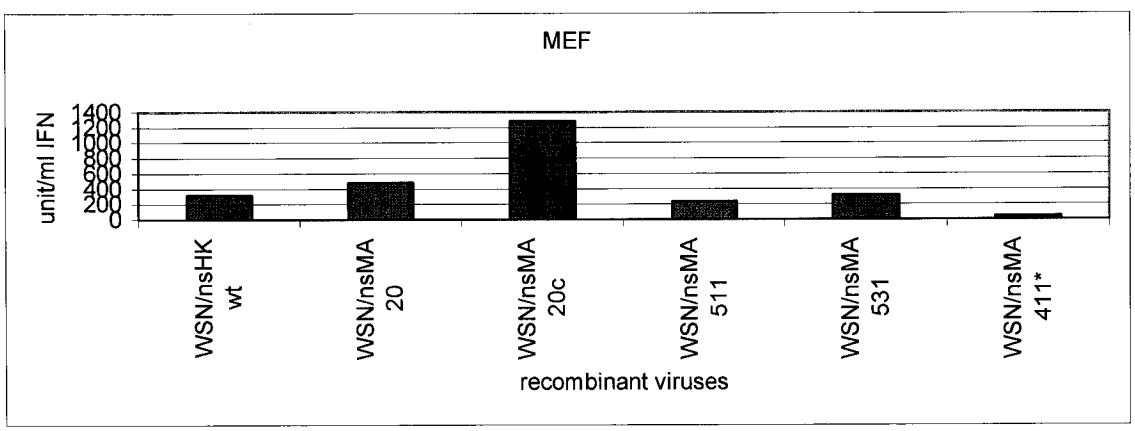
MEF
unit/ml IFN
1400
1200
1000
800
600
400
200
0
WSN/nsHK wt
WSN/nsMA 20
WSN/nsMA 20c
WSN/nsMA 511
WSN/nsMA 531
WSN/nsMA 411*
recombinant viruses

Figure 30a: Absorbance of Different amounts of Human IFN-β.

This graph was made to serve as a standard curve. The IFN titre in the samples can be determined by comparison.

Figure 30b: Absorbance of Human IFN induced by Synthetic Recombinant Viruses (WSN/nsHK or MA#) on A549 Cells.

Samples of two infections on A549 cells of WSN series recombinant viruses were tested. Titres of IFN are read by comparing the absorbance with the standard curve.

Figure 30c: Absorbance of Human IFN induced by Synthetic Recombinant Viruses (WSN/nsHK or MA#) on Hela Cells

Samples of two infections on Hela cells of WSN series recombinant viruses were tested. Titres of IFN are read by comparing the absorbance with the standard curve.

Figure 30d: Absorbance of Human IFN induced by Synthetic Recombinant Viruses (WSN/nsHK or MA#) on MRC5 Cells

Samples of two infections on MRC5 cells of WSN series recombinant viruses were tested. Titres of IFN are read by comparing the absorbance with the standard curve.

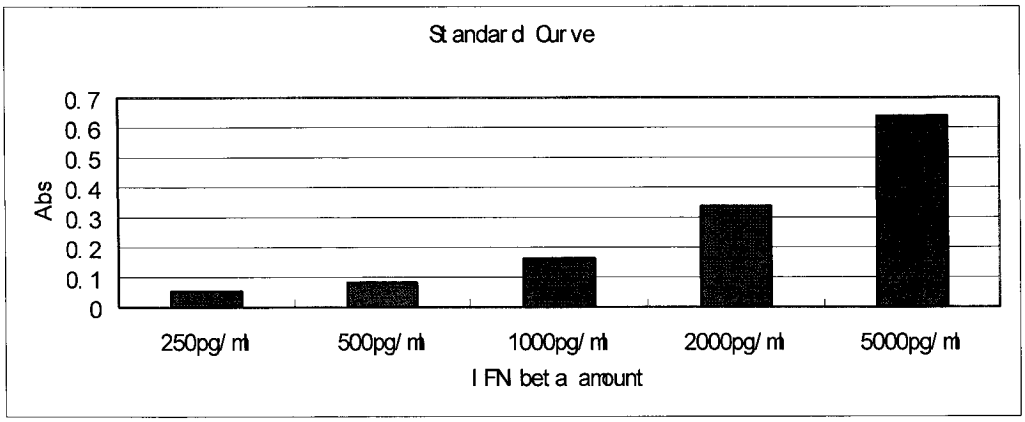
Standard Curve
0.7
0.6
0.5
0.4
0.3
0.2
0.1
0
Abs
250pg/ml
500pg/ml
1000pg/ml
2000pg/ml
5000pg/ml
IFN beta amount

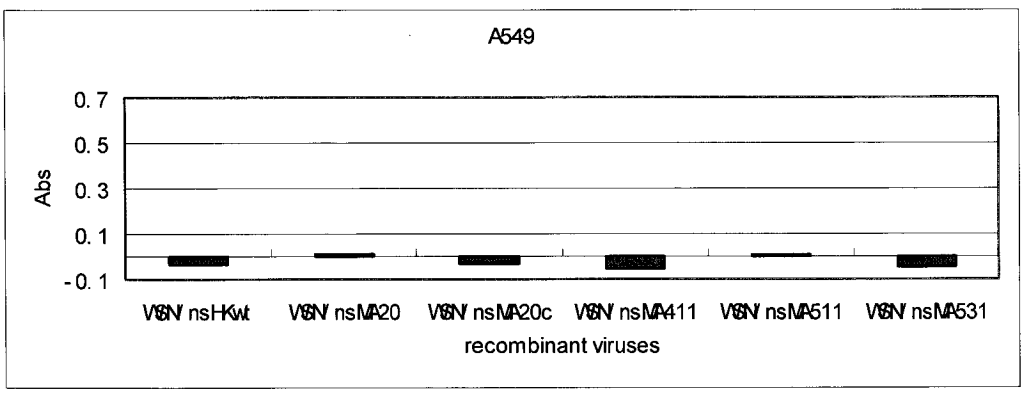
A549
0.7
0.5
0.3
0.1
-0.1
Abs
VSNV nsHKwt
VSNV nsMA20
VSNV nsMA20c
VSNV nsMA411
VSNV nsMA511
VSNV nsMA531
recombinant viruses

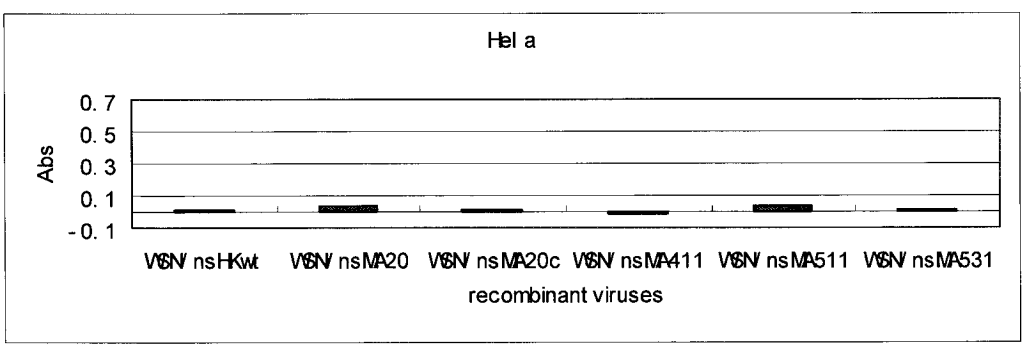
Hela
0.7
0.5
0.3
0.1
-0.1
Abs
VSNV nsHKwt
VSNV nsMA20
VSNV nsMA20c
VSNV nsMA411
VSNV nsMA511
VSNV nsMA531
recombinant viruses

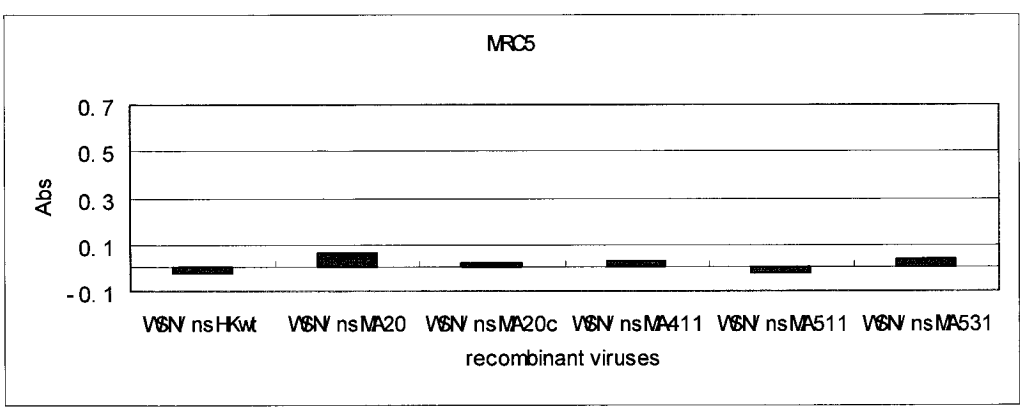
MRC5
0.7
0.5
0.3
0.1
-0.1
Abs
VSNV nsHKwt
VSNV nsMA20
VSNV nsMA20c
VSNV nsMA411
VSNV nsMA511
VSNV nsMA531
recombinant viruses

Discussion

4.1 Introduction

The purpose of this study was to assess the contribution of changes in the interferon antagonist gene, NS1, during the process of adaptation to a new host. It has been clearly demonstrated that the NS1 protein functions as an IFN antagonist and this function is required for normal infection (Donelan et al., 2003; Kittel et al., 2004; Marcus et al., 2005; Talon et al., 2000; Wang et al., 2000). More recently it has been shown that the highly virulent H5N1 z strain is resistant to IFN and infection with this virus results in cytokine hyperinduction which is responsible for inducing the hemophagocytic syndrome in human infection (Fisman 2000; Headley et al., 1997; To et al., 2001). It was reported that H5N1 viruses induced much higher expression of proinflammatory cytokines than did H3N2 or H1N1, particularly TNF-α and IFN-β, in macrophage cell culture (Cheung et al., 2002)

Series of mouse-adapted viruses were studied within this project. Human influenza A virus A/HK/1/68 (H3N2) was chosen for adaptation to mouse because it had no murine adaptation history and was initially avirulent to mice. What makes the mouse model even more useful for influenza A virus study is that the viral pneumonia induced in the mouse resembles the most severe complication of this disease in humans: interstitial pneumonia. Some of the mouse-adapted variants have been demonstrated to dramatically increased virulence to mice and involved mutations almost throughout all gene segments (HKMA20 and HKMA20c) (Brown et al, 2001). Furthermore, these mouse-adapted variants grew faster and to higher titre in mouse lung, which was consistent with their relative virulence to mice (Brown et al., 2001).

Although both innate and adaptive immune responses are involved in clearance of influenza A virus, IFN is the first line of defense by limiting the virus in the first replication site and allow time for the host to develop adaptive immune response. Thus it is important for the virus to overcome its effect as the virus replicates in the host. In this study the question was specifically asked as whether mutations in NS1 protein that are selected during mouse adaptation contribute to an increased ability to resist the antiviral properties of mouse IFN. Adaptation with increased virulence in a new host involves not only mutations that increase virulence in the lung but also aspect of changes in host specific replication ability. Therefore, host specificity of the IFN resistance was assessed by using human and mouse cells for comparison. In addition to host specific there are also differences in cell types. In order to address cell type specificity, IFN response was compared between epithelium, which is the normal substrate for influenza A virus replication, and fibroblast, which is normally resistant to infection by human strains of influenza A viruses.

The initial question was whether NS1 mutations contributed to altered IFN resistance in the new host. The experimental system employed mouse adapted variants of the prototype H3N2 HK strain isolated after serial passage in mice. The first panel of 6 clonally mouse adapted variants were obtained after 20 serial mouse passages and all showed increased virulence in mice. Five out of six had mutations in the NS1 protein, possessing either the V23A mutation or the F103L mutation (See Table 2). Subsequently ten sister clones of A/HK/1/68 isolate were adapted to the mouse lung and sequencing of the NS1 genes from several mouse-adapted clones identified 3 more mutant NS1 genes for analysis. It was showed that all of five NS1 genotypes of mouse-adapted variants were resistant to mouse IFN in MEF.

Although this was consistent with a role of NS1 mutations in increasing IFN resistance, the mutant mouse-adapted variants had different mutant genomic backgrounds and it was not possible to exclude the contribution of mutations on other genome segments to the phenotype. Recombinant influenza viruses were constructed that differed solely due to the presence of individual mutation on their NS1 genes. Using these viruses that differed solely due to the presents of NS1 mutations, it was possible to show that each of these mutations increased resistance to IFN but that this phenotype was in some instances host and tissue type dependent. All mutations conferred IFN resistance in murine epithelium but not necessarily in murine fibroblasts, nor human cells of epithelial or fibroblast origin. Table 9 summarizes data from this study.

4.2 Relationship between Virulence, Murine Lung Infection and Cell Damage

Previous studies on progeny virus HKMA20c and other 20 passage series mouse adapted variants showed that they had lower mLD_{50} and higher yield in mouse lung than their parental virus HK (Brown et al, 2001). The current study extended the observation to mouse lung pathology and cell damage. Mice infected by HKMA20c experienced much more extensive interstitial pneumonia which is the characteristic of viral pneumonia. HKMA20c was able to infect tissues outside bronchioles extensively whereas infection of HK was mainly limited within the bronchioles. According to the extent of cell damage by viral infection, the NS20c protein provides the carrying virus the strongest ability to cause cell damage in both human and murine epithelium and fibroblast. All these data are confirming previous observation on properties of virulence and growth of mutant progeny virus HKMA20c (Brown et al., 2001).

Table 9 Data Summary

§ "m.": murine; "h.": human; "epi": epithelium cell; "fib": fibroblast

§ "R": resistance; "NC": no change; "S": sensitive; "PR": partial resistance; "U": upregulated

§ * indicates that data of WSN/ns411 infection of an MOI of 0.02 whereas that of other viruses is 2

§ + indicates normal growth ability; << indicates reduced growth ability

§ + indicates successful generation of synthetic virus; / indicates no recovery of synthetic virus

§ Blank box indicates no in vivo experiment was done for that particular virus

NS1 protein	mutation	Recombinant viruses WSN/nsHK								
		IFN sensitivity (fold reduction)				IFN induction (unit/ml)		replication ability	rescue in HK backbone	in vivo inf. (MA variants)
		M1 (m. epi.)	MEF (m. fib.)	A549 (h. epi.)	MRC5 (h. fib.)	mouse cell (M1)	human cell (MRC5)			
HKwt		24	46	415	593	160	<10	+	+	bronchioles
MA20	V23A	2 ***R***	19 ***R***	2291 ***S***	245 ***PR***	160	<10	+	/	
MA20c	F103L	3 ***R***	1 ***R***	79 ***R***	26 ***R***	960 ***U***	20	+	/	alveoli and bronchioles
MA411	M106V	3* ***R***	54* ***NC***	3* ***R***	4* ***R***	20*	<10*	<<	/	
MA511	M106I	13 ***R***	47 ***NC***	858 ***S***	350 ***PR***	240	<10	+	+	
MA531	L98S M106I	3 ***R***	9 ***R***	1622 ***S***	155 ***PR***	240	<10	+	+	

4.3 Mapping of the IFN Sensitivity Determining Region of the NS1 Protein

One important finding from these studies was the identification of a region within the NS1 protein, from AA 98 to 106, that possessed a cluster of mouse adapted mutations, and therefore represents a putative IFN sensitivity determining region and also demonstrated instances of convergent evolution. As several host factors have been implicated in binding this region, it is possible that these mutations affect binding of several factors and also changes in binding affinity. It is expected that those mutations with the most profound changes to the most important effectors of IFN resistance are those selected on serial passage in mice. The V23A NS1 protein variant with the mutation located within the dsRNA binding region (Hatada and Futada, 1992; Qian et al, 1995) may be a more effective RNA binding protein that is required to antagonize a stronger IFN response for mouse adapted viruses. Likewise the mutations from AA 98 to 106 are located in a region that lies at the amino terminal boundary of the effector domain that binds to both PKR (Tan and Katze, 1998) and several other protein factors in particular eIF4G (Aragon et al, 2000), whose binding requires AA 81-113 and is not bound by the RNA binding domain alone. Further study is needed to assess the effect of NS1 mutations on binding to eIF4GI as well as other binding partners: the cleavage and polyadenylation specificity factor (CPSF), poly(A)-binding protein II (PABII) which both bind to the carboxy terminal regions at amino acid 186 and 223-237 respectively (Krug et al, 2003); and poly(A)-binding protein 1 (PABPI) which interacts to amino acid 1-81 at the N-terminal region of NS1 (Burgui et al, 2003). Furthermore, there are several other protein factors have also been identified but neither their functions as NS1 binders nor their binding sites have been fine

elucidated and could operate in IFN sensitivity (NS1-BP, human Staufen, and NS1-I) (Falcon et al, 1999). The two mutated regions on MA NS1 protein aa23 and aa98-106 may optimize binding to host factors that result in inhibition of the antiviral response and appears to implicate both RNA and protein binding capability.

There are also functions relating to antagonism of RNA silencing that could be implicated in IFN antagonism. The active site for modulating IFN sensitivity will serve as an excellent set of molecular tools to probe the interactions with know host NS1 binding factors.

4.4 IFN Resistance Is Associated with Growth Attenuation

Another interesting discovery from these studies was the fact that several NS1 mutations were attenuating (on HK backbone) for viral replication as observed in the synthetic recombinant viruses, and thus required compensatory growth enhancing elements (on WSN backbone) in order to be rescued from cloned genes in cell culture. Since WSN strain has been adapted in laboratory culture for long time (since 1933), it is presumed that there are mutations on this strain and it is strongly adapted for growing. The derived viruses had reduced growth ability in the case of the F103L and V106M mutations on NS1 protein.

The fact that the F103L mutation attenuates replication and it is shared with HPAI H5N1 suggests that this mutation may not exist in influenza strains unless accompanied by mutations elsewhere that enhance replication and thus compensate for the attenuating phenotype of this mutation. The existence of this and other attenuating mutations (ie, V23A, F103L and M106V) that enhance IFN resistance suggests that NS1 functions such as binding to host or viral factors in the absence of IFN may inhibit viral replication. Using this information it could be

possible to inhibit viral replication by targeting the active AA 98-106 region for drug intervention.

4.5 Mouse-Adapted NS1 Mutants Have Host Dependent IFN Resistance

In order to more thoroughly assess the nature of NS1 mutations that are associated with mouse-lung adaptation, virus clones derived from several independent series of mouse adaptations of sister clones of HK parental virus were sequenced. NS1 mutations that have been selected independently will give information about the structural regions in NS1 protein that are important for host adaptation to increased virulence. When the panel of 5 mouse-adapted variants was first analyzed to assess whether there were differences in IFN inhibition relative to parental human strain HK virus, it was observed that all the MA mutant NS1 variants were more resistant to IFN inhibition in mouse embryo fibroblasts than in human A549 epithelial cells, where increased IFN sensitivity was seen for HK5MA21-1. The most important observation was that all the mouse-adapted mutants with NS1 mutations were more IFN resistant in mouse cells, which is consistent with the role of IFN resistance as a feature of adaptation to virulence in a novel host species, and therefore identifies IFN sensitivity as a determinant of virulence and host adaptation. Some of the resistance was host dependent since the HK5MA21-1 variant was more sensitive to interferon when assayed in human cells and therefore suggests that some of the mutations may involve modified interaction with host factors in the new host. Because these mouse-adapted variants possess mutations in genes besides NS1, it cannot be concluded that only the NS1 mutations are responsible for the increased IFN resistance in mouse cells. Analysis of IFN induction showed

low levels of induction of IFN of mouse-adapted variants which were similar or less than that of parent virus HK in both human epithelium as well as mouse fibroblasts.

4.6 Confirmation that NS1 Mutations Increase IFN Resistance

The genome of parental virus HK was construction in the POL I based plasmid system for rescue of synthetic virus in 293T cells derived from HEK (human embryonic kidney). Whereas it is a routine process to obtain synthetic WSN virus (which is a highly lab adapted virus that has been passaged in ferrets, chicken embryo and mice), it was not always possible to rescue the HK human isolate obtained from limited lab passaging (2 passages in monkey kidney cells followed by 4 egg passages before clonal isolation in MDCK cells). Although it was possible to derive wild type HK virus, it was not possible after repeated attempts to derive the NS20, NS20c or NS411 mutant NS genes on the HK backbone. This indicated that these NS1 mutations are attenuating for growth in human 293T cells.

To overcome the barrier to rescue attenuating NS1 mutants, attempts to derive the mutants on the WSN backbone were successfully performed and succeeded. All the resulting NS1 variants grew as well as or better than their counterparts on the HK backbone and the wild type WSN virus (synthetic virus with complete eight genome segments of wild type WSN strain) except for the NS411 mutant that was severely attenuated yielding low titre in both MDCK and chicken embryo. Together these data indicate that some NS1 mutations that increase IFN resistance resulted in attenuated replication in various non-murine cell lines.

Resistance to IFN was not enhanced in human lung epithelium except for the F103L mutation derived from NS20c. Surprisingly all the NS1 mutants were more resistant to IFN in human MRC5 fibroblasts with the greatest resistance shown for

NS20c. Also surprisingly, all the NS1 mutations increased replication ability in human MRC5 cells which are lung fibroblasts, which may have contributed to the selective environment of the mouse adaptation process.

IFN resistance was increased in mouse epithelium for all NS1 mutants which demonstrates that NS1 mutations that are selected on mouse adaptation can increase IFN resistance in lung epithelium which presumably provides a selective advantage in these tissues relative to the parental virus HK. The ability to resist IFN in mouse cells was cell type dependent: all the NS1 mutations that were selected on mouse lung adaptation were resistant to IFN in murine epithelial cells whereas only 3 out of 5 variants were more resistant than wt HK NS1 in murine embryo fibroblasts. This was most dramatic again for the MA20c variant where the F103L mutation made the recombinant virus totally resistant to inhibition by mouse IFN. The WSN/NS20c variant was totally resistant to IFN in all cells in both human and mouse epithelium and fibroblasts. The data clearly show that mouse lung adaptation results in selection of variants that can resist mouse IFN in epithelium but not necessarily fibroblast and that this property was not shared in comparisons between human and murine cells.

Highly IFN resistance property is shared by high virulent strains of influenza A virus. A recombinant virus possessing 1918 pandemic NS1 gene was efficient at blocking the expression of IFN stimulated genes (ISG) (Geiss G.K., 2002). It was also documented that highly virulent H5N1 influenza viruses was associated with strong IFN resistance. This effect required Glu at position 92 (Seo S.H., 2002 & 2004).

4.7 HPAI H5N1 Shares the F103L Mutation with HKMA20c and M106I Mutation with HK5MA21-1/ HK5MA21-3

Although previous data by others has shown that the NS1 protein functions to antagonize the antiviral response of IFN, the genetic basis for differences in IFN antagonism are not known. Furthermore the highly pathogenic H5N1 z strain is known to be resistant to IFN effect in vitro and also induces very high levels of IFN (Guan et al, 2002; Li et al, 2004). This is the first demonstration that IFN resistance plays a role in modulating virulence.

Blast analysis shows that the HPAI H5N1 virus has acquired the identical mutations at position 103 and 106 as the HKMA20c and HK5MA21-1/ HK5MA21-3 respectively. Interestingly all of these viruses are IFN resistant and HKMA20c shares the feature of high IFN induction which may actually be a direct consequence of IFN resistance, where due to strong IFN resistance, the virus continues to replicate and therefore induced greater yields of IFN whereas other viruses that are less resistant are more inhibited in the presence of IFN and thus reduced in replication with reduced IFN induction as is seen for IFN-sensitive viruses. In H1N1 and H3N2 infections, circulating IFN level correlated with the viral replication titre (Hayden F.G., 1998; Hill, 1972; Richman D.D., 1976).

The observation that the 103 mutation operates not only in human and murine cells but also in both epithelium and fibroblasts is consistent with the shift in replication from epithelium to fibroblast for HPAI H5N1. Fibroblast replication is known to require enhanced cleavability of the HA but it is also possible that the NS1 103 mutation may also be required to resist the stronger fibroblast IFN response as the HPAI H5N1 strains replicate in both epithelium and fibroblast. In all our

experiments we found that infected fibroblasts produced more IFN than infected epithelium which may be an important factor that restricts influenza replication to lung epithelium.

4.8 Growth Affects of NS1 Mutations

Since NS1 protein functions as an IFN antagonist, it is possible that this property is only beneficial in the presence of IFN and that replication in the absence of exogenous IFN is not a selective property and indeed that increased IFN resistance changes viral replication properties and that these changes are less than optimal. Several of our mutants were so severely attenuated that they could not be rescued on the HK backbone, which was further seen for the NS20c and NS411 mutants when introduced onto the WSN backbone where they had reduced titres in all substrates (MDCK cells, chicken embryo, mouse epithelium and fibroblast as well as human epithelium and fibroblasts). Interestingly the F103L mutation in NS20c was the attenuating but had the strongest IFN antagonism being unaffected by IFN for all cell types.

4.8 Conclusions

1. An influenza A virus that possesses the point mutation Leu at position 103 on NS1 protein is more virulent in murine lung and all the tested human and murine epithelium and fibroblast cell cultures. This mutation confers increased resistance to both human and murine IFN relative to that of wild type HK virus. Furthermore, virus with this mutation also induces higher level of IFN than wt virus HK and other mouse adapted viruses in this study. This may result from its better replication in the presence of the host IFN that in turn stimulates more IFN induction by the host. And this phenomenon may contribute to cytokine hyper-

induction and the high virulence of HKMA20c. Although the underlying mechanisms are unknown, it may involve changes in interaction with host factor(s) in particularly eIF4GI.

2. Point mutation Ala at position 23 of NS1 protein is within the dsRNA binding domain and may have an enhanced ability to bind RNA molecules. Virus possessing this mutation is more resistant to mouse IFN than wt virus HK.
3. One other point mutation on NS1 protein, Ile at 106, also confers resistance to mouse IFN but to a less extent than other mutant NS1 variants.
4. An additional point mutation to Ile at 106 of the NS1 protein, Ser at 98, provides the improved growth as well as better or similar IFN resistance on all tested human and mouse epithelium and fibroblast cell lines.
5. NS1 proteins that possess point mutations Ala at 23, Leu at 103, and Val at 106 produce growth-attenuating phenotype. This could be related to host restrictions that contribute to the species barrier.
6. Viral protein(s) other than NS1 might be also involved to the interaction with IFN response since mouse adapted variants and synthetic recombinant viruses possessing the same NS1 mutation do not showed exactly same IFN resistant pattern.

REFERENCES

Abbas A.K., Lichtman A.H., and Pober J.S. Cellular and molecular immunology. Philadelphia: WB Saunders, 1997

Abe Y., Takashita E., Sugawara K., Matsuzaki Y., Muraki Y., Hongo S. Effect of the addition of oligosaccharides on the biological activities and antigenicity of influenza A/H3N2 virus hemagglutinin. J Virol 2004;78(18):9605-9611

Agris C.H., Nemeroff M.E., Krug R.M. A block in mammalian splicing occurring after formation of large complexes containing U1, U2, U4, U5, and U6 small nuclear ribonucleoproteins. Mol Cell Biol 1989;9(1):259-267

Akarsu H., Burmeister W.P., Petosa C., Petit I., Muller C.W., Ruigrok R.W., Baudin F. Crystal structure of the M1 protein-binding domain of the influenza A virus nuclear export protein (NEP/NS2). EMBO J 2003;22;4646-4655

Alexopoulou L., Holt A.C., Medzhitov R., Flavell R.A. Recognition of double stranded RNA and activation of NF-kB by Toll-like receptor 3. Nature 2001;413:732-738

Alonso-Caplen F.V., Nemeroff M.E., Yun Q., Krug R.M. Nucleocytoplasmic transport: the influenza virus NS1 protein regulates the transport of spliced NS2 mRNA and its precursor NS1 mRNA. Genes & Dev 1992;6:255-267

Allen H., McCauley J., Waterfield M., Gething M.J. Influenza virus RNA segment 7 has the coding capacity for two polypeptides. J Virolo 1987;61:2217-2224

Aragon T., De La Luna S., Novoa I., Carrasco L., Ortin J., Nieto A. Eukaryotic translation initiation factor 4GI is a cellular target for NS1 protein, a translational activator of influenza virus. Mol Cell Biol 2000;20(17):6259-6268

Area E., Martin-Benito J., Gastamionza P., Torreira E., Valpuesta J.M., Carrascosa J.L., Ortin J. 3D structure of the influenza virus polymerase complex: location of subunit domains. Proc Natl Acad Sci USA 2004;101(1):308-313

Arnheiter, H., M. Frese, R. Kamadur, E. Meier, and O. Haller. Mx transgenic mice-animal models of health. Curr Top Microbiol 1996;206;119-147

Asaoka N., Tanaka Y., Sakai T., Fujii Y., Ohuchi R., Ohuchi M. Low growth ability of recent influenza clinical isolates in MDCK cells is due to their low receptor binding affinities. Microbes Infect 2006;8(2):511-519

Aytay S., Schulze I.T. Single amino acid substitutions in the hemagglutinin can alter the host range and receptor binding properties of H1 strains of influenza A virus. J Virol 1991;65(6):3022-3028

Bailly J.E., Brown E.G. Interference by a non-defective variant of influenza A virus is due to enhanced RNA synthesis and assembly. Virus Res 1998;57(1):81-100

Bender B.S., Croghan T., Zhang L. Transgenic mice lacking class I major histocompatibility complex-restricted T cells have delayed viral clearance and increased mortality after influenza virus challenge. J Exp Med 1992;175:1143-1145

Bergmann M., Garcia-Sastre A., Carnero E., Pehamberger H., Wolff K., Palese P., Muster T. Influenza virus NS1 protein counteracts PKR-mediated inhibition of replication. J Virol 2000;74(13):6203-6206

Biron C.A. and Sen G.C. Interferons and other cytokines. In: Knipe D.M., Howley P.M., ed. The field of virology, forth ed. Lippincott Williams & Wilkins. 2001:321-353

Blau D.M., Compans R.W. Polarization of viral entry and release in epithelium cells. Semin Virol 1996;7:245-253

Boyce T.G., Gruber W.C., Coleman-Dockery S.D. et al. Mucosal immune response to trivalent live attenuated intranasal influenza vaccine in children. Vaccine 2000;19:217-226

Brown E.G. Influenza virus genetics. Biomed Pharmacother 2000;54(4):196-209

Brown E.G. Increased virulence of a mouse-adapted variant of influenza A/FM/1/47 virus is controlled by mutations in genome segments 4, 5, 7, and 8. J Virol 1990;64(9):4523-4533

Brown E.G., Bailly J.E. Genetic analysis of mouse-adapted influenza A virus identifies roles for the NA, PB1, and PB2 genes in virulence. Virus Res 1999;61(1):63-76

Brown E.G., Liu H., Kit L.C., Baird S. and Nesrallah M. Pattern of mutation in the genome of influenza A virus on adaptation to increased virulence in the mouse lung: Identification of functional themes. Proc Natl Acad Sci U S A 2001;98(12);6883-6888

Bucher E., Hemmes H., De Haan P., Goldbach R., Prins M. The influenza A virus NS1 protein binds small interfering RNAs and suppresses RNA silencing in plants. J Gen Virol 2004;85(Pt4):983-991

Bui M., Whittaker G., Helenius A. Effect of M1 protein and low PH on nuclear transport of influenza virus ribonucleoproteins. J Virol 1996;70:8391-8401

Bui M., Wills E.G., Hekenius A., Whittaker G.R. Role of the influenza virus M1 protein in nuclear export of viral ribonucleoproteins. J Virol 2000;74;1781-1786

Burgui I, Aragon T., Ortin J. and Nieto A. PABP1 and eIF4G1 associate with influenza virus NS1 protein in viral mRNA translation initiation complexes. J Gen Virol 2003;84(Pt 12):3263-3274

Burnet F.M., Lind P.E. Recombination of characters between two influenza virus strains. Aust J Sci 1949;12:109-110

Cann A.J. Principles of molecular virology, third edition. San Diego: Academic Press, 2001

Castrucci M.R., Kawaoka Y. Biologi importance of neuraminidase stalk length in influenza A virus. J Virol 1993;67(2):759-764

Catchpole A.P., Mingay L.J., Fodor E., Brownlee G.G. Alterative base pairs attenuate influenza A virus when introduced into the duplex region of the conserved viral RNA promoter of either the NS or the PA gene. J Gen Virol 2003;84(Pt 3):507-515

Caton A.J., Gerhard W. The diversity of the CD4+ T cell response in influenza. Semin Immunol 1992;4:85-90

Chanturiya A.N., Basanez G., Schubert U., Henklein P., Yewdell J.W., Zimmerberg J. PB1-F2, an influenza A virus-encoded proapoptotic mitochondrial protein, creates variably sized pores in planar lipid membranes. J Virol 2004;78(12):6304-6312

Chen C., Krug R.M. Selective nuclear export of viral mRNAs in influenza-virus-infected cells. Trends Microbiol 2000;8:376-383

Chen P.K. Outbreak of avian influenza A (H5N1) virus infection in Hong Kong in 1997. Clin Infect Dis 2002;34(2):58-64

Chen Z., Li Y., Krug R.M. Influenza A virus NS1 protein targets poly(A)-binding protein II of the cellular 3' end processing machinery. EMBO J 1999;18:2273-2283

Cheung C.Y., Poon L.L., Lau A.S., Luk W., Lau Y.L., Shortridge K.F., Gordon S., Guan Y., Peiris J.S. Induction of proinflammatory cytokines in human macrophages by influenza A (H5N1) viruses: a mechanism for the unusual severity of human disease? Lancet 2002;360(9348):1831-1837

Chotpitayasunondh T., Ungchusak K., Hanshaoworakul W., Chunsuthiwat S., Sawanpanyalert P., Kijphati R. Human disease from influenza A (H5N1), Thailand, 2004. Emerg Infect Dis 2005;11:201-209

Chu C.M., Tian S.F., Ren G.F., Zhang Y.M., Zhang L.X., Liu G.Q. Occurrence of temperature-sensitive influenza A viruses in nature. J Virol 1982;41(2):353-359

Clements M.L., Betts R.F., Tierney E.L. Serum and nasal wash antibodies associated with resistance to experimental challenge with influenza A wild-type virus. J Clin Microbiol 1986;24:157-160

Compans R.W., Content J., Duesberg P.H. Structure of the ribonucleoprotein of influenza virus. J Virol 1972;10:795-800

Couciero J., Paulson J., Baum L. Influenza virus strains selectively recognize sialyloligosaccharides on human respiratory epithelium; the role of the host cell in selection of hemagglutinin receptor specificity. Virus Res 1993;29:155-165

Cox N.J., Subbarao K. Influenza. Lancet 1999;354:1277-1282

De La Luna S., Martin J., Portela A., Ortin J. Influenza virus naked RNA can be expressed upon transfection into cells co-expressing the three subunits of the polymerase and the nucleoprotein from simian virus 40 recombinant viruses. J Gen Virol 1993;74;535-539

De La Luna S., Fortes P., Beloso A., Ortin J. Influenza virus NS1 protein enhances the rate of translation initiation of viral mRNAs. J Virol 1995;69:2427-2433

Delgadillo M.O., Saenz P., Salvador B., Garcia A., Simon-Mateo C. Human influenza virus NS1 protein enhances viral pathogenicity and acts as an RNA silencing suppressor in plants. J Gen Virol 2004;85(Pt 4):993-999

Deng T., Sharps J., Fodor E., Brownlee G. In vitro assembly of PB2 with a PB1-PA dimmer supports a new model of assembly of influenza A virus polymerase subunits into a functional trimeric coplex. J Virol 2005;79(13):8669-8674

Donelan N.R., Basler C.F., Garcia-Sastre A. A recombinant influenza A virus expressing an RNA-binding-defective NS1 protein induces high levels of beta interferon and is attenuated in mice. J Virol 2003;77(24):13257-13266

Domingo E., Holland J.J. RNA virus mutations and fitness for survival. Annu Rev Microbiol 1997;51:151-178

Douglas R. Prophylaxis and treatment of influenza. New Eng J Med 1990;322(7):443-450

Drake J.W., Holland J.J. Mutation rates among RNA viruses. Proc Natl Acad Sci USA 1999;96(24):13910-13913

Durbin J.E., Hackenmiller R., Simon M.C., Levy D.E. Targeted disruption of the mouse Stat1 gene results in compromised innate immunity to viral disease. Cell 1990;84:443-450

Easterday B.C. Animal influenza. In Kilbourne E.D., ed. The influenza viruses and influenza. Orlando: Academic Press, 1975:449-481

Eckert D.M., Kim P.S. Mechanisms of viral membrane fusion and its inhibition. Annu Rev Biochem 201;70:777-810

Edwards K.M., Dupont W.D., Westrich M.K., et al. A randomized controlled trial of cold-adapted and inactivated vaccines for the prevention of influenza A disease. J Infect Dis 1994;169:68-76

Eichelberger M., Allan W., Zijlstra M. Clearance of influenza virus respiratory infection in mice lacking class I major histocompatibility complex-restricted CD8+ T cells. J Exp Med 1991;174:875-880

Ellis T.M., Bousfield R.B., Bissett L.A., Dyrting K.C., Luk G.S., Tsim S.T. Investigation of outbreaks of highly pathogenic H5N1 avian influenza in waterfowl and wild birds in Hong Kong in late 2001. Avian Pathol 2004;33:492-505

Ennis F.A., Rook A.H., Qi Y.H. HLA-restricted virus-specific cytotoxic T-lymphocyte responses to live and inactivated influenza vaccines. Lancet 1981;2:887-891

Epstein S.L., Misplon J.A., Laswon C.M. β2-microglobulin-deficient mice can be protected against influenza A infection by vaccination with vaccinia-influenza recombinants expressing hemagglutinin and neuraminidase. J Immunol 1993;150:5484-5493

Falcon A.M., Fortes P., Marion R.M., Beloso A., Ortin J. Interaction of influenza virus NS1 protein and the human homologue of Staufen in vivo and in vitro. Nucleic Acids Res 1999;27(11):2241-2247

Fechter P., Mingay L., Sharps J., CHambers A., Fodor E., Brownlee G.G. Two aromatic residues in the PB2 subunit of influenza A RNA polymerase are crucial for cap binding. J Biol Chem 2003;278(22):20381-20388

Fisman D.N. Hemophagocytic syndromes and infection. Emerg Infect Dis 2000;6:601-608

Fleischer T.H., Becht H., Rott R. Recognition of viral antigens by human influenza A virus-specific Y lymphocyte clones. J Immunol 1985;135:2800-2804

Fodor E., Crow M., Mingay L.J., Deng T., Sharps J., Fetchter P., Brownlee G.G. A single amino acid mutation in the PA subunit of the influenza virus RNA polymerase inhibits endonucleolytic cleavage of capped RNAs. J Virol 2002;76(18):8989-9001

Fodor E., Smith M. The PA subunit is required for efficient nuclear accumulation of the PB1 subunit of the influenza A virus RNA polymerase complex. J Virol 2004;78(17):9144-9153

Fortes P., Beloso A., Ortin J. Influenza virus NS1 protein inhibits pre-mRNA splicing and blocks mRNA nucleocytoplasmic transport. EMBO J 1994;13(3):704-712

Fouchier R.A., Munster V., Wallensten A., Bestebroer T.M., Herfst S., Smith D., Rimmelzwaan G.F., Olsen B., Osterhaus A.D. Characterization of a novel influenza A virus hemagglutinin subtype (H16) obtain from black-headed gulls. J Virol 2005;79(5):2814-2822

Garcia-Sastre A., Egorov A., Matassov D., Brandt S., Levy D.E., Durbin J.E., Palese P., Muster T. Influenza A virus lacking the NS1 gene replicates in interferon-deficient systems. Virology 1998;252(2):324-330

Garcia-Sastre A., Durbin R.K., Zheng H., Palese P., Gertner R., Levy D.E., Durbin J.E. The role of interferon in the tropism of influenza virus. J Virol 1998(a);72:8550-8558

Garcia-Sastre A., Inhibition of interferon-mediated antiviral responses by influenza A viruses and other negative-strand RNA viruses. Virology 2001;279(2):375-384

Garfinkel M.S. and Katze M.G. Translational control by influenza virus. J Biol Chem 1993;268(30):22223-22226

Geiss G.K., Salvatore M., Tumpey T.M., Carter V.S., Wang X., Basler C.F., Taubenberger J.K., Bumgarner R.E., Palese P., Katze M.G., and Garcia-Sastre A. Cellular transcriptional profiling in influenza A virus-infected lung epithelial cells: the role of the nonstructural NS1 protein and its potential contribution to pandemic influenza. Proc Natl Acad Sci USA 2002;99(16):10736-10741

Chizhmakov I.V., Geraghty F.M., Ogden D.C., Hayhurst A., Antoniou M., Hay A.J. Selective proton permeability and PH regulation of the influenza virus M2 channel expressed in mouse erythroleukaemia cells. J Physiol 1996;494:329-336

Goto H., Wells K., Takada A., Kawaoka Y. Plasminogen-binding activity of the neuraminidase determines the pathogenicity of influenza A virus. J Virol 2001;75(19):9297-301

Gottschalk A. Neuraminidase: the specific enzyme of influenza virus and Vibrio cholerae. Biochim Biophys Acta 1957;23;645-646

Greenspan D., Palese P., Krystal M. Two nuclear location signals in the influenza virus NS1 nonstructural protein. J Virol 1988;62:3020-3026

Guan Y., Peiris J.S., Lipatov A.S., Ellis T.M., Dyrting K.C., Krauss S., Zhang L.J., Webster R.G., Shortridge K.F. Emergence of multiple genotypes of H5N1 avian influenza viruses in Hong Kong SAR. Proc Natl Acad Sci U S A. 2002;99(13):8950-8955

Haller, O., M. Frese, and G. Kochs. Mx proteins: mediators of innate resistance to RNA viruses. Rev Sci Technol Off Int Epizootol 1998;17;220-230

Harper S.A., Fukuda K., Uyeki T.M., Cox N.J., Bridges C.B. Center for Disease Control and Prevention, Prevention and control of influenza: recommendations of the Advisory Committee on Immunization Practices (ACIP), MMWR Recomm Rep 2004;53(RR-6): 1-40

Hatada E., Futada R. Binding of influenza A virus NS1 protein to dsRNA in vitro. J Gen Virol 1992;73:3325-3329

Hatada E., Saito S., Fukuda R. Mutant influenza viruses with a defective NS1 protein cannot block the activation of PKR in infected cells. J Virol 1999;73(3):2425-2433

Hay A.J. The action of adamantanamines against influenza A viruses: inhibition of the M2 ion channel protein. Semin Virol 1992;3;21-30

Hayden F.G., Scott F.R., Lobo M.C. Local and systemic cytokine response during experimental human influenza A virus infection: relation to symptom formation and host defense. J Clin Invest 1998;101:643-649

Headley A.S., Tolley E., Meduri G.U. Infections and the inflammatory response in acute respiratory distress syndrome. Chest 1997;111:1306-1321

Heggeness M.H., Smith P.R., Ulmanen I. Studies on the helical nucleocapsid of influenza virus. Virology 1982;118;466-470

Helenius A. Unpacking the incoming influenza virus. Cell 1992;69;577-578

Henklein P., Bruns K., Nimtz M., Wray V., Tessmer U., Schubert U. Influenza A virus protein PB1-F2: synthesis and characterization of the biologically active full length protein and related peptides. J Pept Sci 2005;11(8):481-490

Herlocher M.L., Massab H.F., Webster R.G. Molecular and biologically changes in the cold adapted "master strain" A/AA/6/60 (H2N2) influenza virus. Proc Natl Acad Sci USA 1993;90(13):6032-6036

Hernandez L.D., Hoffman L.R., Wolfsberg T.G., White J.M. Virus-cell and cell-cell fusion. Annu Rev Cell Dev Biol 1996;12:627-661

Hill D.A., Baron S., Perkins J.C., Worthington M., Van Kirk J.E., Mills J., Kapikian A.Z., Chanock R.M. Evaluation of an interferon inducer in viral respiratory disease. JAMA 1972;219:1179-1184

Hinshaw V.S., Air G.M., Gibbs A.J., Graves L., Prescott B., Karunakaran D. Antigenic and genetic characterization of a novel hemagglutinin subtype of influenza A viruses from gulls. J Virol 1982;42:865-872

Hirst G. Studies on the mechanism of adaptation of influenza virus to mice. J Exp Med 1947;86:357-366

Honda A., Ueda K., Nagata K., Ishihama A. RNA polymerase of influenza virus: role of NP in RNA chain elongation. J Biochem (Tokyo) 1988;104(6):1021-1026

Horimoto T. and Kawaoka Y. Biologic effects of introducing additional basic amino acid residues into the Hemagglutinin cleavage site of a virulent avian influenza virus. Virus Res 1997;50(1):35-40

Horimoto T., Kawaoka Y. Pandemic threat posed by avian influenza A viruses. Clin Microbiol Rev 2001;14:129-149

Huang T.S., Palese P., Krystal M. Determination of influenza virus proteins required for genome replication. J Virol 1990;64;5669-5673

Huang X., Liu T., Muller J., Levandowski R.A. Ye Z. Effect of influenza virus matrix protein and viral RNA on ribonucleoprotein formation and nuclear export. Virology 2001;287;405-416

Isaacs A., Lindenmann J. Virus interference I, the interferon. Proc R Soc Lond B 1957;147:258-267

Ito T. and Kawaoka Y. Host-range barrier of influenza A viruses. Vet Microbiol 2000;74(1-2):71-75

Jardetzky T.S., Lamb R.A. Virology: a class act. Nature 2004;427:307-308

Johansson B.E., Kilbourne E.D. Supplementation of conventional influenza A vaccine with purified viral neuraminidase results in a balanced and broadened immune response. Vaccine 1998;16:1009-1015

Julkunen I., Sareneva T., Pirhonen J., Ronni T., Melen K., Matikainen S. Molecular pathogenesis of influenza A virus infection and virus-induced regulation of cytokine gene expression. Cytokine Growth Factor Rev 2001;12(2-3):171-180

Julkunen I., Melen K., Nyqvist M., Pirhonen J., Sareneva T., Matikainen S. Inflammatory responses in influenza A virus infection. Vaccine 2001(a);19:S32-S37

Kaplan D.R., Griffith R., Braciale V.L. Influenza virus-specific human cytotoxic T cell clones: heterogeneity in antigenic specificity and restriction by class II MHC products. Cell Immunol 1984;88:193-206

Kawaoka Y.S., Yamnikova S., Chambers T.M., Lvov D.K., Webster R.G. Molecular characterization of a new hemagglutinin, subtype H14, of influenza A virus. Virology 1990;179:759-767

Kittel C., Sereining S., Ferko B., Stasakova J., Romanova J., Wolkerstorfer A., Katinger H., Egorov A. Rescue of influenza virus expressing GFP from the NS1 rreading frame. Virology 2004;324(1):67-73

Kilbourne E.D., In pursuit of influenza: Fort Monmouth to Valhalla (and back). Bioessays 1997;19;641-650

Kimura N., Nishida M., Nafata K., Ishihama A., Oda K., Nakada S. Transcription of a recombinant influenza virus RNA in cells that can express the influenza virus RNA polymerase and nucleoprotein genes. J Gen Virol 1992;73;1321-1328

Kou Z., Lei F.M., Yu J., Fan Z.J., Yin Z.H., Jia C.X., Xiong K.J., Sun Y.H., Zhang X.W., Wu X.M., Gao X.B., and Li T.X. New genotype of avian influenza H5N1 viruses isolated from tree sparrows in China. J Virol 2005;79(24):15460-15466

Krug R.M., Alonso-Caplen F.V., Julkunen I., Katze M.G. Expression and replication of the influenza virus genome. In Krug R.M., ed. The influenza viruses. New York: Plenum, 1989:89-152

Krug R.M., Yuan W., Noah D.L., and Latham A.G. Intracellular warfare between human influenza viruses and human cells: the roles of the viral NS1 protein. Virology 2003;309(2):181-189

Lakey D.L., Treanor J.J., Betts B.F. Recombinant baculovirus influenza A hemagglutinin vaccines are well tolerated and immunogenic in health adults. J Infect Dis 1996;174:838-841

Lamb J.R., Eckels D.D., Lake P. Antigen-specific human T lymphocyte clones: induction, antigen specificity, and MHC restriction of influenza virus-immune clones. J Immunol 1982;128:233-238

Lamb J.R., McMicheal A.J., Rothbard J.B. T-cell recognition of influenza viral antigens. Hum Immunol 1987;19:79-89

Lamb R.A., Choppin P.W., Chanock R.M., Lai C.-J. Mapping of the two overlapping genes for polypeptides NS1 and NS2 on RNA segment 8 of influenza virus genome. Proc Natl Acad Sci USA 1980;77:1857-1861

Lamb R.A., Lai C.-J. Conservation of the influenza virus membrane protein (M1) amino acid sequence and an open reading frame of RNA segment 7 encoding a second protein (M2) in H1N1 and H3N2 strains. Virology. 1981;112:746-751

Lamb R.A., Choppin P.W. The gene structure and replication of influenza virus. Annu Rev Biochem 1983;52;467-506

Lamb R.A., Holsinger L.J., Pinto L.H. The influenza A virus M2 ion channel protein and its role in the influenza virus life cycle. In: Wimmer E, ed. Receptor-mediated virus entry into cells. Cold Spring Harbor, NY: Cold Spring Harbor Press, 1994: 303-321

Lamb R.A., Krug R.M. Orthomyxoviridae: The viruses and their replication. In: Knipe D.M., Howley P.M., ed. The field of virology, fourth ed. Lippincott Williams & Wilkins. 2001: 1487-1533

Lee M.K., Bae S.H., Park C.J., Cheong C., Choi B.S. A single-nucleotide natural variantion (U4 to C4) in an influenza A virus promoter exhibits a large structural change: implications for differential viral RNA synthesis by RNA-dependent RNA polymerase. Nucleic Acids Res 2003;31(4):1216-23

Lee M.T., Bishop K., Medcalf L., Elton D., Digard P., Tiley L. Definition of the minimal viral components required for the initiation of unprimed RNA synthesis by influenza virus RNA polymerase. Nucleic Acids Res 2002;30(2):429-438

Leser G.P., Lamb R.A. Influenza virus assembly and budding in raft-derived microdomains: a quantitative analysis of the surface distributaion of HA, NA and M2 proteins. Virology 2005 ;342(2):215-227

Levy D.E., Adolfo G.-S. The virus battles: IFN induction of the antiviral state and mechanisms of viral evasion. Cytokine Growth Factor Rev 2001:12(2-3):143-156

Li K.S., Guan Y., Wang J., Smith G.J., Xu K.M., Duan L., Rahardjo A.P., Puthavathana P., Buranathai C., Nguyen T.D., Estoepangestie A.T., Chaisingh A., Auewararkul P., Long H.T., Webby R.J., Poon L.L., Chen H., Shortridge K.F., Yuen K.Y., Webster R.G., Peiris J.S. Genesis of a highly pathogenic and potentially pandemic H5N1 influenza virus in eastern Asia. Nature 2004;430(6996):209-213

Li S., Schulman J., Itamura S., Palese P. Glycosylation of neuraminidase determines the neurovirulence of influenza A/WSN/33 virus. J Virol 1993;67(11):6667-6673

Li W.X., Li H., Lu R., Li F., Dus M., Atkinson P., Brydon E.W., Johnson K.L., Garcia-Sastre A., Ball L.A., Palese P., Ding S.W. Interferon antagonist proteins of influenza and vaccinia viruses are suppressors of RNA silencing. Proc Natl Acad Sci USA 2004(a);101(5):1350-1355

Li Y., Yamakita Y., Krug R.M. Regulation of a nuclear export signal by an adjacent inhibitory sequence: the effector domain of the influenza virus NS1 protein. Proc Natl Acad Sci USA 1998;95(9):4864-4869

Li Y., Chen Z.Y., Wang W., Baker C.C., Krug R.M. The 3'-end-processing factor CPSF is required for the splicing of single-intron pre-mRNAs in vivo. RNA 2001;7:920-931

Li Y., Han X., Lai A.L., Bushweller J.H., Cafiso D.S., Tamm L.K. Membrane structures of the hemifusion-inducing fusion peptide mutant G1S and the fusion-blocking mutant G1V of influenza virus hemagglutinin suggest a mechanism for pore opening in membrane fusion. J Virol 2005;79(18):12065-12076

Li Z., Chen H., Jiao P., Deng G., Tian G., Li Y., Hoffmann E., Webster R.G., Matsuoka Y., Yu K. Molecular basis of replication of duck H5N1 influenza viruses in a mammalian mouse model. J Virol 2005;79(18):12058-12064

Liem N.T., Lim W. Lack of H5N1 avian influenza transmission to hospital employees, Hanoi, 2004. Emerg Infect Dis 2005;11:210-215

Lindenmann J. From interference to interferon: abrief historical introduction. Philos Trans R Soc Lond B Biol Sci 1982;299:3-6

Lu Y., Qian X.-Y., Krug R.M. The influenza virus NS1 protein: a novel inhibitor of pre-mRNA splicing. Genes Dev 1994;8:1817-1828

Lu Y., Wambach M., Katze M.G., Krug R.M. Binding of the influenza virus NS1 protein to double-stranded RNA inhibits the activation of the protein kinase that phosphorylates the eIF-2 translation initiation factor. Virology 1995;214(1):222-228

Maassab H.F., DeBorde D.C. Characterization of an influenza A host range mutant. Virology 1983;130(2):342-350

Malet I., Belnard M., Agut H., Cahour A. From RNA to quasispecies: a DNA polymerase with proofreading activity is highly recommended for accurate assessment of viral diversity. J Virol Methods 2003;109(2):161-170

Marcus P.I., Rojek J.M., Sekellick M.J. Interferon induction and/or production and its suppression by influenza A viruses. J Virol 2005;79(5):2880-2890

Marie I., Durbin J.E., Levy D.E. Differential viral induction of distinct interferon-alpha genes by positive feedback through interferon regulatory factor-7. EMBO J 1998;17:6660-6669

Marion R.M., Fortes P., Beloso A., Dotti C., Ortin J., A human sequence homologue of Staufen is an RNA-binding protein that is associated with polysomes and localizes to the rough endoplasmic reticulum. Mol Cell Biol 1999;19(3):2212-2219

Martin K., Helenius A. Nuclear transport of influenza virus ribonucleoproteins: the viral matrix protein (M1) promotes export and inhibits import. Cell 1991;67;117-130

Martin-Benito J., Area E., Ortega J., Liorca O., Valpuesta J.M., Carrascosa J.L., Ortin J. Three-dimensional reconstruction of a recombinant influenza virus ribonucleoprotein particle. EMBO Rep 2001;2:313-317

Mazanec M.B. Kaetzel C.S., Lamm M.E. Intracellular neutralization of virus by immunoglobulin A antibodies. Pro Natl Acad Sci USA 1992;89:6901-6905

Mazanec M.B., Huang Y.T., Pimplikar S.W. Mechanisms of inactivation of respiratory viruses by IgA, including intraepithelial neutralization. Semin Virol 1996;7:285-292

Mena I., de la Luna S., Albo C., Martin J., Nirto A., Ortin J., Portela A. Synthesis of biologically active influenza virus core proteins using a vaccinia virus-T7 RNA polymerase expression system. J Gen Virol 1994;75;2109-2114

Mena I., Jambrina E., Albo C., Perales B., Ortin J., Arrese M., Vallejo D., Portela A. Mutational analysis of influenza A virus nucleoprotein: identification of mutations that affect RNA replication. J Virol 1999 Feb;73(2):1186-1194

Mims C. The pathogenesis of infectious disease. Academic Press, Toronto. 1987:270

Mohler L., Flockerzi D., Sann H., Reichl U. Mathematical model of influenza A virus production in large-scale microcarrier culture. Biotechnol Bioeng 2005;90(1):46-58

Mould J.A., Drury J.E., Frings S.M., Kaupp U.B., Pekosz A., Lamb R.A., Pinto L.H. Permeation and activation of the M2 ion channel of influenza A virus. J Biol Chem 2000;275:31038-31050

Muller U., Steinhoff U., Reis L.F.L., Hemmi S., Pavlovic J., Zinkernagel R.M., Aguet M. Functional role of type I and type II interferons in antiviral defense. Science 1994;264:1918-1921

Murphy B.R., Kasel J.A., Chanock R.M. Association of serum antineuraminidase antibody with resistance to influenza in man. N Engl J Med 1972;286:1329-1332

Murphy B.R., Wood F.T., Massicot J.G., Chanock R.M. Temperature-sensitive mutants of influenza A virus. Transfer of the two ts-1 A2 ts lesions present in the Udorn/72-ts-1A2 donor virus to the influenza A/Alaska/6/77 (H3N2) wild type virus. Arch Virol 1980;65(2):175-186

Murphy B.R. Use of live attenuated cold-adapted influenza A reassortant virus vaccine in infants, children, young adults, and elferly adults. Infect Dis Clin Pract 1993;2:174-181

Murti K.G., Webster R.G., Jones I.M. Localization of RNA polymerase on influenza viral ribonucleoproteins by immunogold labeling. Virology 1988;164;562-566

Nayak D.P., Hui E.K., Barman S. Assembly and budding of influenza virus. Virus Res 2004;106(2):147-165

Nemeroff M.E., Utans U., Kramer A., Krug R.M. Identification of cis-acting intron and extron regions in influenza virus NS1 mRNA that inhibits splicing and cause the formation of aberrantly sedimenting presplicing complexs. Mol Cell Biol 1992;12(3):962-970

Nemeroff M.E., Qian X.Y., Krug R.M. The influenza virus NS1 protein forms multimers in vitro and in vivo. Virology 1995;212(2):422-428

Nemeroff M., Barabino S.M.L., Keller W., Krug R.M. Influenza virus NS1 protein interacts with the 30 kD subunit of cleavage and specificity factor and inhibits 3' end formation of cellular pre-mRNAs. Mol Cell 1998;1:991-1000

Neumann G., Watanabe T., Ito H., Watanabe S., Goto H., Gao P., Hughes M., Perez D.R., Donis R., Hoffmann E., Hobom G., Kawaoka Y. Generation of influenza A viruses entirely from cloned cDNAs. Proc Natl Acad Sci U S A 1999;96(16):9345-9350

Neumann G., Hughes M.T., Kawaoka Y. Influenza A virus NS2 protein mediates vRNA nuclear export through NES-independent interaction with hCRM1. EMBO J 2000;19;6751-6758

Nguyen H., Hiscott J., Pitha P.M. The growing family of interferon regulatory factors. Cytokine Growth Factor Rev 1997;8:293-312

Nichol K.L., Mendelman P.M., Mallon K.P. Effectiveness of live, attenuated intranasal influenza virus vaccine in healthy, working adults: a randomized controlled trail. JAMA 1999;282:137-144

Noah D.L., Twu K.Y., Krug R.M. Cellular antiviral response against influenza A virus are countered at the posttranscriptional level by the viral NS1A protein via its binding to a cellular protein required for the 3' end processing of cellular pre-mRNAs. Virology 2003;307(2):386-395

Ogra P.L., Chow T., Beutner K.R. Clinical and immunologic evaluation of neuraminidase-specific influenza A virus vaccine in humans. J Infect Dis 1977;135:499-506

O'Neill R.E., Jaskunas R., Blobel G., Palese P., Moroianu J. Nuclear import of influenza virus RNA can be mediated by viral nucleoprotein and transport factors required for protein import. J Biol Chem 1995;270:22701-22704

Palese P., Compans R.W. Inhibition of influenza virus replication in tissue culture by 2-deoxy-2,3-dehydro-N-trifluoroacetylneuraminic acid (FANA): mechanism of action. J Gen Virol 1976;33(1):159-163

Parvin J.D., Moscona A., Pan W.T. Measurement of the mutation rates of animal viruses: influenza A virus and poliovirus type I. J Virol 1986;59:377-383

Patterson S., Gross J., Oxford J.S. The intercellular distribution of influenza virus matrix protein and nucleoprotein in infected cells and their relationship to hemagglutinin in the plasma membrane. J Gen Virol 1988;69;1859-1872

Penn C. The role of RNA segment 1 in an in vitro host restriction occurring in an avian influenza virus mutant. Virus Res 1989;12(4):349-359

Perez D.R., Donis R.O. Functional analysis of PA binding by influenza A virus PB1: effects on polymerase activity and viral infectivity. J Virol 2001;75(17):8127-8136

Pinto L.H., Holsinger L.J., Lamb R.A. Influenza virus M2 protein has ion channel activity. Cell 1992;69:517-528

Plotch S.J., Bouloy M., Ulmanen I., Krug R.M. A unique cap (m7GpppXm)-dependent influenza virion endonuclease cleaces capped RNAs to generate the primers that initiate viral RNA transcription. Cell 1981;23;847-858

Potter C.W., Oxford J.S. Determinants of immunity to influenza infection in human. Br Med J 1979;35:69-75

Qian X.Y., Alonso-Caplen F., Krug R.M. Two functional domains of the influenza virus NS1 protein are required for regulation of nuclear export of mRNA. J Virol 1994;68(4):2433-2441

Qian X., Chien C., Lu Y., Montelione G.T., Krug R.M. An amino-terminal polypeptide fragment of the influenza virus NS1 protein possesses specific RNA binding activity and largely helical backbone structure. RNA 1995;1:948-956

Qiu Y., Krug R.M. The influenza virus NS1 protein is a poly(A)-binding protein that inhibits nuclear export of mRNAs containing poly(A). J Virol 1994;68(4):2425-2432

Qiu Y., Nemeroff M., Krug R.M. The influenza virus NS1 protein binds to a specific region in human U6 snRNA and inhibits U6-U2 and U6-U4 snRNA interactions during splicing. RNA 1995;1(3):304-316

Ramalho-Santos J., de Lima M.C. The influenza virus hemaglutinin: a model protein in the study of membrane fusion. Biochim Biophys Acta. 1998;1376(1):147-154

Rao P., Yuan W., Krug R.M. Crucial role of CA cleavage sites in the cap-snatching mechanism for initiating viral mRNA synthesis. EMBO J 2003;22;1188-1198

Raut S., Hurd J., Cureton R.J., Blandford G., Heath R.B. The pathogenesis of infections of the mouse caused by virulent anda virulent variants of an influenza virus. J Med Microbiol 1975;8;127-136

Ray C. Respiratory viruses. In Sherris J. ed. Medical Microbiology. second ed. Elsevier Science Publishing Co. Inc., New York. 1990;499-507

Renegar K.B., Small P.A.jr. Immunoglobulin A mediation of murine nasal anti-influenza virus immunity. J Virol 1991;65:2146-2148

Richman D.D., Murphy B.R., Baron S., Uhlendorf C. Three strains of influenza A virus (H3N2): interferon sensitivity in vitro and interferon production in volunteers. J Clin Microbiol 1976;3:223-226

Rohm C., Zhou N., Suss J., Mackenzie J., Webster R.G. Characterization of a novel influenza hemagglutinin, H15: criteria for determination of influenza A subtypes. Virology 1996;217:508-516

Ronni T., Matikainen S., Sareneva T., Melen K., Pirhonen J., Keskinen P., Julkunen I. Regulation of IFN-alpha/beta, MxA, 2',5'-oligoadenylate synthetase, and HLA gene expression in influenza A-infected human lung epithelial cells. J Immunol 1997;158(5):2363-2374

Ruigrok R.W.H., Calder L.J., Wharton S.A. Electron microscopy of the influenza virus submembranal structure. Virology 1989;73;311-316

Sakaguchi T., Leser G.P., Lamb R.A. The ion channel activity of the influenza virus M2 protein affects transport through the Golgi apparatus. J Cell Biol 1996;133;733-747

Samuel C.E. Antiviral actions of interferons. Clin Microbiol Rev 2001;14;778-809

Scherle P.A., Palladino G., Gerhard W. Mice can recover from pulmonary influenza virus infection in the absence of class I-restricted cytotoxin T cells. J Immunol 1992;148:212-217

Schmitt A.P., Lamb R.A. Influenza virus assembly and budding at the viral budzone. Adv Virus Res 2005;64:383-416

Scholtissek C., Spring S.B. Extragenic suppression of temperature-sensitive mutations in RNA segment 8 by replacement of different RNA segments with those of other influenza A virus prototype trains. Virology 1982;118(1):28-34

Schulman J.L., Palese P. Virulence factors of influenza A viruses: WSN virus neuraminidase required for plaque production in MDBK cells. J Virol 1977;24:170-176

Schulze I.T. The structure of influenza virus II, a model based on the morphology and composition of subviral particles. Virology 1972;47;181-196

Sen G.C., Ransohoff R.M. Interferon-induced antiviral actions and their regulation. Adv Virus Res 1993;42:57

Sen G.C., Sarkar S.N. Transcriptional signaling by double-stranded RNA: role of TLR3. Cytokine Growth Factor Rev 2005;16(1):1-14

Seo S.H., Hoffmann E., Webster R.G. Lethal H5N1 influenza viruses escape host anti-viral cytokine responses. Nat Med 2002;8(9):950-954

Seo S.H., Hoffmann E., Webster R.G. The NS1 gene of H5N1 influenza viruses circumvents the host anti-viral cytokine responses. Virus Res 2004;103(1-2):107-113

ShapiroG.I., Gurney T.Jr. Krug R.M. Influenza virus gene expression: comtrol mechanism at early and late times of infection and nuclear-cytoplasmic transport of virus-specific RNAs J Virol 1987;61:764-773

Shi L., Summers D.F., Peng Q., Galarz J.M. Influenza A virus RNA polymerase subunit PB2 is the endonuclease which cleaves host cell mRNA and functions only as the trimeric enzyme. Virology 1995;208(1):38-47

shinya K., Hamm S., Hatta M., Ito H., Ito T., Kawaoka Y. PB2 amino acid at position 627 affects replicative efficiency, but not cell tropism, of Hong Kong H5N1 influenza A viruses in mice. Virology 2004;320(2):258-266

Skehel J.J., Wiley D.C. Receptor binding and membrane fusion in virus entry: the influenza hemagglutinin. Annu Rev Biochem 2000;69:531-569

Smeenk C.A., Brown E.G. The influenza virus variant A/FM/1/47-MA possesses single amino acid replacements in the hemagglutinin, controlling virulence, and in the matrix protein, controlling virulence as well as growth. J Virol 1994;68(1):530-534

Smeenk C.A., Wrignt K.E., Burns B.F., Thaker A.J., Brown E.G. Mutations in the hemagglutinin and matrix genes of a virulent influenza virus variant, A/FM/1/47-MA, control different stages in pathogenesis. Virus Res 1996;44(2):79-95

Smith E.J., Marie I., Prakash A., Garcia-Sastre A., and Levy D.E. IRF3 and IRF7 phosphorylation in virus-infected cells does not require double-stranded RNA-dependent protein kinase R or Ikappa B kinase but is blocked by vaccinia virus E3L protein. J Bio Chem 2001;276(12):8951-8957

Smith P.L., Lombardi G., Foster G.R. Type I interferons and the innate immune response—more than just antiviral cytokines. Mol Immunol 2005;42(8):869-877

Staeheli, P., F. Pitossi, and J. Pavlovic. Mx proteins: GTPases with antiviral activity. Trends Cell Biol 1993;3;268-272

Sterkers G., Michon J., Henin Y. Fine specificity analysis of human influenza-specific cloned cell lines. Cell Immunol 1985;94:394-405

Subbarao E.K., London W., Murphy B.R. A single amino acid in the PB2 gene of influenza A virus is a determinant of host range. J Virol 1993;67(4):1761-1764

Subbarao K., Webster R.G., Kawaoka Y., Murphy B.R. Are there alternative avian influenza viruses for generation of stable attenuated avian-human influenza A reassortant viruses? Virus Res 1995;39(2-3):105-118

Sugrue R.J., Bahadur G., Zambon M.C. et al. Specific structural alteration of the influenza haemagglutinin by amantadine. EMBO J 1990;9:3469-3476

Sugrue R.J., Hay A.J. Structural characteristics of the M2 protein of the influenza A viruses: evidence that it forms a tetrameric channel. Virology 1991;180;617-624

Suzuki T., Takahashi T., Guo C.T., Hidari K.I., Miyamoto D., Goto H., Kawaoka Y., Suzuki Y. Sialidase activity of influenza A virus in an endocytic pathway enhances viral replication. J Virol 2005;79(18):11705-11715

Sweet C., Smith H. Pathogenicity of influenza virus. Microbiol 1980;44;303-330

Takeda K., Akira S. TLR signaling pathways. Semin Immunol 2004;16(1):3-9

Takeda K., Akira S. Microbial recognition by Toll-like receptors. J Dermatol Sci 2004(a);34(2):73-82

Takeuchi K., Lamb R.A., Influenza virus M2 protein ion channel activity stabilizes the native form of fowl plaque virus hemagglutinin during intracellular transport. J Virol 1994;68:911-919

Talon J., Horvath C.M., Polley R., Basler C.F., Muster T., Palese P., Garcia-Sastre A. Activation of interferon regulatory factor 3 is inhibited by the influenza A virus NS1 protein. J Virol 2000;74(17):7989-7996

Talon J., Salvatore M., O'Neill R.E., Nakaya Y., Zheng H., Muster T., Garcia-Sastre A., Palese P. Influenza A and B viruses expressing altered NS1 proteins: a vaccine approach. Proc Natl Acad Sci USA 2000(a);97(8):4309-4314

Tan S.L., Katze M.G. Biochemical and genetic evidence for complex formation between the influenza A virus NS1 protein and the interferon-induced PKR protein kinase. J Interferon Cytokine Res 1998;18(9):757-766

Taubenberger J.K., Reid A.H., Lourens R.M., Wang R., Jin G., Fanning T.G. Characterization of the 1918 influenza virus polymerase genes. Nature 2005;437(7060):889-893.

Taubenberger J.K., Reid A.H., Fanning T.G. Capturing a killer flu virus. Sci Am 2005(a);292(1):48-57

To K.-F., Chan K.F., Lee W.K., Lam W.Y., Wong K.F., Tang N.L., Tsang D.N., Sung R.Y., Buckley T.A., Tam J.S., Cheng A.F. Pathology of fatal human infection associated with avian influenza A H5N1 virus. J Med Virol 2001;63:242-246

Von Itzstein M., Dyason J.C., Oliver S.W., White H.F., Wu W.Y., Kok G.B., Pegg M.S. A study of the active site of influenza virus sialidase: an approach to the rational design of novel anti-influenza drugs. J Med Chem 1996;39(2):388-391

Wagner R., Herwig A., Azzouz N., Klenk H.D. Acylation-mediated membrane anchoring of avian influenza virus hemagglutinin is essential for fusion pore formation and virus infectivity. J Virol 2005;79(10):6449-6458

Wang M.Z., Tai C.Y., Mendel D.B. Mechanism by which mutations at his274 alter sensitivity of influenza A virus N1 neuraminidase to oseltamivir carboxylate and zanamivir. Antimicrob Agents Chemother 2002;46(12):3809-3816

Wang W., Krug R.M. The RNA-binding and effector domains of the viral NS1 protein are conserved to different extents among influenza A and B viruses. Virology 1996;223(1):41-50

Wang W., Krug R.M. U6atac snRNA, the highly divergent counterpart of U6 snRNA, is the specific target that mediates inhibition of AT-AC splicing by the influenza virus NS1 protein. RNA 1998;4(1):55-64

Wang W., Riedel K., Lynch P., Chien C.Y., Montelione G.T., Krug R.M. RNA binding by the novel helical domain of the influenza virus NS1 protein requires its demer structure and a small number of specific basic amino acids. RNA 1999;5(2):195-205

Wang X., Li M., Zheng H., Muster T., Palese P., Beg A.A., Garcia-Sastre A. Influenza A virus NS1 protein prevents activation of NF-kappaB and induction of alpha/beta interferon. J Virol 2000;74(24):11566-11573

Ward A.C. Changes in the neuraminidase of neurovirulent influenza virus strains. Virus Genes 1995;10(3):253-260

Ward A.C. Neurovirulence of influenza A virus. J Neurovirol 1996;2(3):139-151

Ward A.C. Virulence of influenza A virus for mouse lung. Virus Genes 1997;14;187-194

Ward A.C., Koning-Ward T.F. Changes in the hemagglutinin gene of the neurovirulent influenza virus strain A/WSN/33. Virus Genes 1995(a);10:179-183

Ward A.C., Azad A.A., McKimm-Breschkin J.L. Changes in the NS gene of neurovirulent strains of influenza affect splicing. Virus Genes 1995(b);10(1):91-94

Weaver B.K., Kumar K.P., Reich N.C. Interferon regulatory factor 3 and CREB-binding protein/p300 are subunits of double-stranded RNA-activated transcription factor DRAF1. Mol Cell Biol 1998;18:1359-1368

Weber, F., O. Haller, and G. Kochs. MxA GTPase blocks reporter gene expression of reconstituted Thogoto virus ribonucleoprotein complexes. J Virol 2000;74;560-563

Webster R.G., Air G.M., Metzger D.W., Colman P.M., Varghese J.N., Baker A.T. Laver W.G. Antigenic structure and variation in an influenza virus N9 neuraminidase. J Virol 1987;61(9):2910-2916

Webster R.G., Bean W.J., Gorman O.T., Chambers T.M., Kawaoka Y. Evolution and ecology of influenza A viruses. Microbiol Rev 1992;56:152-179

Weis W., Brown J.H., Cusack S. Structure of the influenza virus haemagglutinin complexed with its receptor, sialic acid. Nature 1988;333:426-431

Whittaker G., Bui M., Helenius A. Nuclear trafficking of influenza virus ribonucleoproteins in heterokaryons. J Virol 1996;70:2743-2756

Wiley D.C., Skehel J.J. The structure and function of the hemagglutinin membrane glycoprotein of influenza virus. Annu Rev Biochem 1987;56:365-394

Wolff T., O'Neill R.E., Palese P. Interaction cloning of NS1-I, a human protein that binds to the nonstructural NS1 proteins of influenza A and B viruses. J Virol 1996;70(8):5363-5372

Wolff T., O'Neill R.E., Palese P. NS1-binding protein (NS1-BP): a novel human protein that interacts with the influenza A virus nonstructural NS1 protein is relocalized in the nuclei of infected cells. J Virol 1998;72(9):7170-7180

Wright P.F., Webster R.G. Orthomyxoviruses. In: Knipe D.M., Howley P.M., ed. The field of virology, forth ed. Lippincott Williams & Wilkins. 2001:1533-1579

Wyde P.R., Cate T.R. Cellular changes in lungs of mice infected with influenza virus: characterization of the cytotoxic response. Infect Immunol 1978;15;221-229

Yewdell J.W., Hackett C.J. The specificity and function of T lymphocytes induced by influenza viruses. In: Krug R. ed. The influenza viruses. New York: Plenum Press, 1989

Zoueva O.P., Bailly J.E. Nicholls R., Brown E.G. Aggregation of influenza virus ribonucleocapsids at low PH. Virus Res 2002;85(2):141-149

APPENDIX I : SOLUTIONS

Carnoy's Fixative

3 parts methanol with 1 part acetic acid

Coomassie Brilliant Blue

25% Methanol

7% Acetic Acid

0.1% Coomassie Brilliant Blue

LB (Luria-Bertani) Medium

Per liter:

10 g Bacto-tryptone

5 g Bacto-yeast extract

10 g NaCl

Adjust PH to 7.5 with sodium hydroxide.

Sterilize by autoclaving

LB Medium Containing Agar

Make up liquid media according to the appropriate formula given above. Just before autoclaving, add (per litre) of the following:

15 g Agar

When preparing plates, media that containing agar should be sterilized by autoclaving and allowed to cool to 55°C before 100 µg/µl ampicilline are added. Plates can be poured directly from flask and waited for hardening.

Lysis Solution

1% SDS

0.2 N NaOH

PBS (Phosphate Buffered Saline)

8.0 mM Na_2HPO_4

2.5 mM NaH_2PO_4

145 mM NaCl

PH 7.4

Sterilize by autoclaving

S.O.C. Medium

Per liter:

20 g Bacto-tryptone

5 g Yeast extract

0.5 g NaCl

Adjust PH to 7.5 with potassium hydroxide and sterilize by autoclaving. Just before use, add 20 ml of sterile 1 M glucose, sterilize by filtration through 0.22 μm filter.

STE Buffer

100 mM Tris-HCl (PH 8.0)

1 M NaCl

10 mM EDTA (PH 8.0)

sterilize by autoclaving

Suspension Solution

50 mM Tris

10 mM EDTA

PH: 8.0

TBE Buffer

89 mM boric acid

89 mM Tris

20 mM EDTA

sterilize by autoclaving

TE Buffer

10 mM Tris-HCL PH 7.4

1 mM EDTA PH 8.0

PH 7.4

sterilize by autoclaving

APPENDIX II : OLIGONUCLEOTIDE PRIMERS

All primers are written 5' to 3'. Unless otherwise indicated, the primers were used for RT-PCR. Negative sense primers are indicated by an asterisk.

Universal

*10234 CCGCAGTAGAAACAAGG

Universal for segment 1, 2, 3, and 6

10232 CCGCTAGCGAAAGCAGG

RTG GGGGAGCGAAAGCAGG

Universal for segment 4, 5, 7, and 8

10231 CCGCTAGCAAAAGCAGG

RTA GGGGAGCAAAAGCAGG

Segment 1

KC12 GGGGAGCGAAAGCAGGTCAATTATATTC

*KC4 GGTTATTAGTAGAAACAAGGTCGTTTTTAAAC

*10235 CCGCAGTAGAAACAAGGTCG

*S1 GGTTATTAGTAGAAACAAGGTCG

Segment 2

KC13 GGGGAGCGAAAGCAGGCAAACCATTTGA

*KC5 GGTTATTAGTAGAAACAAGGCATTTTTTC

*10236 CCGCAGTAGAAACAAGGCAT

*S2 GGTTATTAGTAGAAACAAGGCAT

Segment 3

KC14 GGGGAGCGAAAGCAGGTACTGATTC

*KC6 GGTTATTAGTAGAAACAAGGTACTTTTTTG

*10237 CCGCAGTAGAAACAAGGTAC

*S3 GGTTATTAGTAGAAACAAGGTAC

Segment 4

KC15 GGGGAGCAAAAGCAGGGGATAATTC

*KC7 GGTTATTAGTAGAAACAAGGGTGTTTTTAATTAC

*10238 CCGCAGTAGAAACAAGGGTG

*S48 GGTTATTAGTAGAAACAAGGGTG

Segment 5

KC16 GGGGAGCAAAAGCAGGGTAGATAATC

*KC8 GGTTATTAGTAGAAACAAGGGTATTTTTC

*10239 CCGCAGTAGAAACAAGGGTA

*S5 GGTTATTAGTAGAAACAAGGGTA

Segment 6

KC17 GGGGAGCGAAAGCAGGAGTGAAAATG

*KC9 GGTTATTAGTAGAAACAAGGAGTTTTTTTC

*10240 CCGCAGTAGAAACAAGGAGT

*S6 GGTTATTAGTAGAAACAAGGAGT

Segment 7

KC18 GGGGAGCAAAAGCAGGTAGATATTG

*KC10 GGTTATTAGTAGAAACAAGGTAGTTTTTTTAC

*10241 CCGCAGTAGAAACAAGGTAG

*S7 GGTTATTAGTAGAAACAAGGTAG

Segment 8

KC19 GGGGAGCAAAAGCAGGGTGACAAAG

*KC11 GGTTATTAGTAGAAACAAGGGTGTTTTTTTATC

*10238 CCGCAGTAGAAACAAGGGTG

*S48 GGTTATTAGTAGAAACAAGGGTG

APPENDIX III : SIZES OF PLAQUES OF SYNTHETIC RECOMBINANT VIRUSES (WSN/ns# SERIES) FORMED ON MDCK CELLS AND THEIR REPLICATION TITRES ON STOCK PREPARATIONS

All the synthetic recombinant viruses yielded around 10^7 to 10^8 pfu/ml from different stock preparation approaches: P1 (one passage on MDCK), P2 (two passages on MDCK), P1E(10d)1 (one passage on MDCK followed by one passage on 10-day-old chicken embryo), and P1E(7d)1 (one passage on MDCK followed by one passage on 7-day-old chicken embryo) where WSN/ns20c got only 10^6 pfu/ml from egg stock and WSN/ns411 got 10^4 to 10^5 from both cell and egg stocks (See Figure 18).

All synthetic viruses formed two sizes of plaques on MDCK cells, large one and small one. Among viruses from egg stocks, similar size was seen for different viruses in the same preparation group (See Figure 36 and 38): in P1E(10d)1 group, around 3~4 milimetre for the large plaques and 1 milimetre for the small plaques; in P1E(7d)1 group, around 4~5 milimetre for the large plaques and 2 milimetre for the small plaques. However, among viruses from MDCK stocks, WSN/nsMA411 had significantly smaller size of plaques while the others shared similar sizes in the same preparation group (See Figure 32 and 34). In P1 group, all the synthetic viruses had around 3~4 milimetre for the large plaques and 1 milimetre for the small plaques, except that WSN/nsMA411 had 1.5 milimetre for the large plaques and 0.5 milimetre for the small plaques. In P2 group, all the synthetic viruses had around 4 milimetre for the large plaques and 2 milimetre for the small plaques, except that WSN/nsMA411 had 2 milimetre for the large plaques and 0.5 milimetre for the small plaques.

For each virus stocks, titres of its large plaque forming virus population and small plaque forming virus population are different. Collectively, for viruses from all different stock preparations, their titres of large plaque forming virus are 10 fold higher than small plaque forming virus, except for WSN/ns411's MDCK stocks which have similar titres between large and small plaque forming virus populations (See Figure 31, 33, 35, and 37).

Figure 31: Replication Titres of Large Plaque Population and Small Plaque Population of Synthetic Recombinant Viruses (WSN/nsHK or MA#) of One Passage on MDCK Cells.

Each bar represents the large/small plaque population from one plaque assay titration of one growth experiment. The rescued wild type WSN (as control), all synthetic recombinant viruses in WSN backbone are shown. Titres are expressed as common logarithm.

P1: one passage on MDCK cells

Large plaque population: blue

Small plaque population: pink

Figure 32: Plaque Sizes of Large Plaque Population and Small Plaque Population of Synthetic Recombinant Viruses (WSN/nsHK or MA#) of One Passage on MDCK Cells.

Each spot represents the average diameter of ten plaques from one population. Each virus forms two sizes of plaques: large one and small one.

P1: one passage on MDCK cells

1: WSN/nsHKwt 2: WSN/nsMA20

3: WSN/nsMA20c 4: WSN/nsMA411

5: WSN/nsMA511 6: WSN/nsMA531

7: wt WSN

Large size: square

Small size: triangle

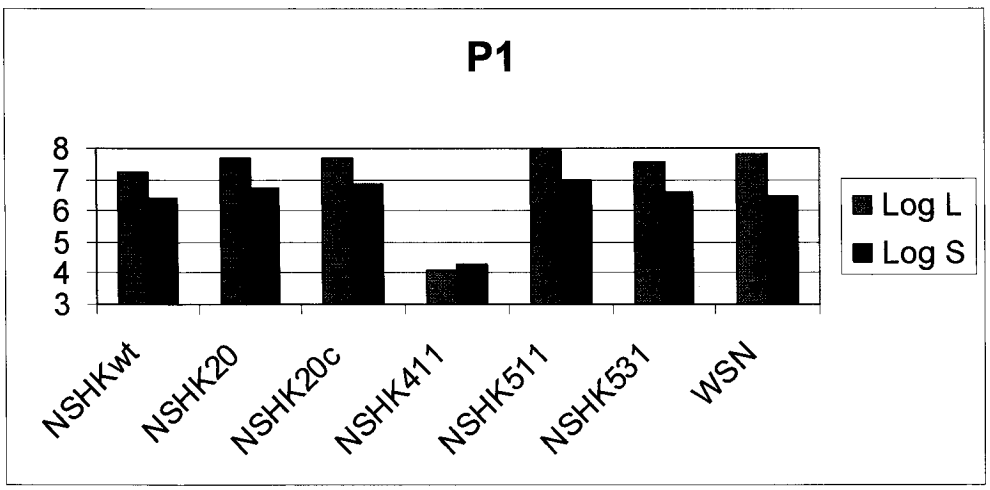
P1
8
7
6
5
4
3
Log L
Log S
NSHKwt
NSHK20
NSHK20c
NSHK411
NSHK511
NSHK531
WSN

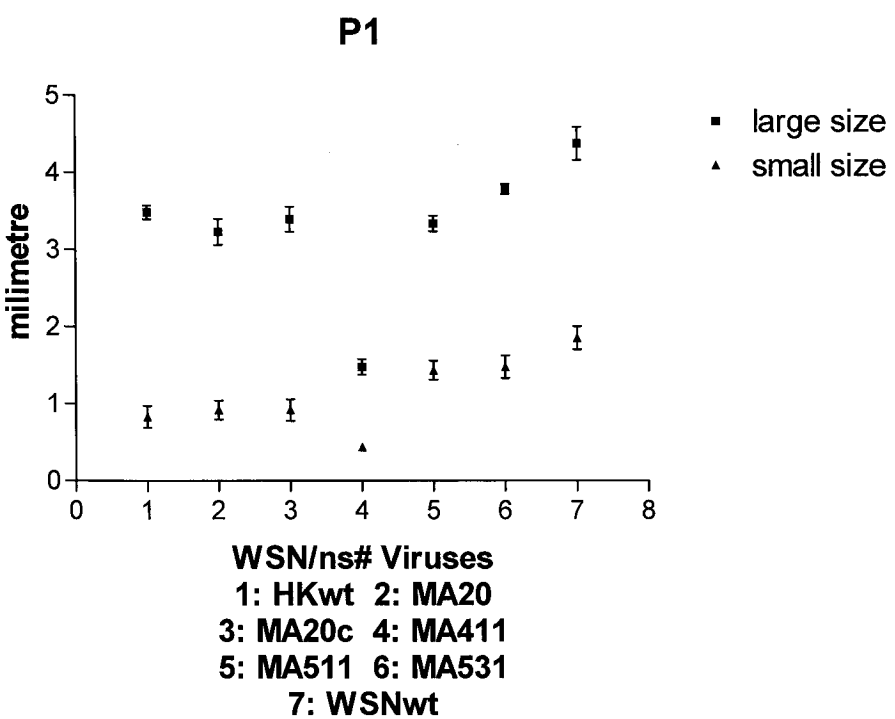
P1
5
4
3
2
1
0
milimetre
0
1
2
3
4
5
6
7
8
large size
small size
WSN/ns# Viruses
1: HKwt 2: MA20
3: MA20c 4: MA411
5: MA511 6: MA531
7: WSNwt

Figure 33: Replication Titres of Large Plaque Population and Small Plaque Population of Synthetic Recombinant Viruses (WSN/nsHK or MA#) of Two Passages on MDCK Cells.

Each bar represents the large/small plaque population from one plaque assay titration of one growth experiment. The rescued wild type WSN (as control), all synthetic recombinant viruses in WSN backbone are shown. Titres are expressed as common logarithm.

P2: two passages on MDCK cells

Large plaque population: blue

Small plaque population: pink

Figure 34: Plaque Sizes of Large Plaque Population and Small Plaque Population of Synthetic Recombinant Viruses (WSN/nsHK or MA#) of Two Passages on MDCK Cells.

Each spot represents the average diameter of ten plaques from one population. Each virus forms two sizes of plaques: large one and small one.

P2: two passages on MDCK cells

1: WSN/nsHKwt 2: WSN/nsMA20

3: WSN/nsMA20c 4: WSN/nsMA411

5: WSN/nsMA511 6: WSN/nsMA531

7: wt WSN

Large size: square

Small size: triangle

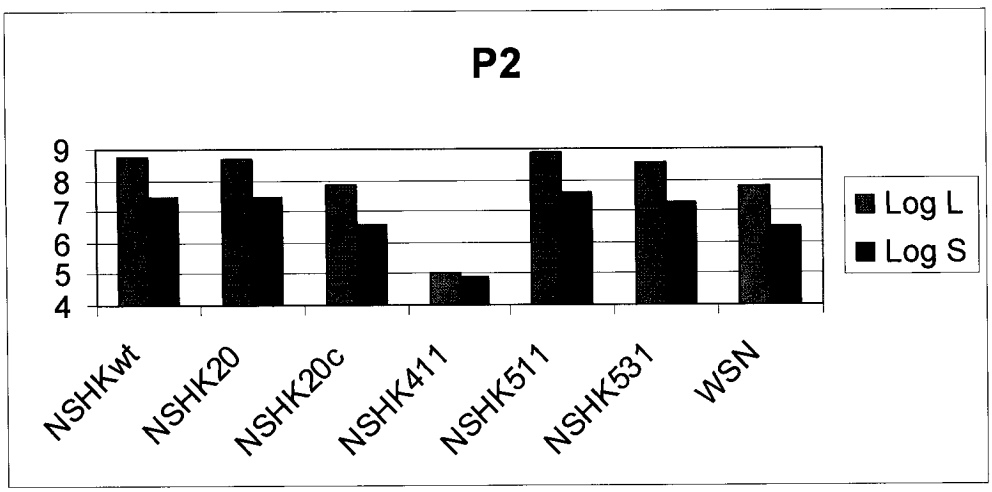
P2
9
8
7
6
5
4
Log L
Log S
NSHKwt
NSHK20
NSHK20c
NSHK411
NSHK511
NSHK531
WSN

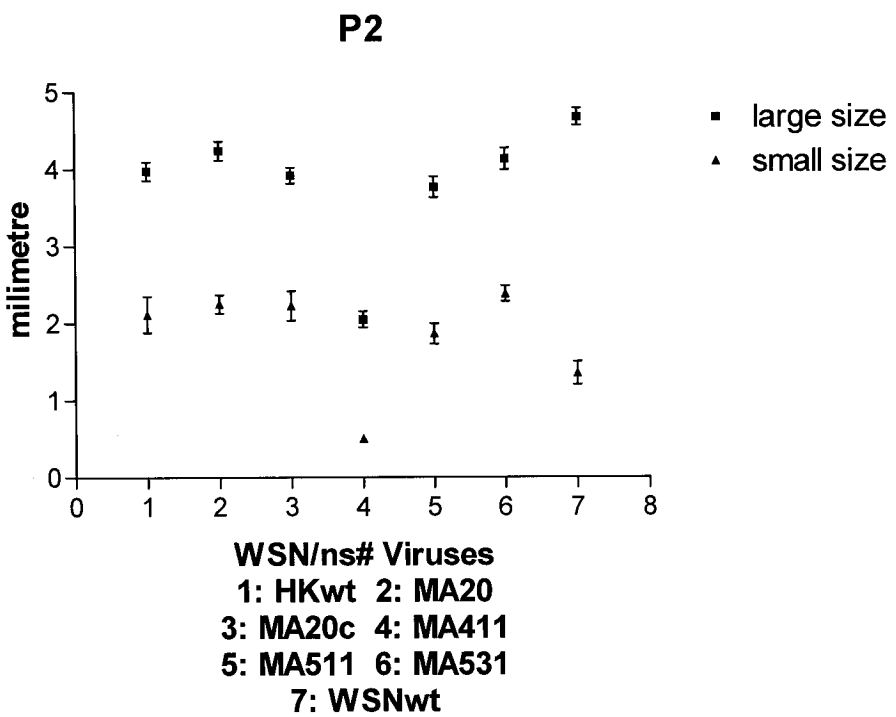
P2
5
4
3
2
1
0
milimetre
0
1
2
3
4
5
6
7
8
large size
small size
WSN/ns# Viruses
1: HKwt 2: MA20
3: MA20c 4: MA411
5: MA511 6: MA531
7: WSNwt

Figure 35: Replication Titres of Large Plaque Population and Small Plaque Population of Synthetic Recombinant Viruses (WSN/nsHK or MA#) of One Passage on MDCK Cells Followed by One Passage in 10-day Old Embryonated Eggs.

Each bar represents the large/small plaque population from one plaque assay titration of one growth experiment. All synthetic recombinant viruses in WSN backbone are shown. Titres are expressed as common logarithm.
P1E(10D)1: one passage on MDCK cells followed by one passage in 10-day old embryonated eggs

Large plaque population: blue

Small plaque population: pink

Figure 36: Plaque Sizes of Large Plaque Population and Small Plaque Population of Synthetic Recombinant Viruses (WSN/nsHK or MA#) of One Passage on MDCK Cells Followed by One Passage in 10-day Old Embryonated Eggs.

Each spot represents the average diameter of ten plaques from one population. Each virus forms two sizes of plaques: large one and small one.

P1E(10D)1: one passage on MDCK cells followed by one passage in 10-day old embryonated eggs

1: WSN/nsHKwt 2: WSN/nsMA20

3: WSN/nsMA20c 4: WSN/nsMA411

5: WSN/nsMA511 6: WSN/nsMA531

Large size: square

Small size: triangle

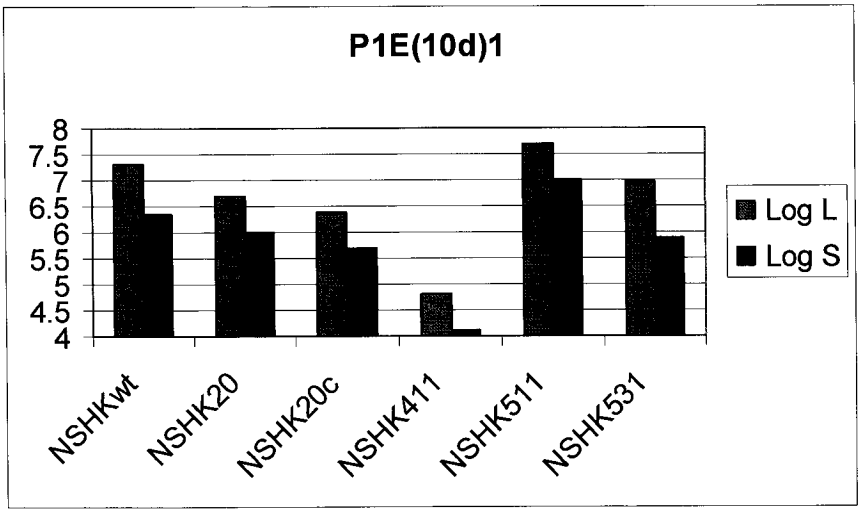
P1E(10d)1
8
7.5
7
6.5
6
5.5
5
4.5
4
Log L
Log S
NSHKwt
NSHK20
NSHK20c
NSHK411
NSHK511
NSHK531

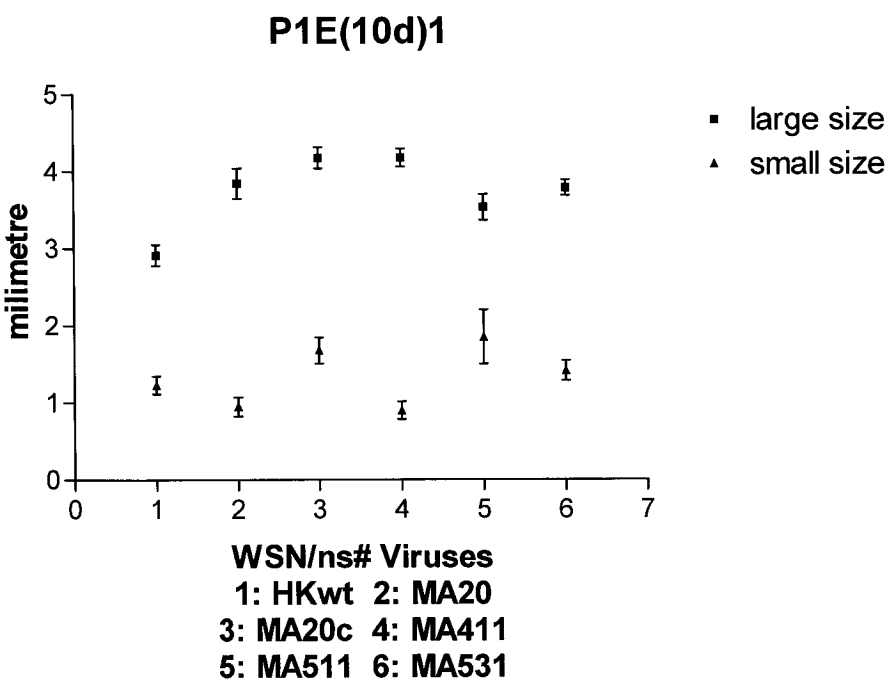
P1E(10d)1
milimetre
5
4
3
2
1
0
0
1
2
3
4
5
6
7
large size
small size
WSN/ns# Viruses
1: HKwt 2: MA20
3: MA20c 4: MA411
5: MA511 6: MA531

Figure 37: Replication Titres of Large Plaque Population and Small Plaque Population of Synthetic Recombinant Viruses (WSN/nsHK or MA#) of One Passage on MDCK Cells Followed by One Passage in 7-day Old Embryonated Eggs.

Each bar represents the large/small plaque population from one plaque assay titration of one growth experiment. All synthetic recombinant viruses in WSN backbone are shown. Titres are expressed as common logarithm.

P1E(7D)1: one passage on MDCK cells followed by one passage in 7-day old embryonated eggs

Large plaque population: blue

Small plaque population: pink

Figure 38: Plaque Sizes of Large Plaque Population and Small Plaque Population of Synthetic Recombinant Viruses (WSN/nsHK or MA#) of One Passage on MDCK Cells Followed by One Passage in 7-day Old Embryonated Eggs.

Each spot represents the average diameter of ten plaques from one population. Each virus forms two sizes of plaques: large one and small one.

P1E(7D)1: one passage on MDCK cells followed by one passage in 7-day old embryonated eggs

1: WSN/nsHKwt 2: WSN/nsMA20

3: WSN/nsMA20c 4: WSN/nsMA411

5: WSN/nsMA511 6: WSN/nsMA531

Large size: square

Small size: triangle

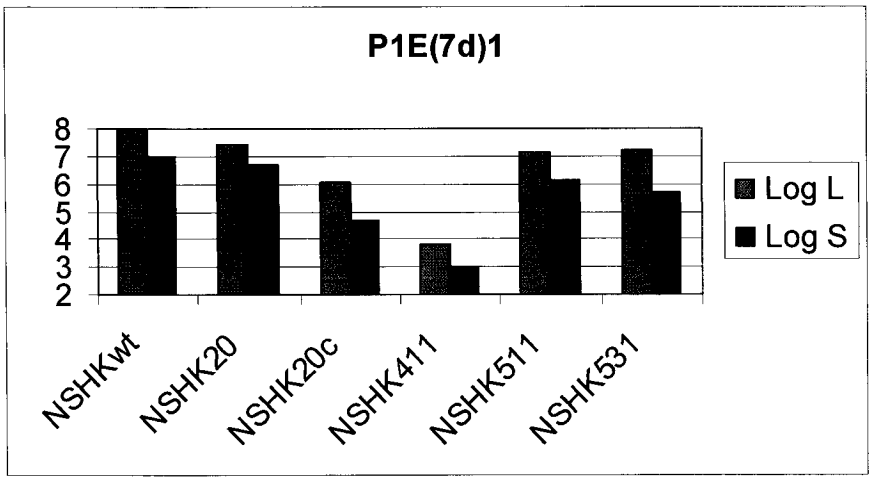
P1E(7d)1
8
7
6
5
4
3
2
Log L
Log S
NSHKwt
NSHK20
NSHK20c
NSHK411
NSHK511
NSHK531

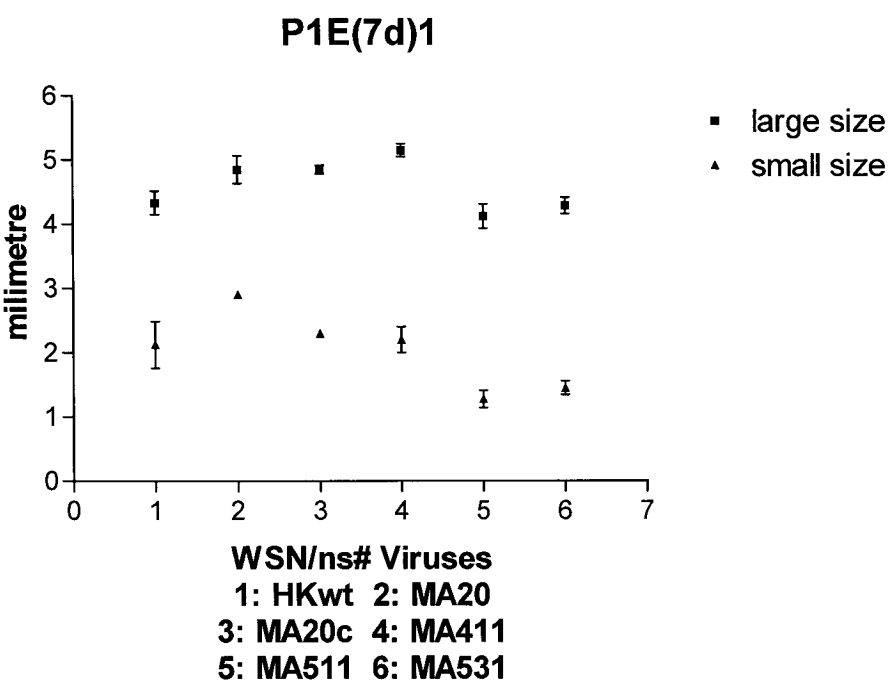
P1E(7d)1
milimetre
6
5
4
3
2
1
0
0
1
2
3
4
5
6
7
large size
small size
WSN/ns# Viruses
1: HKwt 2: MA20
3: MA20c 4: MA411
5: MA511 6: MA531

APPENDIX IV : Unit Standard of Commercial IFN for IFN Assay

To set up the system of IFN assay, different amounts of vesicular stomatitis virus (VSV) were used to infect cells per well in a 96-well dish in order to make it exactly one unit of commercial IFN to protect one well of cells from that amount of VSV infection. Figure 56 showed the IFN titration experiment on 2,000 pfu/well of VSV infection on L929 cell. Since volume of 100 µl of IFN sample was incubated in one well, the titre of IFN of the sample that successfully protected cells of one well should be 10 unit/ml.

Figure 39. Commercial IFN Standard

Picture represents cell culture in a 96-well dish. Left column represents cell culture without IFN incubation, some of them are infected by 2,000 pfu/well VSV. Right column are cell culture infected by the same amount of VSV and incubated with different amount of IFN. Picture shows that exactly one unit of IFN protects one dish cells from 2,000 pfu/well VSV infection.

Commercial IFN Standard